Sujung Jun, Allele-Specific Effects of Extracellular Superoxide Dismutase on Expression and Disease susceptibility. Doctor of Philosophy (Biochemistry and Molecular Biology), November, 2010, 161 pp., 1 tables, 26 illustrations, references, 105 titles.

Our lab previously reported a new allele for extracellular superoxide dismutase (ecSOD), expressed in 129P3/J mice (129), which differs from the wild-type, expressed in C57BL/6J and other strains. The newly discovered allele is associated with significantly increased circulating and heparin-releasable ecSOD activity and amount. To examine the properties of the two forms of ecSOD in an identical environment, I have generated congenic mice expressing either ecSOD allele on C57BL/6 genomic background. The congenic mice plasma ecSOD phenotypes show the same differences reported in the founder mice, indicating that the ecSOD genotype is largely responsible for the observed differences in the ecSOD phenotypes of the C57 and 129 strains. Tissue enzyme distribution of *129* allele is associated with higher levels of enzyme in most tissues; despite profoundly lower levels of the corresponding mRNA levels in the tissues. These results also suggest significant allele-specific differences in the regulation of ecSOD synthesis and intracellular processing/secretion of ecSOD. The increased rates of synthesis and secretion of *129* ecSOD relative to *wt* ecSOD is confirmed by using stably transfected CHO cells with either of ecSOD allele. The effects of the increased ecSOD levels in tissues on the susceptibility to asbestos-induced lung injury as well as bacterial infections were also investigated in congenic mice. Accordingly congenic mice with the *129* allele were significantly resistant to asbestos-induced fibrosis and injury. On the other hand, the expression of 129 allele significantly aggravated susceptibility to *Listeria*

and *Streptococcus* infection compared to C57 allele and ecSOD KO mice, suggesting that ecSOD plays an important role in the modulation of immune responses triggered by bacterial infection. Overall this study confirmed the ecSOD allele-specific effects on the ecSOD phenotype and on the disease susceptibilities. In conclusion, the congenic mice offer an excellent model to examine the regulatory mechanisms of ecSOD expression and the role of ecSOD in various diseases involving oxidative stress.

ALLELE-SPECIFIC EFFECTS OF EXTRACELLULAR SUPEROXIDE DISMUTASE ON EXPRESSION AND DISEASE SUSCEPTIBILITY

DISSERTATION

Presented to the Graduate Council of the
Graduate School of Biomedical Sciences
University of North Texas
Health Science Center at Fort Worth

In Partial Fulfillment of the Requirements

For the Degree of

DOCTOR OF PHILOSOPHY

By

Sujung Jun, B.S., M.S.
Fort Worth, Texas
November 2010

ACKNOWLEDGEMENTS

I would like to thank the faculty and staff of the Department of Molecular Biology and Immunology at The University of North Texas Health Science Center for their support and assistance throughout my graduate career. I would also like to thank the members of my Advisory Committee, including Dr. Andras Lacko, Dr. Laszlo Prokai, Dr. Wolfram Siede, and Dr. James Simpkins for their continual support and helpful suggestions. My sincere gratitude is extended to the members of Dr. Dory's laboratory, including Dr. Bhalchandra Kudchodkar for his helpful discussions and guidance, Dr. Anson Pierce who has developed the foundation for my dissertation project, Dr. Andrej Mirossay who helped me with initial projects, and also my coworkers, Ms. Alicia Benson and Mr. Pratik Desai for their wonderful animal care as well as technical support. My deepest gratitude is given to my mentor, Dr. Ladislav Dory, who provided me with the opportunity, knowledge, and the critical mindset to accomplish my goals including being a scientist. Without his wonderful guidance, I would not have this successful graduate career. I appreciate all my collaborators including Dr. Cheryl Fattman's group at The University of Pittsburg, Dr. Rance Berg, Dr. Harlan Jones of the Department of Molecular Biology and Immunology, and Dr. Nathalie Sumien and Dr. Michael Forster of the Department of Pharmacology and Neuroscience at The University of North Texas Health Science Center for their passion for this project. Also, I would not have gotten this far without the support of my family in Korea, who were always dedicated to my success. Lastly, I would like to thank my husband, Dr. Byung-Jin Kim, who has stood by my side every step of the way, and encouraged me throughout my graduate education with many sacrifices.

TABLE OF CONTENTS

LIST OF TABLES

CHAPTER II

LIST OF ILLUSTRATIONS

CHAPTER VI

CHAPTER I

INTRODUCTION

1. Reactive Oxygen Species and Oxidative stress

The term reactive oxygen species (ROS) is a general term for any oxygen-containing radical such as superoxide ($O_2^{\bullet -}$) or non-radical oxidant, such as hydrogen peroxide (H_2O_2)[1]. The ROS are generated as products of normal cellular metabolism by (i) mitochondria-catalyzed electron transport reactions (ii) neutrophils and macrophages during inflammation (iii) metal-catalyzed reactions [2] or generated during irradiation by U.V. light, X-rays and gamma rays [3]. ROS are known to play a dual role in biological systems; they can be either harmful or beneficial to living systems [3]. Under physiological conditions, low levels of ROS regulate the function of a number of cellular signaling pathways involved in the expression of a number of genes. An example of another physiological function of ROS is the defense against infectious agents during innate immune response. When overproduced however, a state generally referred to as oxidative stress, they become harmful to living organisms [4]. Oxidative stress can cause damage to proteins, lipids, carbohydrates, and nucleic acids [4]. Oxidative modification of biomolecules can lead to the generation of powerful inflammatory mediators, the activation or inactivation of key proteins or their regulators, and the disintegration of DNA. As a result, it has been suggested that damage caused by oxidative stress plays a key role in the initiation or progression of numerous disorders, including chronic pathological conditions including aging [5]. Continuous exposure to oxidative stress has prompted organisms to develop a series of enzymatic and non-enzymatic

antioxidant defense mechanisms for protection against the damage caused by ROS. Besides the endogenous antioxidants, they may also be acquired via diet. Excess of ROS may accumulate, therefore, when their generation exceeds the system's antioxidant capability to neutralize or eliminate them. Thus, the various roles of antioxidants in the protection against oxidative stress as well as the role of specific ROS molecules in disease progression are major topics of current research.

As illustrated in **Figure 1**, the superoxide anion radical is formed by the process of reduction of molecular oxygen mediated by NAD(P)H oxidases and xanthine oxidase or non-enzymatically, by the mitochondrial electron transport chain or hemoglobin-mediated oxygen transport. Superoxide radicals are dismutated by superoxide dismutase (SOD) to hydrogen peroxide. Hydrogen peroxide is most efficiently scavenged by glutathione peroxidase (GPx) or catalase. NO• is an abundant reactive radical generated in biological tissues by specific nitric oxide synthases (NOSs), which metabolize arginine to citrulline with the formation of NO• [6]. NO• acts as an important signaling molecule in a large variety of diverse physiological processes, including regulation of blood pressure, neurotransmission, defense mechanisms, and immune regulation [7]. NO• produced by the cells of the immune system (neutrophils, monocyte/macrophages etc.) is an effective antimicrobial agent. Cells of the immune system produce both, $O_2^{\bullet-}$ and NO• during the oxidative burst triggered during inflammatory processes. Under these conditions, $O_2^{\bullet-}$ and NO• react together to produce significant amounts of highly toxic peroxynitrite anion ($ONOO^-$), a potent oxidizing agent that can cause DNA fragmentation and lipid oxidation [9]. Thus, it is very important that the level of superoxide be controlled precisely. SODs are the only enzymes that regulate the levels of $O2^{\bullet-}$ by catalyzing its dismutation to hydrogen peroxide and because of the interaction of $O2^{\bullet-}$ and NO•, SODs

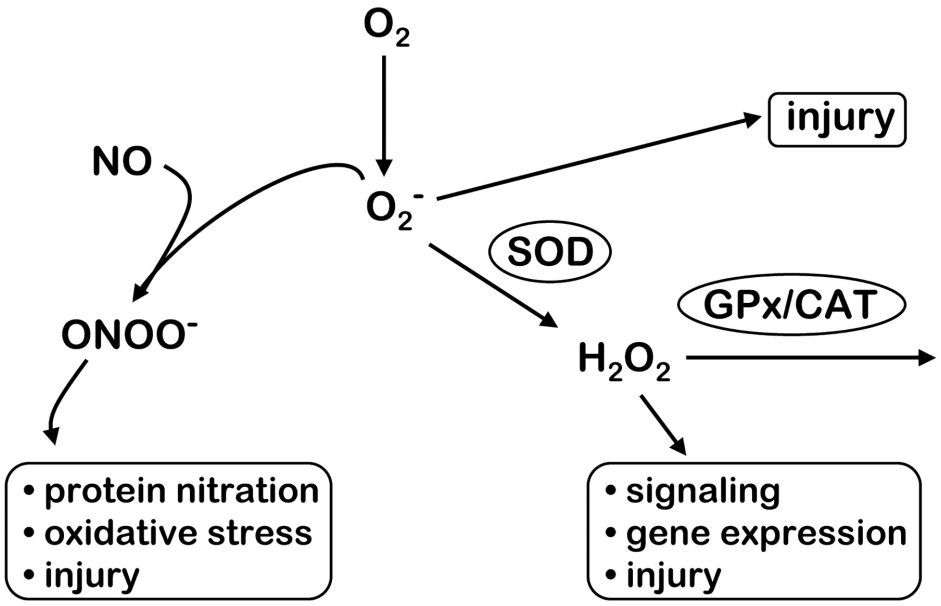

Figure 1. Schematic illustration of the inter-relationships between various ROS and NO. $O2^{\bullet-}$ is produced from molecular oxygen (O_2) by a variety of sources and can directly produce injury or can be converted by SOD to H_2O_2. H_2O_2 is an important signaling molecule, but in combination with Fe^{2+}, H_2O_2 can also produce injury by forming hydroxyl radical, a highly reactive ROS. H_2O_2 can also be degraded by various glutathione peroxidases (GPx) or catalase (CAT). Superoxide can react with NO to form peroxynitrite ($ONOO^-$). This extremely efficient reaction results in a decrease in NO bioavailability and normal NO-mediated signaling. In addition, $ONOO^-$ can indirectly produce additional increases in superoxide and oxidative. (Adapted from Faraci et al. [8])

effectively regulate the bio-availability of NO•. SODs thus play a significant role in regulating ROS and cellular oxidative stress.

2. Superoxide Dismutase

The mammalian superoxide dismutase family of enzymes (EC 1.15.1.1) contains three isoforms; copper/zinc SOD (Cu/Zn SOD or SOD1), manganese SOD (MnSOD or SOD2) and extracellular SOD (ecSOD or SOD3)[10]. SOD functions to remove superoxide from the cellular environment by catalyzing the dismutation of two superoxide radicals to hydrogen peroxide and oxygen. The kinetics of the dismutation reaction is near first order ($k = 3 \times 10^9 M^{-1} s^{-1}$) and limited by the speed with which superoxide can diffuse to the active site [11]. SOD activity can be found in all organisms of the phylogenetic tree, with the exception of a few strict anaerobes, though even they possess manganese salts that mimic SOD activity. Mitochondria (as well as many prokaryotes), possess manganese-dependent SOD (MnSOD). MnSOD is a 96 kDa homotetramer found in the mitochondrial inner membrane, and protects mitochondria from superoxide generated by single electron reduction of oxygen from the electron transport chain. Reduced MnSOD activity in mice is associated with an increased incidence of cancer and DNA damage, but not acceleration of aging. The loss of MnSOD has been associated with neonatal death [12]. Cytosolic Cu/Zn SOD is a 64kDa homodimer composed of two 32kDa subunits and is present in the cytosol and nucleus of cells, as the major intracellular SOD. Cu/Zn SOD, as its name implies, contains a copper and zinc ion and is the major intracellular scavenger of superoxide. The gene for Cu/Zn SOD is located on human chromosome 21. It was first discovered by Fridovich and was found to be the enzyme responsible for hemocuperin activity

[13]. Misfolded Cu/Zn SOD is responsible for the inherited human disease familial amyotrophic lateral sclerosis, which contributes 5-10% of all lateral sclerosis cases and is characterized by progressive degeneration of motor neurons [14].

3. Extracellular Superoxide Dismutase

The extracellular isoform of SOD (ecSOD) was discovered in 1982 by Marklund and coworkers [15], and is the only enzyme that protects the extracellular matrix (ECM) from superoxide.

3.1 Structure

The enzyme is secreted, as a slightly hydrophobic glycoprotein. It exists as a 135kDa homotetramer composed of four 28kDa subunits [16]. Two of these are linked through disulfide bridges formed between the carboxyl terminal cysteine residues located in each subunit. Each subunit binds one copper and zinc ion [17], and is roughly 60% homologous to the intracellular Cu/Zn SOD [10] with little homology to mitochondrial MnSOD. The location of the ecSOD gene has been mapped to human chromosome 4 and to mouse chromosome 5; both of them are composed of two exons and one intron, with the coding sequence contained entirely in one exon [18, 19]. Mouse ecSOD gene is 82% identical to rat ecSOD, but only 60% identical to human ecSOD [20, 21].

The mouse ecSOD mRNA encodes a 251 amino acid pre-propeptide, with a signal sequence (see **Figure 2**), whose predicted cleavage site occurs between amino acids 20 and 21 to

yield a 231 amino acid peptide [21]. However, based on NH_2-terminal sequencing of purified ecSOD from mouse lung, the mature protein is only 227 amino acids long [21]. Amino acids 21-24 are not found in the mature protein; the site of the cleavage of these residues has yet to be identified with certainty. The mature form of mouse ecSOD can be divided into three functional domains: (1) the amino terminal residues 1-97 contain a glycosylation site at Asn 97; (2) residues 98-193, containing the active site with a strong homology with Cu/Zn SOD; (3) C-terminal amino acids 194-227, containing a group of six positively charged amino acids (4 arginines, 2 lysines), referred to as the heparin-binding domain.

Because of its heparin-binding domain, ecSOD is well suited to interact with the negatively charged heparan sulfate proteoglycans and glycocalyx, present in the ECM and on the surface of cells, as well as type I collagen [22]. Here, the enzyme can protect tissues from the superoxide ion and limit its interaction with NO•, giving ecSOD the distinction as a major determinant of NO• bioavailablility. This action also prevents the excessive formation of the highly reactive peroxynitrite. This is particularly important in the vasculature, where nitric oxide induces vasodilation and has several anti-atherogenic properties.

Since the heparin binding domain can be cleaved, enzyme fractionation by heparin-sepharose affinity chromatography yields three distinct tetramers of enzyme: type A ecSOD, which has no affinity for heparin, type B ecSOD with intermediate affinity for heparin, and type C, which has strong heparin affinity [23]. Types A and B are found circulating in plasma, while type C remains bound to the ECM but can be released into the circulation by displacing it with heparin [24, 25]. The tissue-bound form represents approximately 90-99% of the total body ecSOD [24, 26]. The various affinities for heparin can be explained by proteolysis of the heparin-binding domain, which can occur partially, to produce type B ecSOD, and completely,

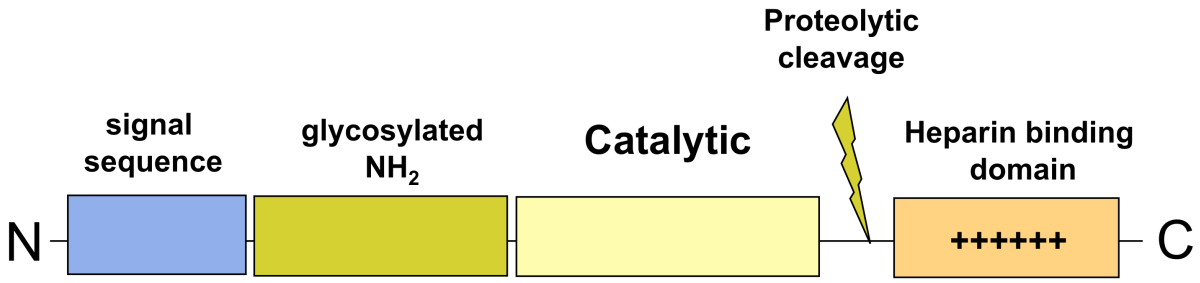

Figure 2. Schematic diagram of ecSOD functional domains in protein.

The ecSOD gene has two exons; the coding sequence is contained entirely in one exon. The ecSOD gene can be divided into four functional domains: (1) the signal sequence, cleaved during synthesis, (2) the glycosylated N-terminus, (3) the catalytic region, which bears the highest level homology to Cu/Zn SOD, (4) the positively charged heparin-binding domain.

to produce type A tetramer in which all of the 4 subunits lack the C-terminal heparin-binding domain [27]. Cleavage of the C-terminal heparin-binding domain can be accomplished by an intracellular furin-like protease [28]; however the precise mechanism and physiological significance of this cleavage is unknown. Cleavage of the heparin binding domain is thought to control the tissue distribution, and shortens its half-life from ~85h (uncleaved type C) to ~7h (cleaved type A) [29].

3.2 Regulation of expression

In contrast to intracellular CuZn-SOD and MnSOD, the expression of ecSOD appears to be restricted to only a few cell types in several tissues. High levels of ecSOD are present in alveolar type II cells, proximal renal tubular cells, lung macrophages, vascular smooth muscle cells, some fibroblast lines, glial and endothelial cells [26]. In mammals, the enzyme concentration is highest in the lung, kidney, and aorta [21], while the heart and brain have lesser amounts. In the lung interstitium, ecSOD is localized in areas containing high amounts of type 1 collagen fibers, where the enzyme may protect it from oxidative degradation. ecSOD mRNA is highly expressed in blood vessels, lung and kidneys of the mouse [18, 22]. The mechanism regulating such specific expression is not yet well-understood, but Zelko et al reported that Ets, Kruppel, and MZF-1 transcription factors determine the cell-specific expression of murine ecSOD [30]. Zelko *et al.* reported that transcription of the murine ecSOD is regulated, at least in part, by Sp1/Sp3 transcription factors [31]. Furthermore, they found that the Sp1/Sp3 transcription factors are the major trans-activating factors activating basal gene transcription of human ecSOD [32]. Interestingly, there is a disparity between protein and mRNA levels of

ecSOD in the cell, indicating a role for post-transcriptional regulation in maintaining optimal enzyme levels in various tissues [18]. Compared to the number of studies on transcriptional regulation mechanisms, posttranscriptional modulation of ecSOD, such as rates of protein synthesis and secretion, and the extent of degradation are not known.

In human vascular smooth muscle cells and lung alveolar type II cells, inflammatory cytokines such as interferon (IFN)-γ and IL-4 can upregulate the expression of ecSOD mRNA and protein while tumor necrosis factor (TNF)-α downregulate them [33]. Common to many of the cytokine pathways is the stimulation of transcription by NF-κB. It is therefore interesting to note that there exists a putative NF-κB binding motif in the promoter region of human as well as mouse ecSOD [18, 34]. TNF-α and IFN-γ appear to be a potent combination for the induction of ecSOD expression in rat alveolar type II pneumocytes through NF-κB activation [35]. Also, ecSOD expression can be regulated by hormones such as angiotensin II, estrogen and progesterone, a wide variety of oxidizing agents such as xanthine oxidase, paraquat, and t-butyl hydroperoxide in fibroblasts [36], and dietary zinc intake [37, 38]. Vasoactive factors such as histamine, vasopressin, oxytocyn, endothelin-1, serotonin, and heparin markedly increase enzyme levels in cultured arterial smooth muscle cells [39]. Further, exercise training increases the production of nitric oxide in mouse vessel endothelial cells which, in turn, up-regulates the expression of ecSOD in adjacent smooth muscle cells [40]. Thus, increased concentration of ecSOD prevents the degradation of NO by oxygen radicals. Angiotensin II strongly induces ecSOD activity in mouse aortas [41] and in cultured human smooth muscle cells [39] through transcriptional activation and stabilization of mRNA.

Copper, a redox active metal, is an essential element for ecSOD function. Fukai and colleagues determined that copper delivery to ecSOD modulates its enzymatic activity [42].

Intracellular copper availability is extraordinarily restricted, as the intracellular milieu has a great capacity to chelate copper. However, in the cytoplasm, copper is distributed among several proteins, known as copper chaperones, which includes antioxidant protein 1 (Atox1). Copper chaperones compete with chelators for copper and directly insert the cofactor into the target enzymes, such as cytochrome C oxidase, CuZn-SOD, and Menkes ATPase, thus converting the latter from an inactive to an active state (holo-cuproenzymes). Menkes ATPase serves as a copper efflux pump that regulates the amount of copper leaving the cell and supplies copper to secreted cuproenzymes, including ecSOD [43]. Like copper, iron is a redox active metal that is critical to cellular homeostasis. The addition of $FeCl_2$ to smooth muscle cell cultures induces ecSOD protein expression in a dose-dependent fashion [44]. In addition, low concentrations of iron increase secretion of ecSOD to the medium, whereas higher concentration inhibits both ecSOD expression and secretion. The mechanisms by which iron may modulate ecSOD are currently unknown.

3.3 ecSOD polymorphism in human and mouse

A substitution of arg-213 with gly (R213G), localized in the center of the carboxyl-terminal cluster of positively charged amino acid residues of the heparin-binding domain, is a common human gene variant of ecSOD [45]. Although this variant does not affect ecSOD enzymatic activity, it apparently reduces its affinity for ECM; plasma concentrations of ecSOD are increased up to a 30-fold in the population that carries the gene variant (2-5% of the global population) [45]. Interestingly, the R213G gene product is resistant to proteolysis by trypsin and neutrophil-derived proteases [46]. The clinical significance of $ecSOD_{(R213G)}$ has been

investigated in several association studies. Patients with diabetes and end-stage renal disease that carry $ecSOD_{(R213G)}$ have increased 5-year mortality rates, with significantly higher death rates from ischemic heart disease and cerebrovascular disease, than non-carriers [47]. Also, the R213G gene variant appeares to accelerate the progression of renal failure and atherosclerosis in uremic patients. Finally, a study in Denmark detected a 2.3-fold increase in risk of ischemic heart disease in heterozygotes carrying $ecSOD_{(R213G)}$ [48]. These results demonstrate the importance of tissue-bound ecSOD for protection against oxidative stress.

Recently, Dahl et al. identified novel polymorphisms in human ecSOD that are associated with altered lung function or chronic obstructive pulmonary disease (COPD) [49]. They occur in the non-coding 5' untranslated region (E1) and first intron (I1) of the ecSOD gene. Both the E1 and I1 polymorphisms are associated with lower levels of lung tissue ecSOD; E1/I1 homozygotes have reduced forced vital capacity, indicating reduced lung function, and greater risk of clinical COPD in terms of hospitalizations. Arcaroli et al. also confirmed the association between haplotypes in ecSOD and mortality in patients with infection-associated acute lung injury, which usually develops in response to a major insult such as sepsis, trauma, pneumonia, and multiple transfusions [50]. These data suggest that ecSOD polymorphism has a profound effect on lung function and disease. Several other variants of the ecSOD gene have also been described in humans, including A40T and a silent mutation, L53L (CTG to TTG) [19, 51]. The A40T substitution is located in the amino-terminal domain of ecSOD, where it is thought to be involved in the tetramerization of the enzyme. The A40T polymorphism appears to be associated with the susceptibility in type 2 diabetes patients to insulin resistance and hypertension [52]. Rosta et al. recently reported that this polymorphism is associated with pre-eclampsia which is characterized by hypertension and proteinuria developed after midgestation, when the disease

was complicated by severe fetal growth restriction [53].

Our group previously reported a variant of the ecSOD allele found in the 129P3/J strain of mice (129) and referred to it as *129* ecSOD*,* which is different from the wild-type allele, found in the C57 and other strains (*wt* ecSOD) [54]. The *129* ecSOD has a 10bp deletion in the 3'UTR and several point mutations in the coding sequence. Only two of these point mutations result in amino acid substitutions: 1) in the signal peptide sequence (N21D) and 2) in the catalytic domain (A186S). This genotype is associated with 2-3 fold higher enzyme activity and amount in the circulation when compared to C57 mice, which express *wt* ecSOD. The amino acid substitution in the catalytic domain does not appear to have a major effect since the changes in enzyme amount parallel the changes in activity in the plasma, as shown by Pierce et al [54] (see **Figure 3**). The effects of change within the signal peptide or 10bp deletion in the 3'UTR have not been investigated yet.

Interestingly, the C57 and the 129 strains of mice are the two most widely used animal models for human diseases. The 129 mice are used as embryonic stem cell donors for the creation of most C57 strain gene knockout or transgenic mice. Extensive backcrossing to the C57 strain is used to eliminate as many of the 129 genes as possible. In spite of this, a small genomic contamination from 129 can remain and affect the phenotype of the manipulated mouse model. Awareness of this fact is especially important for the studies in which these two strains respond differently to the induction of the same disease. A genetic disruption or transfer acquired from different species or strains of the same species may trigger alterations in the expression of other genes in the recipient species in response to physiological modulators. In contrast, congenic mice provide a convenient tool that eliminates many of these problems, since they have identical

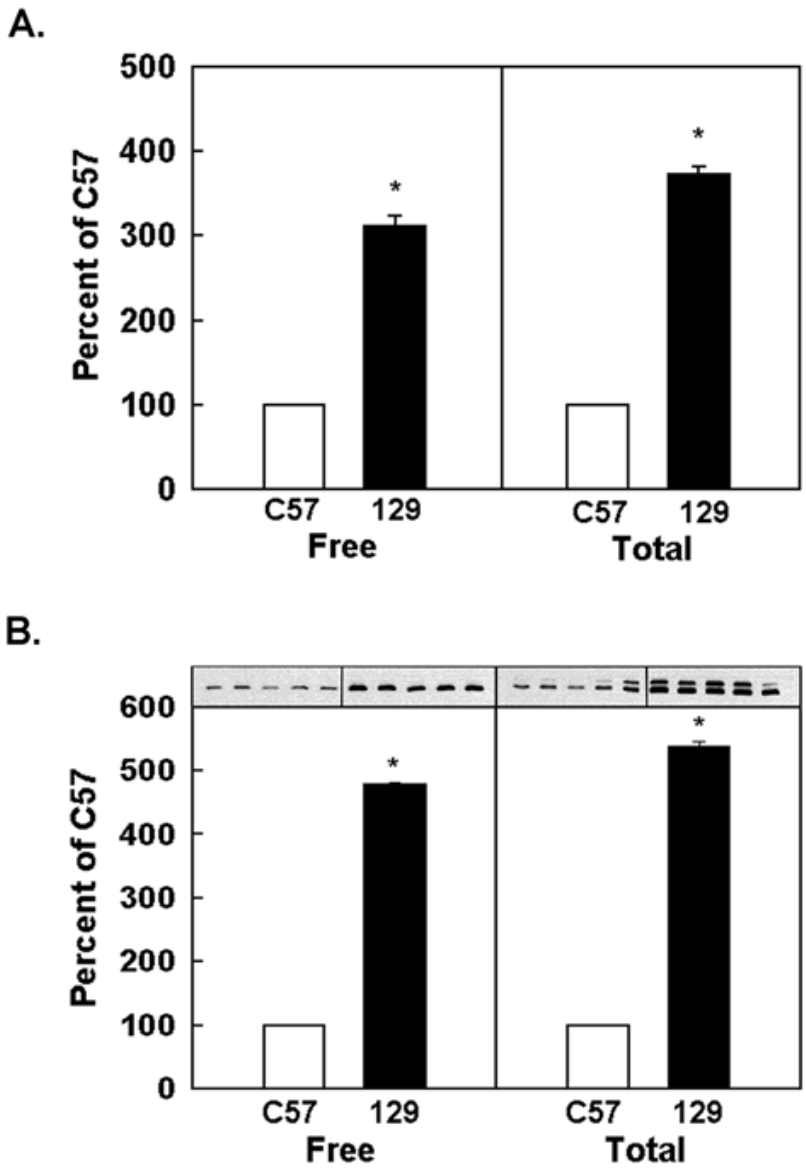

Figure 3. Plasma ecSOD activity and amount in C57 and 129 strain [54].

Free (open) and total (free plus heparin-releasable, matrix-bound) ecSOD (filled) were measured in 6 month old C57 and 129 mice. Total values represent ecSOD activity after heparin injection (100U). Extracellular SOD activity (A), a tyypical Western blot for ecSOD and the densitometry (B) is shown.

genetic background and differ only in the genetic loci of interest. In fact, the 129 and C57 mice differ significantly in their response to proliferative lung disease, brain ischemia, vascular remodeling, susceptibility to atherosclerosis [55-58], as well as development of tolerance against global and focal cerebral ischemia [59] by hyperbaric oxygen treatment. None of these studies identified specific gene(s) that may account for the observed differences in the response of these strains. Given the potentially important role of ecSOD in maintaining the redox environment of the ECM, it is important to examine the specific effects of this allele, independent of the genetic environment, on the overall ecSOD and disease susceptibility phenotype.

Recently, Ganguly et al. [60] reported that mouse ecSOD is also associated with the complex traits of dead space volume (VD) and total lung capacity by genomewide linkage analysis of C3H/HeJ (C3H) and JF1/Msf (JF1) mouse strains which differ the most in measured lung function. They also reported that JF1 strains produce significantly lower transcript and protein levels of ecSOD than C3H. The JF1 strain possesses 3 SNPs compared to wild type (C3H) mice. Those are N21D, E57Q, and A186S. Note that two of these (N21D and A186S) are common between 129 and JF1 strains; the 10bp deletion is not observed in ecSOD of JF1 (Jun et al, unpublished observations). Thus, it is very important to understand which of the polymorphisms is responsible for the phenotype.

3.4 ecSOD and disease

There is compelling evidence that increased oxidative stress plays an important role in the pathophysiology of many diseases such as cardiovascular disease, cancer, diabetes mellitus and neurodegenerative diseases [5]. Protection from global cerebral ischemia, preservation of post-

ischemic myocardial function, reduction of lung injury during inflammation, and reduction in aging-induced cognitive impairment is shown in transgenic mice expressing human ecSOD [61]. Adenoviral-delivery of human ecSOD to rabbits protected them from myocardial stunning. Evidence for the participation of ecSOD in the aging process exists based on the finding that the decline in ecSOD activity is a factor responsible for decreased telomere shortening in fibroblast donor cells. Thus ecSOD may be considered as a useful therapeutic target for the treatment of oxidative stress and inflammatory disorders in the future [62, 63].

1. Cardiovascular disease

ecSOD is highly expressed in blood vessels, particularly arterial walls [22, 64], and is the predominant form of SOD in the aortas of baboons and humans, constituting up to 70% of the SOD activity in this tissue [64]. Because superoxide, either alone or in combination with nitric oxide, has been associated with the progression of atherosclerosis, the regulation of ecSOD levels in vessels may be particularly important in the pathogenesis of this disease [65]. For example, ecSOD expression is substantially reduced in patients with coronary artery disease, suggesting that reduced ecSOD activity contributes to endothelial dysfunction in patients with this disease [66]. This is supported by the fact that overexpression of ecSOD in vascular endothelial cells can protect against the oxidation of LDL, a major contributing factor to the formation of atherosclerosis [67]. Lund et al showed that endogenous ecSOD also plays an important role in protection against decreased-vasomotor function during aging [68]. This research group also showed that 1) vascular dysfunction associated with aging is mediated in part by increased levels of superoxide, 2) gene transfer of ecSOD reduces vascular superoxide and dysfunction in old animals, and 3) beneficial effects of ecSOD in old rats require the heparin-

binding domain of ecSOD, since gene transfer of the human variant form R213G did not have a protective effects [69]. Activation of membrane-bound NADPH oxidase by angiotensin II has been shown to be a significant source of ROS in blood vessels [70], and the hypertension caused by angiotensin II can be abrogated by treatment with membrane-targeted forms of SOD [71]. Gene transfer of ecSOD, with a strict requirement for its heparin-binding domain, reduces systemic vascular resistance and arterial pressure in a genetic model of hypertension [72].

The beneficial effects of ecSOD in reducing myocardial infarct size and preserving cardiac function have been found in numerous laboratories. Initial studies using recombinant ecSOD demonstrated preserved cardiac function and reduced levels of tissue ROS following ischemia/reperfusion in rat hearts [73, 74]. ecSOD-transgenic mice expressing a 5-fold higher level of ecSOD showed greater preservation of myocardial function after global ischemia/reperfusion than their wild-type counterparts [75]. Li and coworkers have shown that increasing ecSOD levels in rabbit hearts confers both protection against myocardial stunning [76] and reduces reperfusion infarct size [77] following ischemia/reperfusion. Similar ecSOD-mediated protection has been demonstrated in other tissue models of ischemia/reperfusion injury including cerebral ischemia and renal ischemia in the rabbit kidney [78, 79].

2. Asbestos-induced lung disease

Asbestos is a naturally occurring mineral fiber. Inhalation of asbestos fibers causes interstitial pulmonary fibrosis in both man and experimental animals. Although occupational exposures to asbestos fibers has decreased in recent years, the 20 to 40 year delay from exposure to manifestation of disease has resulted in increased incidence of asbestosis in exposed

populations [80]. Thus, this disease is currently and will remain as a significant health problem. Even though much work has been done to investigate both the pathogenesis and treatment of asbestos-related diseases, there are no effective therapeutic approaches because it is not clear how this fibroproliferative process is mediated at the biochemical and molecular levels.

A number of studies suggest that ROS-mediated inflammation and tissue damage contribute to the interstitial pulmonary fibrosis in both human and experimental animal models after asbestos exposure (reviewed in [81]). Thus, a number of antioxidant enzymes, including manganese superoxide dismutase and catalase [82, 83], as well as the addition of iron chelators [84] have been tested and shown to be protective in models of asbestos-induced lung disease.

ecSOD may be a key therapeutic target, since it is expressed at especially high levels in mammalian lungs, compared with other tissues [24, 26]. Previous studies have found that asbestos-induced lung injury is accompanied by loss of ecSOD from the alveolar septa and accumulation of the enzyme in the bronchoalveolar lavage fluid [85]. Furthermore, ecSOD knock-out mice show enhanced lung injury and inflammation compared with wild-type mice in asbestos-induced lung injury [86]. These studies also show that ecSOD plays an important role in protecting mice from asbestos induced lung injury and inflammation [85]. The mechanism of this protection by ecSOD, however, is not fully understood. Recent studies indicate that inhibition of oxidative fragmentation of ECM probably represents one mechanism by which ecSOD inhibits inflammation in response to lung injury [87].

Interestingly, the 129P3/J mice are significantly more resistant to asbestos-induced pulmonary fibrosis than the C57BL/6 mice [55]. This phenotype is also associated with reduced expression of pro-fibrotic cytokines including transforming growth factor (TGF) β and TNF α at sites of fiber deposition. These findings of a delayed and/or reduced response to injury in a

subset of 129 mouse strain both commercially derived inbred and genetically-manipulated backcrosses, along with similar results in primary mouse lung cells in vitro, suggest that the 129 mouse strain can be a useful model for defining susceptibility gene(s) that control responses to lung injury. However, no studies have defined the susceptibility gene(s) yet. Our findings suggest that the newly found ecSOD allele in the 129 strain might be a susceptibility gene that controls inflammatory or fibrotic responses to asbestos exposure.

3. Bacterial infection

Inflammation is a response of the organism to injury related to physical or chemical noxious stimuli or microbiological toxins, which are involved in multiple pathologies. Inflammatory response is intended to inactivate or destroy invading organisms, remove irritants, and set the stage for tissue repair [88]. Conventionally, ROS have been considered to function primarily in host defense as antimicrobial factors [89]. Phagocytic cells including neutrophil and macrophages are among the most important components of the innate immune response, which is the first line of host defense and those phagocyte-derived ROS are of crucial importance for host resistance to microbial pathogens [1]. Two of the most important antimicrobial systems of phagocytic cells are the NADPH oxidase and inducible nitric oxide synthase (iNOS) pathways, which are responsible for the generation of superoxide and nitric oxide radicals, respectively [1]. Nitric oxide may play regulatory roles at virtually every stage of the development of inflammation, in particular, in the regulation of pro-inflammation properties of endothelium and in the early stages of inflammatory cell transmigration into the sites of inflammation [88].

Superoxide and hydrogen peroxide also have been associated with many stages of the inflammation.

It is very interesting to note that SODs control the level of superoxide by dismutation and, in the case of ecSOD, play a major role in regulating the levels of nitric oxide. Furthermore, by limiting the availability of superoxide, the level of peroxinitrite can also be controlled by these enzymes (**Figure 1**). Although many studies have revealed the importance of ROS as bactericidal, the role of ecSOD during bacterial infection has not been studied in detail. A limited number of studies has shown that exogenous SOD can inhibit killing of *Listeria* [90, 91]; macrophages from mice that overexpress human SOD1 are also impaired in their ability to kill *E. coli* [92]. These studies imply that ecSOD may impair the ability to mount a proper innate immune response against invading microorganisms**.** Other studies show that mice overexpressing human ecSOD have increased survival rates and decreased neutrophil recruitment in response to LPS stimulation when compared to wild-type mice [93]. On the other hand, mice lacking ecSOD show increased lung neutrophil recruitment and injury in response to LPS [94]. The overexpression of human ecSOD also protects mice from lung injury due to influenza virus infection [95]. These studies indicate that ecSOD is important for protecting tissues from oxidative damage by dampening immune responses. The immunosuppressive effect may be counterproductive during acute infections. Thus, understanding how ecSOD expression is regulated and how ecSOD regulates ROS during bacterial infection is important.

4. Brain function and behavior

Increasing evidence suggests that oxidative stress plays a central role in a variety of neurological disorders including Alzheimer's disease, amyotrophic lateral sclerosis,

Huntingdon's disease, and Parkinson's disease (reviewed in [96]). Thus, the proper function of brain antioxidant mechanisms may be of considerable importance in the prevention of these neurological disorders. Although ecSOD expression is much lower in the brain when compared to other organs [24, 26], the extracellular space in the brain is relatively small and, therefore, the actual concentration of ecSOD in the brain may be considerably higher than initially thought [65]. Investigations into the role of ecSOD in normal brain function and a variety of neurological disorders have been performed. These studies suggest that the regulation of brain extracellular superoxide concentration by ecSOD may be of importance with regard to cognitive function. Thus genetically altered mice that expressed either higher-than- or lower-than normal levels of ecSOD displayed impaired learning and memory functions [97-99]. For example, ecSOD-transgenic mice exhibited a reversible impairment of long-term potentiation in hippocampal area CA1 that is related to impaired long-term, but not short-term, memory in contextual fear conditioning [100]. In other studies involving choice accuracy in a radial arm maze, both ecSOD transgenic and knockout mice had particular difficulty in making accurate choices under a low motivational state [97]. However, it should be noted that these mice were not incapable of learning; they showed significant progress under the high motivation conditions [101]. These studies demonstrate that, rather than being exclusively a neurotoxic molecule, brain extracellular superoxide may be vital in maintaining adequate learning function [97]. These results also may have important implications for attention deficit hyperactivity disorder, characterized by cognitive impairments related to motivational states. In this regards, it is very interesting that C57 mouse strains differ substantially from 129 mouse strains on almost all measures of locomotor behavior [102] and on hypoactive anxious phenotype in the 129 strain [103].

3.5 Therapeutic applications of ecSOD

A considerable number of studies suggests that the administration of a wide variety of enzymatic and nonenzymatic antioxidants can protect against oxidant-induced tissue injury, both in animal models and in the human [65]. Since ecSOD level and/or activity is decreased in several diseases, it is interesting to entertain the idea of ecSOD as a potential target for therapy to improve antioxidant capacity and restore the free radical balance. Thus, a further understanding of the role of ecSOD in the pathogenesis of oxidant-mediated diseases as well as the regulatory mechanism of ecSOD expression will provide better insight into the potential therapeutic possibilities of ecSOD.

5. Project Goals

Many diseases display involvement with oxidative stress and could potentially benefit from antioxidant therapy designed to restore the balance between reductive and oxidative factors. Even though ecSOD is considered as one of the target antioxidant enzyme, the functional significances of the gene polymorphism in mice in disease progression as well as in the expression are not studied yet.

The first phase of my work involved generation of congenic mice (C57.129-*sod3*) expressing either *wt* or *129* ecSOD allele on C57 background and characterization of the tissue phenotype of ecSOD distribution.

The second phase of my work focuses on the effect of polymorphism on cellular aspects of ecSOD synthesis and secretion.

The third and fourth phases of my work investigate the effect of ecSOD expression level on disease susceptibility, including asbestos-induced lung fibrosis and bacterial infection.

6. Note on Materials Used in the Dissertation

Overall results presented in Chapter II were published in the Journal of Free Radical Biology and Medicine (2010) [104]. The initial work for Chapter III was published in Biochemical and Biophysical Research Communications (2007) [105] and the results presented in Chapter III are in preparation for submission. The material from Chapter IV is in review in the Journal of Free Radical Biology and Medicine.

REFERENCES

[1] Fang, F. C. Antimicrobial reactive oxygen and nitrogen species: Concepts and controversies. *Nat. Rev. Microbiol.***2:**820-832; 2004.

[2] Cadenas, E. Biochemistry of oxygen toxicity. *Annu. Rev. Biochem.***58:**79-110; 1989.

[3] Valko, M.; Izakovic, M.; Mazur, M.; Rhodes, C. J.; Telser, J. Role of oxygen radicals in DNA damage and cancer incidence. *Mol. Cell. Biochem.***266:**37-56; 2004.

[4] Valko, M.; Rhodes, C. J.; Moncol, J.; Izakovic, M.; Mazur, M. Free radicals, metals and antioxidants in oxidative stress-induced cancer. *Chem. Biol. Interact.***160:**1-40; 2006.

[5] Valko, M.; Leibfritz, D.; Moncol, J.; Cronin, M. T.; Mazur, M.; Telser, J. Free radicals and antioxidants in normal physiological functions and human disease. *Int. J. Biochem. Cell Biol.***39:**44-84; 2007.

[6] Ghafourifar, P.; Cadenas, E. Mitochondrial nitric oxide synthase. *Trends Pharmacol. Sci.***26:**190-195; 2005.

[7] Bergendi, L.; Benes, L.; Durackova, Z.; Ferencik, M. Chemistry, physiology and pathology of free radicals. *Life Sci.***65:**1865-1874; 1999.

[8] Faraci, F. M.; Didion, S. P. Vascular protection: Superoxide dismutase isoforms in the vessel wall. *Arterioscler. Thromb. Vasc. Biol.***24:**1367-1373; 2004.

[9] Carr, A. C.; McCall, M. R.; Frei, B. Oxidation of LDL by myeloperoxidase and reactive nitrogen species: Reaction pathways and antioxidant protection. *Arterioscler. Thromb. Vasc. Biol.***20:**1716-1723; 2000.

[10] Zelko, I. N.; Mariani, T. J.; Folz, R. J. Superoxide dismutase multigene family: A comparison of the CuZn-SOD (SOD1), mn-SOD (SOD2), and EC-SOD (SOD3) gene structures, evolution, and expression. *Free Radic. Biol. Med.***33:**337-349; 2002.

[11] Forman, H. J.; Fridovich, I. Superoxide dismutase: A comparison of rate constants. *Arch. Biochem. Biophys.***158:**396-400; 1973.

[12] Robinson, B. H. The role of manganese superoxide dismutase in health and disease. *J. Inherit. Metab. Dis.***21:**598-603; 1998.

[13] McCord, J. M.; Fridovich, I. Superoxide dismutase. an enzymic function for erythrocuprein (hemocuprein). *J. Biol. Chem.***244:**6049-6055; 1969.

[14] Liochev, S. I.; Fridovich, I. Mutant cu,zn superoxide dismutases and familial amyotrophic lateral sclerosis: Evaluation of oxidative hypotheses. *Free Radic. Biol. Med.***34:**1383-1389; 2003.

[15] Marklund, S. L.; Holme, E.; Hellner, L. Superoxide dismutase in extracellular fluids. *Clin. Chim. Acta***126:**41-51; 1982.

[16] Marklund, S. L. Human copper-containing superoxide dismutase of high molecular weight. *Proc. Natl. Acad. Sci. U. S. A.***79:**7634-7638; 1982.

[17] Tibell, L.; Hjalmarsson, K.; Edlund, T.; Skogman, G.; Engstrom, A.; Marklund, S. L. Expression of human extracellular superoxide dismutase in chinese hamster ovary cells and characterization of the product. *Proc. Natl. Acad. Sci. U. S. A.***84:**6634-6638; 1987.

[18] Folz, R. J.; Crapo, J. D. Extracellular superoxide dismutase (SOD3): Tissue-specific expression, genomic characterization, and computer-assisted sequence analysis of

the human EC SOD gene. *Genomics***22:**162-171; 1994.

[19] Miao, L.; St Clair, D. K. Regulation of superoxide dismutase genes: Implications in disease. *Free Radic. Biol. Med.***47:**344-356; 2009.

[20] Hendrickson, D. J.; Fisher, J. H.; Jones, C.; Ho, Y. S. Regional localization of human extracellular superoxide dismutase gene to 4pter-q21. *Genomics***8:**736-738; 1990.

[21] Folz, R. J.; Guan, J.; Seldin, M. F.; Oury, T. D.; Enghild, J. J.; Crapo, J. D. Mouse extracellular superoxide dismutase: Primary structure, tissue-specific gene expression, chromosomal localization, and lung in situ hybridization. *Am. J. Respir. Cell Mol. Biol.***17:**393-403; 1997.

[22] Stralin, P.; Karlsson, K.; Johansson, B. O.; Marklund, S. L. The interstitium of the human arterial wall contains very large amounts of extracellular superoxide dismutase. *Arterioscler. Thromb. Vasc. Biol.***15:**2032-2036; 1995.

[23] Marklund, S. L. Analysis of extracellular superoxide dismutase in tissue homogenates and extracellular fluids. *Methods Enzymol.***186:**260-265; 1990.

[24] Marklund, S. L. Extracellular superoxide dismutase in human tissues and human cell lines. *J. Clin. Invest.***74:**1398-1403; 1984.

[25] Adachi, T.; Yamada, H.; Futenma, A.; Kato, K.; Hirano, K. Heparin-induced release of extracellular-superoxide dismutase form (V) to plasma. *J. Biochem.***117:**586-590; 1995.

[26] Marklund, S. L. Extracellular superoxide dismutase and other superoxide dismutase isoenzymes in tissues from nine mammalian species. *Biochem. J.***222:**649-655; 1984.

[27] Karlsson, K.; Edlund, A.; Sandstrom, J.; Marklund, S. L. Proteolytic modification of the heparin-binding affinity of extracellular superoxide dismutase. *Biochem. J.***290 (Pt 2):**623-626; 1993.

[28] Bowler, R. P.; Nicks, M.; Olsen, D. A.; Thogersen, I. B.; Valnickova, Z.; Hojrup, P.; Franzusoff, A.; Enghild, J. J.; Crapo, J. D. Furin proteolytically processes the heparin-binding region of extracellular superoxide dismutase. *J. Biol. Chem.***277:**16505-16511; 2002.

[29] Karlsson, K.; Sandstrom, J.; Edlund, A.; Marklund, S. L. Turnover of extracellular-superoxide dismutase in tissues. *Lab. Invest.***70:**705-710; 1994.

[30] Zelko, I. N.; Folz, R. J. Myeloid zinc finger (MZF)-like, kruppel-like and ets families of transcription factors determine the cell-specific expression of mouse extracellular superoxide dismutase. *Biochem. J.***369:**375-386; 2003.

[31] Zelko, I. N.; Folz, R. J. Sp1 and Sp3 transcription factors mediate trichostatin A-induced and basal expression of extracellular superoxide dismutase. *Free Radic. Biol. Med.***37:**1256-1271; 2004.

[32] Zelko, I. N.; Mueller, M. R.; Folz, R. J. Transcription factors sp1 and sp3 regulate expression of human extracellular superoxide dismutase in lung fibroblasts. *Am. J. Respir. Cell Mol. Biol.***39:**243-251; 2008.

[33] Stralin, P.; Marklund, S. L. Multiple cytokines regulate the expression of extracellular superoxide dismutase in human vascular smooth muscle cells. *Atherosclerosis***151:**433-441; 2000.

[34] Brady, T. C.; Chang, L. Y.; Day, B. J.; Crapo, J. D. Extracellular superoxide dismutase is upregulated with inducible nitric oxide synthase after NF-kappa B

activation. *Am. J. Physiol.***273:**L1002-6; 1997.

[35] Ookawara, T.; Matsuura, N.; Oh-ishi, T.; Okazaki, M.; Kizaki, T.; Suzuki, K.; Hitomi, Y.; Suzuki, K.; Ohno, H. Serum extracellular superoxide dismutase in pediatric patients with various diseases as judged by an ELISA. *Res. Commun. Mol. Pathol. Pharmacol.***107:**291-296; 2000.

[36] Stralin, P.; Marklund, S. L. Effects of oxidative stress on expression of extracellular superoxide dismutase, CuZn-superoxide dismutase and mn-superoxide dismutase in human dermal fibroblasts. *Biochem. J.***298 (Pt 2):**347-352; 1994.

[37] Davis, C. D.; Milne, D. B.; Nielsen, F. H. Changes in dietary zinc and copper affect zinc-status indicators of postmenopausal women, notably, extracellular superoxide dismutase and amyloid precursor proteins. *Am. J. Clin. Nutr.***71:**781-788; 2000.

[38] Olin, K. L.; Golub, M. S.; Gershwin, M. E.; Hendrickx, A. G.; Lonnerdal, B.; Keen, C. L. Extracellular superoxide dismutase activity is affected by dietary zinc intake in nonhuman primate and rodent models. *Am. J. Clin. Nutr.***61:**1263-1267; 1995.

[39] Fukai, T.; Siegfried, M. R.; Ushio-Fukai, M.; Griendling, K. K.; Harrison, D. G. Modulation of extracellular superoxide dismutase expression by angiotensin II and hypertension. *Circ. Res.***85:**23-28; 1999.

[40] Fukai, T.; Siegfried, M. R.; Ushio-Fukai, M.; Cheng, Y.; Kojda, G.; Harrison, D. G. Regulation of the vascular extracellular superoxide dismutase by nitric oxide and exercise training. *J. Clin. Invest.***105:**1631-1639; 2000.

[41] Gongora, M. C.; Qin, Z.; Laude, K.; Kim, H. W.; McCann, L.; Folz, J. R.; Dikalov, S.; Fukai, T.; Harrison, D. G. Role of extracellular superoxide dismutase in hypertension. *Hypertension***48:**473-481; 2006.

[42] Jeney, V.; Itoh, S.; Wendt, M.; Gradek, Q.; Ushio-Fukai, M.; Harrison, D. G.; Fukai, T. Role of antioxidant-1 in extracellular superoxide dismutase function and expression. *Circ. Res.***96:**723-729; 2005.

[43] Qin, Z.; Itoh, S.; Jeney, V.; Ushio-Fukai, M.; Fukai, T. Essential role for the menkes ATPase in activation of extracellular superoxide dismutase: Implication for vascular oxidative stress. *FASEB J.***20:**334-336; 2006.

[44] Stralin, P.; Jacobsson, H.; Marklund, S. L. Oxidative stress, NO* and smooth muscle cell extracellular superoxide dismutase expression. *Biochim. Biophys. Acta***1619:**1-8; 2003.

[45] Adachi, T.; Yamada, H.; Yamada, Y.; Morihara, N.; Yamazaki, N.; Murakami, T.; Futenma, A.; Kato, K.; Hirano, K. Substitution of glycine for arginine-213 in extracellular-superoxide dismutase impairs affinity for heparin and endothelial cell surface. *Biochem. J.***313 (Pt 1):**235-239; 1996.

[46] Adachi, T.; Morihara, N.; Yamazaki, N.; Yamada, H.; Futenma, A.; Kato, K.; Hirano, K. An arginine-213 to glycine mutation in human extracellular-superoxide dismutase reduces susceptibility to trypsin-like proteinases. *J. Biochem.***120:**184-188; 1996.

[47] Yamada, H.; Yamada, Y.; Adachi, T.; Fukatsu, A.; Sakuma, M.; Futenma, A.; Kakumu, S. Protective role of extracellular superoxide dismutase in hemodialysis patients. *Nephron***84:**218-223; 2000.

[48] Juul, K.; Tybjaerg-Hansen, A.; Marklund, S.; Heegaard, N. H.; Steffensen, R.; Sillesen, H.; Jensen, G.; Nordestgaard, B. G. Genetically reduced antioxidative protection and increased ischemic heart disease risk: The copenhagen city heart study. *Circulation***109:**59-65; 2004.

[49] Dahl, M.; Bowler, R. P.; Juul, K.; Crapo, J. D.; Levy, S.; Nordestgaard, B. G. Superoxide dismutase 3 polymorphism associated with reduced lung function in two large populations. *Am. J. Respir. Crit. Care Med.***178:**906-912; 2008.

[50] Arcaroli, J. J.; Hokanson, J. E.; Abraham, E.; Geraci, M.; Murphy, J. R.; Bowler, R. P.; Dinarello, C. A.; Silveira, L.; Sankoff, J.; Heyland, D.; Wischmeyer, P.; Crapo, J. D. Extracellular superoxide dismutase haplotypes are associated with acute lung injury and mortality. *Am. J. Respir. Crit. Care Med.***179:**105-112; 2009.

[51] Yamada, H.; Yamada, Y.; Adachi, T.; Goto, H.; Ogasawara, N.; Futenma, A.; Kitano, M.; Miyai, H.; Fukatsu, A.; Hirano, K.; Kakumu, S. Polymorphism of extracellular superoxide dismutase (EC-SOD) gene: Relation to the mutation responsible for high EC-SOD level in serum. *Jpn. J. Hum. Genet.***42:**353-356; 1997.

[52] Tamai, M.; Furuta, H.; Kawashima, H.; Doi, A.; Hamanishi, T.; Shimomura, H.; Sakagashira, S.; Nishi, M.; Sasaki, H.; Sanke, T.; Nanjo, K. Extracellular superoxide dismutase gene polymorphism is associated with insulin resistance and the susceptibility to type 2 diabetes. *Diabetes Res. Clin. Pract.***71:**140-145; 2006.

[53] Rosta, K.; Molvarec, A.; Enzsoly, A.; Nagy, B.; Ronai, Z.; Fekete, A.; Sasvari-Szekely, M.; Rigo, J.,Jr; Ver, A. Association of extracellular superoxide dismutase (SOD3) Ala40Thr gene polymorphism with pre-eclampsia complicated by severe fetal growth restriction. *Eur. J. Obstet. Gynecol. Reprod. Biol.***142:**134-138; 2009.

[54] Pierce, A.; Whitlark, J.; Dory, L. Extracellular superoxide dismutase polymorphism in mice. *Arterioscler. Thromb. Vasc. Biol.***23:**1820-1825; 2003.

[55] Warshamana, G. S.; Pociask, D. A.; Sime, P.; Schwartz, D. A.; Brody, A. R. Susceptibility to asbestos-induced and transforming growth factor-beta1-induced fibroproliferative lung disease in two strains of mice. *Am. J. Respir. Cell Mol.*

*Biol.***27:**705-713; 2002.

[56] Fujii, M.; Hara, H.; Meng, W.; Vonsattel, J. P.; Huang, Z.; Moskowitz, M. A. Strain-related differences in susceptibility to transient forebrain ischemia in SV-129 and C57black/6 mice. *Stroke***28:**1805-10; discussion 1811; 1997.

[57] Paigen, B.; Ishida, B. Y.; Verstuyft, J.; Winters, R. B.; Albee, D. Atherosclerosis susceptibility differences among progenitors of recombinant inbred strains of mice. *Arteriosclerosis***10:**316-323; 1990.

[58] Ward, N. L.; Moore, E.; Noon, K.; Spassil, N.; Keenan, E.; Ivanco, T. L.; LaManna, J. C. Cerebral angiogenic factors, angiogenesis, and physiological response to chronic hypoxia differ among four commonly used mouse strains. *J. Appl. Physiol.***102:**1927-1935; 2007.

[59] Prass, K.; Wiegand, F.; Schumann, P.; Ahrens, M.; Kapinya, K.; Harms, C.; Liao, W.; Trendelenburg, G.; Gertz, K.; Moskowitz, M. A.; Knapp, F.; Victorov, I. V.; Megow, D.; Dirnagl, U. Hyperbaric oxygenation induced tolerance against focal cerebral ischemia in mice is strain dependent. *Brain Res.***871:**146-150; 2000.

[60] Ganguly, K.; Schulz, H. Association studies of lung function in mice. *Dtsch. Tierarztl. Wochenschr.***115:**276-284; 2008.

[61] Qin, Z.; Reszka, K. J.; Fukai, T.; Weintraub, N. L. Extracellular superoxide dismutase (ecSOD) in vascular biology: An update on exogenous gene transfer and endogenous regulators of ecSOD. *Transl. Res.***151:**68-78; 2008.

[62] Yasui, K.; Baba, A. Therapeutic potential of superoxide dismutase (SOD) for resolution of inflammation. *Inflamm. Res.***55:**359-363; 2006.

[63] Salvemini, D.; Cuzzocrea, S. Therapeutic potential of superoxide dismutase mimetics as therapeutic agents in critical care medicine. *Crit. Care Med.***31:**S29-38; 2003.

[64] Oury, T. D.; Day, B. J.; Crapo, J. D. Extracellular superoxide dismutase in vessels and airways of humans and baboons. *Free Radic. Biol. Med.***20:**957-965; 1996.

[65] Fattman, C. L.; Schaefer, L. M.; Oury, T. D. Extracellular superoxide dismutase in biology and medicine. *Free Radic. Biol. Med.***35:**236-256; 2003.

[66] Landmesser, U.; Merten, R.; Spiekermann, S.; Buttner, K.; Drexler, H.; Hornig, B. Vascular extracellular superoxide dismutase activity in patients with coronary artery disease: Relation to endothelium-dependent vasodilation. *Circulation***101:**2264-2270; 2000.

[67] Takatsu, H.; Tasaki, H.; Kim, H. N.; Ueda, S.; Tsutsui, M.; Yamashita, K.; Toyokawa, T.; Morimoto, Y.; Nakashima, Y.; Adachi, T. Overexpression of EC-SOD suppresses endothelial-cell-mediated LDL oxidation. *Biochem. Biophys. Res. Commun.***285:**84-91; 2001.

[68] Lund, D. D.; Chu, Y.; Miller, J. D.; Heistad, D. D. Protective effect of extracellular superoxide dismutase on endothelial function during aging. *Am. J. Physiol. Heart Circ. Physiol.* 2009.

[69] Brown, K. A.; Chu, Y.; Lund, D. D.; Heistad, D. D.; Faraci, F. M. Gene transfer of extracellular superoxide dismutase protects against vascular dysfunction with aging. *Am. J. Physiol. Heart Circ. Physiol.***290:**H2600-5; 2006.

[70] Griendling, K. K.; Ushio-Fukai, M. Reactive oxygen species as mediators of angiotensin II signaling. *Regul. Pept.***91:**21-27; 2000.

[71] Laursen, J. B.; Rajagopalan, S.; Galis, Z.; Tarpey, M.; Freeman, B. A.; Harrison, D. G. Role of superoxide in angiotensin II-induced but not catecholamine-induced hypertension. *Circulation***95:**588-593; 1997.

[72] Chu, Y.; Iida, S.; Lund, D. D.; Weiss, R. M.; DiBona, G. F.; Watanabe, Y.; Faraci, F. M.; Heistad, D. D. Gene transfer of extracellular superoxide dismutase reduces arterial pressure in spontaneously hypertensive rats: Role of heparin-binding domain. *Circ. Res.***92:**461-468; 2003.

[73] Sjoquist, P. O.; Carlsson, L.; Jonason, G.; Marklund, S. L.; Abrahamsson, T. Cardioprotective effects of recombinant human extracellular-superoxide dismutase type C in rat isolated heart subjected to ischemia and reperfusion. *J. Cardiovasc. Pharmacol.***17:**678-683; 1991.

[74] Sjoquist, P. O.; Marklund, S. L. Endothelium bound extracellular superoxide dismutase type C reduces damage in reperfused ischaemic rat hearts. *Cardiovasc. Res.***26:**347-350; 1992.

[75] Chen, E. P.; Bittner, H. B.; Davis, R. D.; Folz, R. J.; Van Trigt, P. Extracellular superoxide dismutase transgene overexpression preserves postischemic myocardial function in isolated murine hearts. *Circulation***94:**II412-7; 1996.

[76] Li, Q.; Bolli, R.; Qiu, Y.; Tang, X. L.; Murphree, S. S.; French, B. A. Gene therapy with extracellular superoxide dismutase attenuates myocardial stunning in conscious rabbits. *Circulation***98:**1438-1448; 1998.

[77] Li, Q.; Bolli, R.; Qiu, Y.; Tang, X. L.; Guo, Y.; French, B. A. Gene therapy with extracellular superoxide dismutase protects conscious rabbits against myocardial infarction. *Circulation***103:**1893-1898; 2001.

[78] Nilsson, U. A.; Haraldsson, G.; Bratell, S.; Sorensen, V.; Akerlund, S.; Pettersson, S.; Schersten, T.; Jonsson, O. ESR-measurement of oxygen radicals in vivo after renal ischaemia in the rabbit. effects of pre-treatment with superoxide dismutase and heparin. *Acta Physiol. Scand.***147:**263-270; 1993.

[79] Erlansson, M.; Bergqvist, D.; Marklund, S. L.; Persson, N. H.; Svensjo, E. Superoxide dismutase as an inhibitor of postischemic microvascular permeability increase in the hamster. *Free Radic. Biol. Med.***9:**59-65; 1990.

[80] Kamp, D. W.; Weitzman, S. A. Asbestosis: Clinical spectrum and pathogenic mechanisms. *Proc. Soc. Exp. Biol. Med.***214:**12-26; 1997.

[81] Kinnula, V. L.; Fattman, C. L.; Tan, R. J.; Oury, T. D. Oxidative stress in pulmonary fibrosis: A possible role for redox modulatory therapy. *Am. J. Respir. Crit. Care Med.***172:**417-422; 2005.

[82] Mossman, B. T.; Marsh, J. P.; Sesko, A.; Hill, S.; Shatos, M. A.; Doherty, J.; Petruska, J.; Adler, K. B.; Hemenway, D.; Mickey, R. Inhibition of lung injury, inflammation, and interstitial pulmonary fibrosis by polyethylene glycol-conjugated catalase in a rapid inhalation model of asbestosis. *Am. Rev. Respir. Dis.***141:**1266-1271; 1990.

[83] Mossman, B. T.; Surinrut, P.; Brinton, B. T.; Marsh, J. P.; Heintz, N. H.; Lindau-Shepard, B.; Shaffer, J. B. Transfection of a manganese-containing superoxide dismutase gene into hamster tracheal epithelial cells ameliorates asbestos-mediated cytotoxicity. *Free Radic. Biol. Med.***21:**125-131; 1996.

[84] Panduri, V.; Weitzman, S. A.; Chandel, N.; Kamp, D. W. The mitochondria-regulated death pathway mediates asbestos-induced alveolar epithelial cell apoptosis. *Am. J. Respir. Cell Mol. Biol.***28:**241-248; 2003.

[85] Tan, R. J.; Fattman, C. L.; Watkins, S. C.; Oury, T. D. Redistribution of pulmonary EC-SOD after exposure to asbestos. *J. Appl. Physiol.***97:**2006-2013; 2004.

[86] Fattman, C. L.; Tan, R. J.; Tobolewski, J. M.; Oury, T. D. Increased sensitivity to asbestos-induced lung injury in mice lacking extracellular superoxide dismutase. *Free Radic. Biol. Med.***40:**601-607; 2006.

[87] Gao, F.; Koenitzer, J. R.; Tobolewski, J. M.; Jiang, D.; Liang, J.; Noble, P. W.; Oury, T. D. Extracellular superoxide dismutase inhibits inflammation by preventing oxidative fragmentation of hyaluronan. *J. Biol. Chem.***283:**6058-6066; 2008.

[88] Guzik, T. J.; Korbut, R.; Adamek-Guzik, T. Nitric oxide and superoxide in inflammation and immune regulation. *J. Physiol. Pharmacol.***54:**469-487; 2003.

[89] Fialkow, L.; Wang, Y.; Downey, G. P. Reactive oxygen and nitrogen species as signaling molecules regulating neutrophil function. *Free Radic. Biol. Med.***42:**153-164; 2007.

[90] Bortolussi, R.; Vandenbroucke-Grauls, C. M.; van Asbeck, B. S.; Verhoef, J. Relationship of bacterial growth phase to killing of listeria monocytogenes by oxidative agents generated by neutrophils and enzyme systems. *Infect. Immun.***55:**3197-3203; 1987.

[91] Peck, R. Gamma interferon induces monocyte killing of listeria monocytogenes by an oxygen-dependent pathway; alpha- or beta-interferons by oxygen-independent pathways. *J. Leukoc. Biol.***46:**434-440; 1989.

[92] Mirochnitchenko, O.; Inouye, M. Effect of overexpression of human cu,zn superoxide dismutase in transgenic mice on macrophage functions. *J. Immunol.***156:**1578-1586; 1996.

[93] Bowler, R. P.; Nicks, M.; Tran, K.; Tanner, G.; Chang, L. Y.; Young, S. K.; Worthen, G. S. Extracellular superoxide dismutase attenuates lipopolysaccharide-induced neutrophilic inflammation. *Am. J. Respir. Cell Mol. Biol.***31:**432-439; 2004.

[94] Ueda, J.; Starr, M. E.; Takahashi, H.; Du, J.; Chang, L. Y.; Crapo, J. D.; Evers, B. M.; Saito, H. Decreased pulmonary extracellular superoxide dismutase during systemic inflammation. *Free Radic. Biol. Med.***45:**897-904; 2008.

[95] Suliman, H. B.; Ryan, L. K.; Bishop, L.; Folz, R. J. Prevention of influenza-induced lung injury in mice overexpressing extracellular superoxide dismutase. *Am. J. Physiol. Lung Cell. Mol. Physiol.***280:**L69-78; 2001.

[96] Delanty, N.; Dichter, M. A. Oxidative injury in the nervous system. *Acta Neurol. Scand.***98:**145-153; 1998.

[97] Levin, E. D.; Brady, T. C.; Hochrein, E. C.; Oury, T. D.; Jonsson, L. M.; Marklund, S. L.; Crapo, J. D. Molecular manipulations of extracellular superoxide dismutase: Functional importance for learning. *Behav. Genet.***28:**381-390; 1998.

[98] Levin, E. D.; Christopher, N. C.; Lateef, S.; Elamir, B. M.; Patel, M.; Liang, L. P.; Crapo, J. D. Extracellular superoxide dismutase overexpression protects against aging-induced cognitive impairment in mice. *Behav. Genet.***32:**119-125; 2002.

[99] Levin, E. D. Extracellular superoxide dismutase (EC-SOD) quenches free radicals and attenuates age-related cognitive decline: Opportunities for novel drug development in aging. *Curr. Alzheimer Res.***2:**191-196; 2005.

[100] Thiels, E.; Urban, N. N.; Gonzalez-Burgos, G. R.; Kanterewicz, B. I.; Barrionuevo, G.; Chu, C. T.; Oury, T. D.; Klann, E. Impairment of long-term potentiation and associative memory in mice that overexpress extracellular superoxide dismutase. *J.*

*Neurosci.***20:**7631-7639; 2000.

[101] Levin, E. D.; Brucato, F. H.; Crapo, J. D. Molecular overexpression of extracellular superoxide dismutase increases the dependency of learning and memory performance on motivational state. *Behav. Genet.***30:**95-100; 2000.

[102] Paulus, M. P.; Dulawa, S. C.; Ralph, R. J.; Mark, A. G. Behavioral organization is independent of locomotor activity in 129 and C57 mouse strains. *Brain Res.***835:**27-36; 1999.

[103] Kalueff, A. V.; Tuohimaa, P. Contrasting grooming phenotypes in C57Bl/6 and 129S1/SvImJ mice. *Brain Res.***1028:**75-82; 2004.

[104] Jun, S.; Pierce, A.; Dory, L. Extracellular superoxide dismutase polymorphism in mice: Allele-specific effects on phenotype. *Free Radic. Biol. Med.***48:**590-596; 2010.

[105] Mirossay, A.; Jun, S.; Dory, L. Cloning and characterization of two alleles of the murine extracellular superoxide dismutase gene. *Biochem. Biophys. Res. Commun.***352:**739-743; 2007.

CHAPTER II

EXTRACELLULAR SUPEROXIDE DISMUTASE POLYMORPHISM IN MICE: ALLELE-SPECIFIC EFFECTS ON TISSUE PHENOTYPE

ABSTRACT

Extracellular superoxide dismutase (ecSOD) protects the extracellular matrix (ECM) from oxidative stress. We previously reported a new allele for ecSOD, expressed in 129P3/J mice (129), which differs from the wild-type (wt), expressed in C57BL/6J and other strains, by two amino acid substitutions and a 10 bp deletion in the 3' UTR of the mRNA [1]. The newly discovered allele is associated with a phenotype of significantly increased circulating and heparin-releasable enzyme activities and levels. In order to examine the properties of the two forms of ecSOD in an identical environment, we generated, by extensive backcrossing of ecSOD heterozygous progeny to C57BL/6J females, a congenic C57 strain with the 129 (or wt) allele of ecSOD. These mice are homozygous for nearly 5,000 SNPs across all chromosomes, as determined by Affymetrix Parallele Mouse 5K SNP panel. The present study describes the generation of the congenic mice (genetically >99.8 % identical) and their ecSOD phenotype. The congenic mice plasma ecSOD activities before and after heparin administration recapitulate the differences reported in the founder mice. Tissue enzyme distribution is similar in both congenic groups, although the 129 allele is associated with higher levels of enzyme expression despite lower levels of enzyme mRNA. In these characteristics the phenotype is also allele driven, with little impact by the rest of the genome. The congenic mice carrying the 129 allele have mRNA levels that are in between those found in the founder 129P3/J and C57BL/6J strains. We

conclude that the ecSOD phenotype in most aspects of enzyme expression is allele- driven, with the exception of tissue mRNA levels, where a significant contribution by the surrounding (host) genome is observed. These results also suggest potential allele-specific differences in the regulation of ecSOD synthesis and intracellular processing/secretion of ecSOD, independent of the genotype context. Most importantly, the congenic mice offer an excellent model to examine the regulatory mechanisms of ecSOD expression and the role of ecSOD in various diseases involving oxidative stress.

INTRODUCTION

Extracellular superoxide dismutase (ecSOD, also referred to as SOD3) is the only antioxidant enzyme in the extracellular compartment [including the extracellular matrix (ECM), endothelial cell surface and tissue fluids] that provides protection against superoxide and regulates the bioavailability of nitric oxide [2-4]. This is accomplished through the conversion of superoxide to hydrogen peroxide and diminished formation of peroxinitrite from nitric oxide. While hydrogen peroxide is also an oxidant, it also can serve as a signaling molecule and potentiate endothelium- dependent relaxation [5-7]. The physiological importance of this enzyme is illustrated by problems in mice lacking this enzyme: their increased sensitivity to lung injury, increased endothelial dysfunction and impaired neovascularization [8-10]. Over-expression of the human form of the enzyme on the other hand protects mice from global cerebral ischemia [11], preserves post-ischemic myocardial function [12], reduces lung injury during inflammation [13] and reduces aging-induced cognitive impairment [14]. More recent studies indicate that the protective effect of ecSOD on the oxidative fragmentation of the ECM components [15-17] is a key factor in controlling the inflammatory response in lung injury.

In mice, like humans, ecSOD is a glycosylated homotetramer localized mainly in the ECM and on cell surfaces, anchored to heparan sulfate proteoglycans and type I collagen through an interaction of a heparin binding domain (HBD) containing 6 positively charged amino acids in the C-terminal region of each monomer [18-20]. The C-terminal region can be proteolytically cleaved and, depending on the extent of monomer processing, ecSOD can be present in three types: type A, lacking heparin affinity (all monomers in the tetramer are devoid of the HBD); B, with intermediate affinity (some monomers are cleaved); and C, with strong affinity (all monomers in the tetramer are intact) [21]. Thus type A is normally found circulating in plasma,

and types B and C are mostly tissue bound. Over 90% of the total body ecSOD is thus estimated to be associated with tissue extracellular matrix, including vascular tissue and, to a lesser extent, endothelial cell surface [22-24].

We previously observed that the 129 inbred strain of mice expresses a variant of the ecSOD mRNA, which includes the A61G and G556T point mutations and a 10bp deletion in the 3'UTR of the transcript [1]. Other strains tested thus far (C57BL/6J, C3H and Swiss-Webster) carry the "wild-type" (*wt*) allele [1]. The *129* allele is associated with a very different ecSOD phenotype; these mice have significantly higher activity and amount of circulating and heparin-releasable ecSOD, when compared to C57BL/6J mice. Co-incidentally, the 129 and C57 mice differ significantly in their response to proliferative lung disease, brain ischemia, vascular remodeling, susceptibility to atherosclerosis [25-28], as well as development of tolerance against global and focal cerebral ischemia [29] by hyperbaric oxygen treatment. None of these studies identified specific gene(s) that may account for the observed differences in the response of these strains.

When we reported on the different ecSOD phenotype between these two strains [1], we were unable to ascertain the magnitude of the contribution to these differences by the ecSOD allele itself and the effects of the surrounding milieu. In order to examine the contribution of the genetic environment vs. the ecSOD allele to the observed ecSOD phenotype, we bred congenic mice (**C57.129-*sod3***) that carry either of the ecSOD alleles in an otherwise identical C57BL/6J background. Our results clearly demonstrate that the ecSOD phenotype is largely due to the allele-specific effects independent of other strain-specific factors. Our results also suggest significant allele-specific differences in the regulation of ecSOD synthesis and intracellular processing/secretion, independent of the genotype/strain context.

METHODS

Animals: C57BL/6J and 129P3/J mice were obtained from Jackson Laboratories (Bar Harbor, ME) and were maintained on normal chow and water. All experimental protocols were approved by the UNT HSC Institutional Animal Care and Use Committee.

Selection of microsatellite markers: The microsatellite polymorphism markers between the C57BL/6J and 129P3/J strains were selected from the Jackson mouse informatics database. Only markers with at least a 6 bp difference in the size of the amplicons were chosen and are listed in **Table 1**.

DNA isolation and genotyping: DNA was isolated from small amount of tail tissue incubated with 200µl of lysis buffer (Viagen) with proteinase K for 18hr at 56 ^{o}C. EcSOD genotyping was carried out as previously described [1], using primers spanning bp -33 to +94 (forward: 5'-GGGGACATTCCACAGGTGCAG–3', reverse: 5' –TGTCTGCTAGGTCGAAGCTGGAC–3') of the ecSOD gene. The amplicons were then digested with *Mbo*I (Promega) for 3 hr. at 37 ^{o}C. Undigested and digested amplicons were fractionated using 12% PAGE with ethidium bromide staining. For microsatellite genotyping, the primer sets listed in Table 1 were used and the resulting amplicons were separated using 12% or 15% PAGE.

Sample collection: For free (circulating) plasma ecSOD measurements blood was collected from anesthetized 6-8 wk old female mice into heparinized capillary tubes from the retro-orbital plexus. Blood was also collected 10 min after a tail vein injection of small M.W. heparin (100 U) to measure heparin-releasable ecSOD. Upon sacrifice, tissues were perfused with ice-cold PBS via cardiac puncture to remove residual blood. Tissues/organs were removed and

immediately snap-frozen in liquid nitrogen for subsequent analyses or were kept in RNAlater (Ambion) for RNA analyses.

Analyses: Frozen tissues were ground to a fine powder in liquid nitrogen, and homogenized with 50 mM potassium phosphate buffer containing 0.3 M KBr and 3 mM EDTA, pH 7.4 containing a 1:1000 dilution of a protease inhibitor cocktail (100 μM 4-(2-aminoethyl) benzensulfonyl fluoride, 10 μM leupeptin, 10 μM E-64, 1 μM bestatin, 15 nM aprotinin, 1.0 μM pepstatin-A). The protein concentration of tissue homogenate was determined by Lowry assay [30]. RNA isolation was carried out by TRIreagent® (Molecular Research Center) extraction of tissues stored in RNAlater® (Ambion) and concentrations measured by a ND-1000 spectrophotometer (NanoDrop).

Plasma and tissue ecSOD activities: ecSOD was partially purified using ConA Sepharose (Sigma) as described [31], using 100 μl of plasma or 2-6 mg of tissue homogenate protein. The columns (0.5x10 mm) were washed with 50mM Na-HEPES (pH 7.0) and 0.25 M NaCl, and ecSOD was eluted with a washing buffer containing 0.5 M α-methyl mannoside (Sigma), pH 6.0. ConA-Sepaharose efficiency and binding capacity were monitored by Western blotting of the wash.

The activity of ecSOD (released from ConA) was determined using a system based on the oxidation of NAD(P)H [32]. Briefly, 23.5μl of sample was combined with 187μl of 100 mM triethanolamine/diethanolamine-HCl buffer pH 7.4, 6μl of 100mM EDTA/50mM $MnCl_2$ solution, and 10μl 7.5 mM NAD(P)H. The reaction was started with the addition of 23.5μl of 10 mM ß-mercaptoethanol. Samples were tested for NAD(P)H oxidase activity before the addition of ß-mercaptoethanol. Dismutase activity was estimated from a standard curve constructed by

measuring the activity of increasing and known amounts of Cu/Zn SOD (Sigma, cat. #S2515). Activities are therefore expressed as ng of Cu/Zn SOD equivalents.

Western blots: Rabbit anti-mouse ecSOD antiserum was produced against a synthetic mouse-specific 21-amino acid peptide corresponding to the N-terminus of the mature protein, as previously described [1]. Aliquots equivalent to 0.25µL of whole plasma or 10-100µg of tissue protein were dissolved and boiled in Laemmli buffer containing 5% β-mercaptoethanol [33] for 5 min, separated by 12% SDS-PAGE at 100 V for 3.5 hours and transferred to polyvinylidine fluoride membranes (Bio-Rad) for 2 hours. After blocking for 1 hour the membranes were incubated with the primary antibodies for ecSOD (1:20,000) and/or β-actin (1:5,000) rabbit anti-mouse antiserum (Sigma) overnight at 4 ˚C. Secondary antibodies (goat anti-rabbit IgG), conjugated to horseradish peroxidase (Jackson Immunoresearch) were added for 2 hours at RT (1:5,000 dilution). EcSOD and ß-actin bands were visualized by the ECL system (Amersham) using FluorChem® FC2 Imaging System (Alpha Innotech) and densitometric analysis was done using the software supplied (AlphaEaseFC) for the instrument. Transfer efficiency between runs was checked and corrected for by using aliquots of pooled mouse plasma in each of the outside lanes. Moreover, scans were also corrected for loading by detecting ß-actin in all tissue samples except blood.

Quantitative Real-Time PCR (qRT-PCR): cDNA was synthesized from 2µg of total RNA (Retro-Script kit, Ambion) using oligo-dT primers. One eighth (0.25µg) of this reaction mixture was used in the subsequent qRT-PCR reactions, using the following primers for ecSOD: forward, 5' –AGGACGACCTGGGTAAAGGT–3'; reverse: 5' –AGTGGTCTTGCACTCGCTCT–3' and

S15, (a ribosomal protein, as an internal standard): forward: 5' – CGGGCCGGCCGTGCTTCACG–3', reverse: 5' –TTCCGCAAGTTCACCTACC–3' on the Mastercycler realplex^2 (Eppendorf) using *Taq* ReadyMix^{TM} JumpStart^{TM} mix containing SYBR® Green (Sigma) to visualize the amplified product. For all reactions, the cycle threshold (Ct) values of ecSOD were normalized by the Ct of S15 (a ribosomal protein) as an internal standard by the following formula: $\Delta Ct = Ct_{ecSOD} - Ct_{S15}$. The ΔCt value of the *sod3*^{wt} liver was considered as the calibrator of ecSOD mRNA expression. Thus the abundance of each tissue ecSOD mRNA was expressed a fold change relative to *sod3*^{wt} liver by $2^{-\Delta\Delta Ct}$, where $\Delta\Delta Ct = \Delta Ct_{tissue} - \Delta Ct_{sod3wt\ liver}$.

Statistical Analyses: Results from the experiments are reported as means ± SEM. Statistical significance was determined using one- or two- way ANOVA (SPSS 14.0 for Windows and Prism). A p-value of <0.05 was considered statistically significant.

RESULTS

Generation of congenic (C57.129-*sod3*) mice on C57BL/6J background

In order to examine the phenotypic effects of the allelic differences in an otherwise essentially identical environment, we generated C57.129-*sod3* mice, expressing the wild-type (C57.129-$sod3^{wt}$) or the 129 allele for ecSOD (C57.129-$sod3^{129}$). Briefly, an F1 generation male of the C57BL/6J x 129P3/J cross (heterozygous for the ecSOD gene) was backcrossed to C57BL/6J female (N2). Heterozygous male progeny were backcrossed to C57BL/6J females for 10 generations. Each time the male litter was genotyped for ecSOD as well as for six additional microsatellite polymorphism markers (as shown in Table 1). Two of the markers are on chromosome 5, including one 13cM away from the ecSOD locus at 31cM. Heterozygous males with the most C57BL/6J - matching microsatellite markers were chosen for breeding with the C57 females. The extensive (10 generations) backcrossing and the use of strain-specific markers assures theoretically at least a 99.8% homozygosity of the congenic mice with the C57BL/6J strain (% homozygosity = $[1-(1/2)^{n-1}]$). By generation N5 all of the chosen markers in **Table 1**, including ones on Ch5, were homozygous with the C57BL/6J background. The homozygosity of the congenic mice with the C57BL/6J strain was also confirmed by analyzing nearly 5,000 SNPs across all chromosomes using the Affymetrics Parallele Mouse 5K SNP panel (courtesy of Dr. Aldons Lusis, UCLA).

Plasma ecSOD activities and protein levels in congenic mice

We previously reported large differences in the plasma pre- and post-heparin ecSOD activities between the two founder strains. The 129P3/J strain had significantly higher plasma ecSOD activity (as well as amounts), both before as well as after heparin administration [1], when

Chromosome	Locus (cM)	Marker	Primer	Primer sequence	Strain	Fragment size (bp)	Size difference
Chr 1	106.3	D1Mit362	D1Mit362	TGTGTGACTGCTTGGAAGATG CTGAGTCCCTAAAGTTGTCCTTG	129P3/J C57BL/6J	148 120	28
Chr 5	18	D5Mit388	D5Mit388	TTTCAGAGGGTGGGAGGTAA CCTGGACTCATGGAAGCATT	129P3/J C57BL/6J	183 192	11
Chr 5	1	D5Mit346	D5Mit346	TCAAACTCCTCTAATATGGAAGTGC CTGTCTCATTAATCCATGGATCC	129P3/J C57BL/6J	141 121	21
Chr 6	0.9	D6Rp2	TB6F TB6R	TCCTTATAAATCAGTTTCTTAG GCAATGGAGGTAGAAAACTG	129P3/J C57BL/6J	179 165	14
Chr 7	3.9	D7Msu1	pA pB	ATTCCAAAGTGTTCAATGCC ACTTCCCAGCTGATGTGACT	129P3/J C57BL/6J	175 185	10
Chr 11	20	D11Mit188	D11Mit188	CTATTTCCTCAGTGCTCGGC AGCATGTACCTTGAAAACCAGA	129P3/J C57BL/6J	122 128	6

Table 1. Selected microsatellite polymorphism markers between the C57Bl/6J and 129P3/J strains that were used for the selection of male heterozygous ecSOD progeny for subsequent backcrossing into C57 females.

compared to the C57BL/6J mice. As shown in **Figure 1**, these differences are recapitulated in the congenic mice as well. The *sod3*^{129} mice have higher activity and amount of ecSOD in the circulation, both before and after heparin administration, than the *sod3*^{wt} congenic mice. Moreover, these mice also have a significantly larger heparin-accessible pool of ecSOD. Based on these findings we conclude that the phenotypic differences in ecSOD expression in plasma are largely strain- independent and allele-specific.

Tissue distribution of ecSOD in congenic mice

Tissue distribution of ecSOD activity is shown in Figure 2, both before (A) and after (B) heparin administration. The highest enzyme activity was measured in the lung, followed by the heart and aorta. The liver, kidney and brain enzyme have the lowest activity. This observation can be misleading; although the activity of the enzyme in liver homogenates is low, because of its high protein content the total pool of the enzyme is equivalent to the lung pool (data not shown). With the exception of the brain and heart, in all tissues examined, the *sod3*^{129} mice have higher, or in the case of aorta and liver, significantly higher enzyme activity than the *sod3*^{wt} mice. Heparin administration does not significantly change the activity of ecSOD of the brain or lung in either group; a significant fraction of enzyme was lost from the liver, kidney (>50%) and heart (30%) of *sod3*^{129} mice, but not the *sod3*^{wt} mice, as shown in (B).

Tissue ecSOD levels were assessed by Western blotting and are shown in Figure 3, both before (A) and after (B) heparin administration with typical Western blots (C). The levels of enzyme, as determined by Western blotting closely parallel the activity data shown in Figure 2; with the exception of the brain, the *sod3*^{129} mice have higher, or in the case of liver, significantly higher enzyme levels than the *sod3*^{wt} mice. The effects of heparin on enzyme release are also

similar to those shown in Figure 2, except that the liver and kidney of both congenic groups loose a similar fraction of the ecSOD pool.

Data in **Figures 2 and 3** suggest that heparin administration has little effect on the brain and lung enzyme content (both, activity and level). Overall, only tissues from the *sod3*^{129} mice (heart, liver and kidney) release statistically significant amounts of enzyme. The greatest phenotypic difference in this respect is seen in the liver; heparin releases well over 50% of the enzyme activity and mass in the *sod3*^{129} mice, while the release from the livers of *sod3*^{wt} is much smaller, and statistically not significant. These data lead us to conclude that a significantly greater proportion of the liver, kidney and heart enzyme in the *sod3*^{129} mice resides on the endothelial interface, where it is accessible to heparin action. Surprisingly, heparin administration consistently leads to small increases in enzyme content (both activity and amount) of the aorta (the total of ascending, arch, descending and abdominal aorta).

ecSOD mRNA levels in tissues of congenic mice

We next examined the abundance of ecSOD mRNA in the selected tissues. In **Figure 4** we compare ecSOD mRNA abundance in *sod3*^{wt} (equivalent to the founder C57BL/6J mice) to that of *sod3*^{129} mice as well as the founder 129P3/J mice. In agreement with published data [34], ecSOD mRNA abundance is highest in the kidney, lung and aorta, and lower in the brain, heart and liver, regardless of the strain. With the exception of the liver, tissues of the *sod3*^{129} mice, much like the founder 129P3/J mice, have consistently lower levels of ecSOD mRNA, statistically significantly so in the brain, lung and kidney, even though enzyme expression levels are similar or higher. The highest discrepancy is observed in the brain: the levels of ecSOD mRNA driven by the *129* allele in this organ range from 45-50% of those driven by the *wt* allele,

and yet ecSOD expression is similar. Although the mRNA levels of the *sod3*^{129} mice trend with those of the 129P3/J founder strain, they are generally higher. Overall, our mRNA data therefore suggest that the ecSOD mRNA abundance phenotype may be determined partially by the strain (the C57BL/6J genome) and partially be allele-specific.

Figure 1. Plasma ecSOD expression in congenic mice before and after heparin administration.

Plasma ecSOD activities (A) and protein levels (B) were measured in aliquots of plasma, as described in Materials and Methods. A typical Western blot is shown in C. C57.129-*sod3*^{wt} (black bars) mice are compared to the C57.129-*sod3*^{129} (grey bars) congenic mice before (-) and after (+) heparin administration. (A) Activities were measured following partial purification by ConA-Sepharose affinity chromatography and are expressed as ng of Cu/Zn SOD equivalents/mL of plasma; (B) ecSOD protein levels were assessed by Western blotting of a 20μL of diluted plasma (equivalent to 0.25 μL of whole plasma), resolved by 12% SDS-PAGE; (C) a typical blot of plasma ecSOD from 2 mice in each of the experimental groups. The single band in the plasma sample represents the HBD-cleaved form of ecSOD; an additional band of higher molecular weight, representing the uncleaved monomers, appears after heparin administration. The efficiency of transfer was monitored by standard pooled plasma aliquots applied to both outside lanes. Results in (A) and (B) represent means ± SEM of 5 animals per group. All comparisons were done with two-way ANOVA. The heparin releasable pool of ecSOD activity or amount are significantly greater ($p<0.044$ and $p<0.001$, respectively) in the C57.129-*sod3*^{129} mice.

A

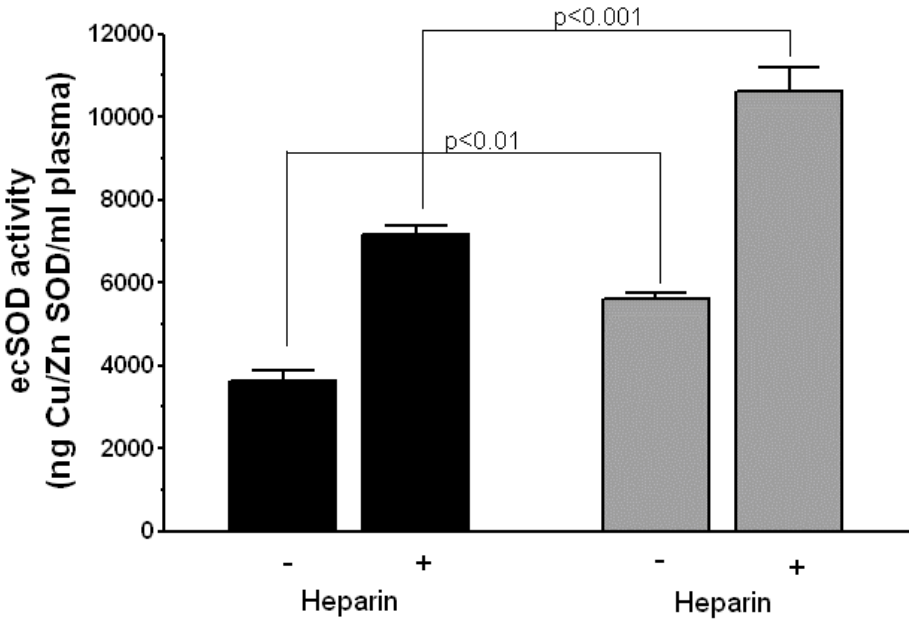
p<0.001
p<0.01
12000
10000
8000
6000
4000
2000
0
ecSOD activity
(ng Cu/Zn SOD/ml plasma)
-
+
-
+
Heparin
Heparin

B

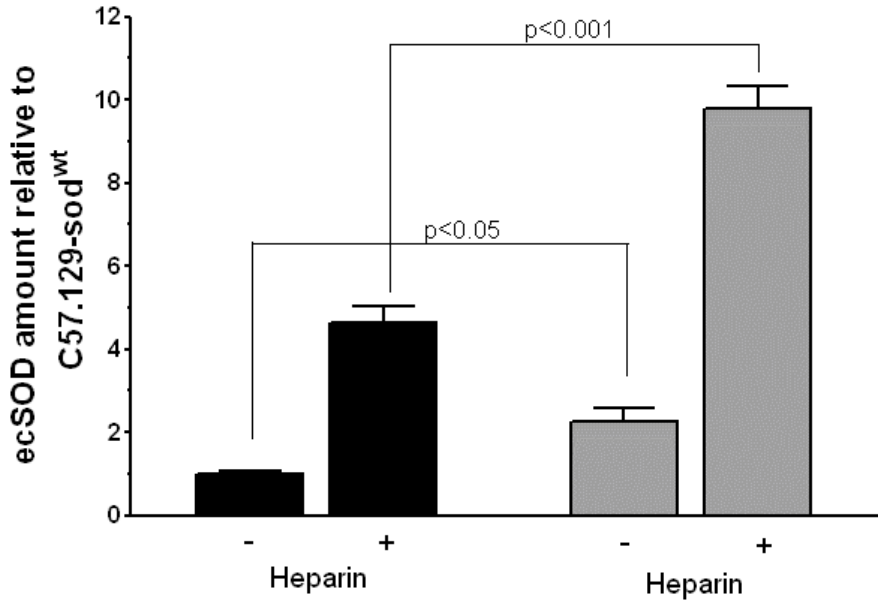
p<0.001
p<0.05
12
10
8
6
4
2
0
ecSOD amount relative to
C57.129-sod^wt
-
+
-
+
Heparin
Heparin

C


sod^wt
sod^129
Heparin
-
+
-
+

Figure 2. **ecSOD activity in selected tissues of congenic mice before and after heparin administration.**

Enzyme activities were determined before (A) and after (B) heparin administration in C57.129-*sod3*^{wt} (black bars) and C57.129-*sod3*^{129} (grey bars) mice. For activity assays, equal amounts of homogenate protein were loaded to ConA columns and eluted, as described in Materials and Methods. Results represent a mean ± SEM of 5 mice/group.

* indicates a significant difference (at $p<0.05$) from C57.129-*sod3*^{wt} mice (black bars).

# indicates a significant difference (at $p<0.05$) from pre-heparin values.

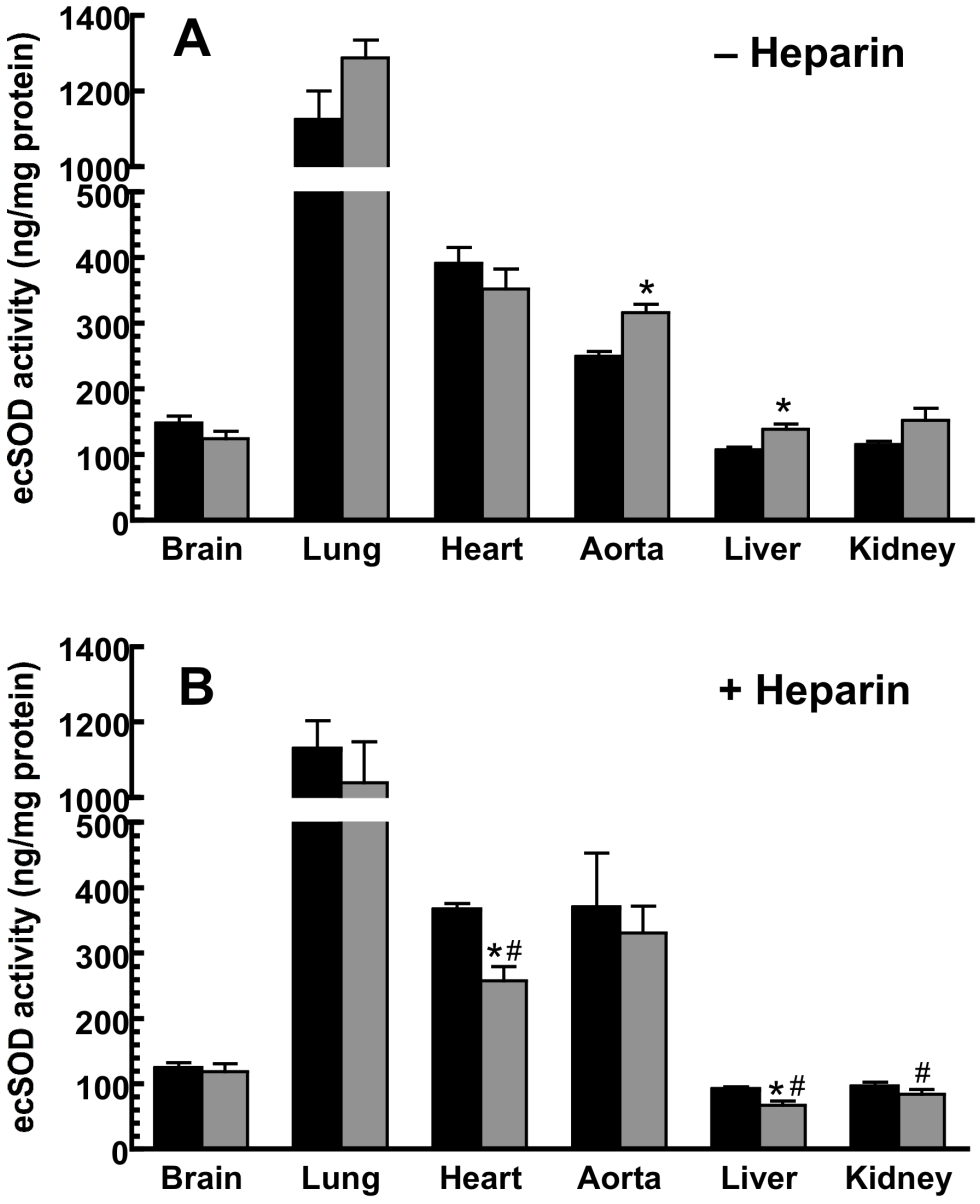
A
– Heparin
ecSOD activity (ng/mg protein)
1400
1200
1000
500
400
300
200
100
0
*
*
Brain
Lung
Heart
Aorta
Liver
Kidney
B
+ Heparin
ecSOD activity (ng/mg protein)
1400
1200
1000
500
400
300
200
100
0
*#
*#
#
Brain
Lung
Heart
Aorta
Liver
Kidney

Figure 3. **ecSOD protein levels in selected tissues of congenic mice before and after heparin administration.**

Enzyme levels were determined by Western blotting before (A) and after (B) heparin administration in C57.129-*sod3*^{wt} (black bars) and C57.129-*sod3*^{129} (grey bars) mice. Also shown are typical blots of tissue ecSOD in each of the experimental groups (C). Tissue homogenate proteins (10 – 100µg) were resolved by 12% SDS-PAGE and transferred to PVDF membranes and scans quantified, as described in the Materials and Methods. Protein loading within each tissue/organ was corrected by ß-actin loading. Transfer efficiency was also monitored by using a sample of pooled standard plasma on both sides of each gel. Results represent a mean ± SEM of 5 mice/group.

* indicates a significant difference (at $p<0.05$) from C57.129-*sod3*^{wt} mice (black bars).

# indicates a significant difference (at $p<0.05$) from pre-heparin values.

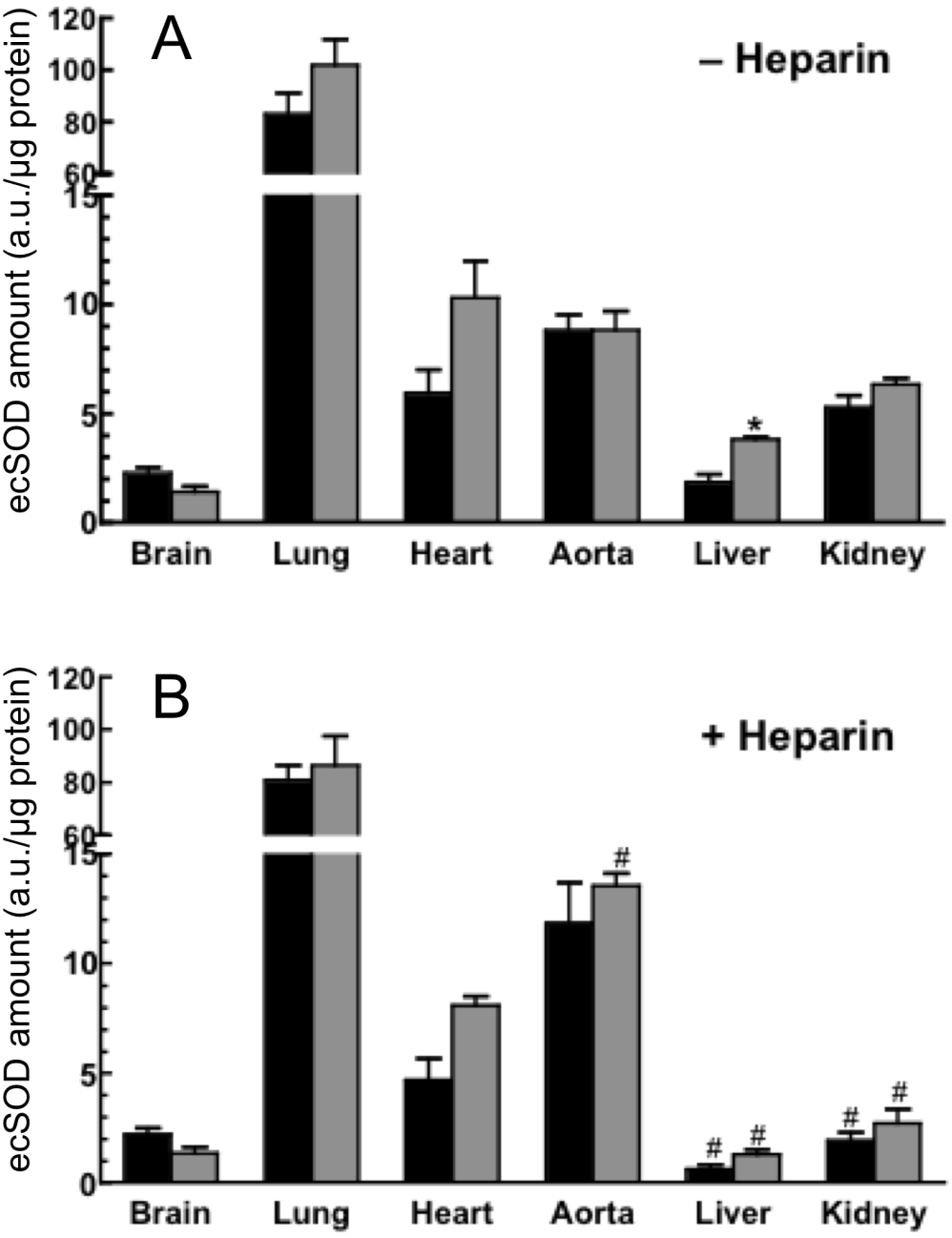
A
– Heparin
ecSOD amount (a.u./µg protein)
120
100
80
60
15
10
5
0
*
Brain
Lung
Heart
Aorta
Liver
Kidney
B
+ Heparin
ecSOD amount (a.u./µg protein)
120
100
80
60
15
10
5
0
#
#
#
#
#
Brain
Lung
Heart
Aorta
Liver
Kidney

C

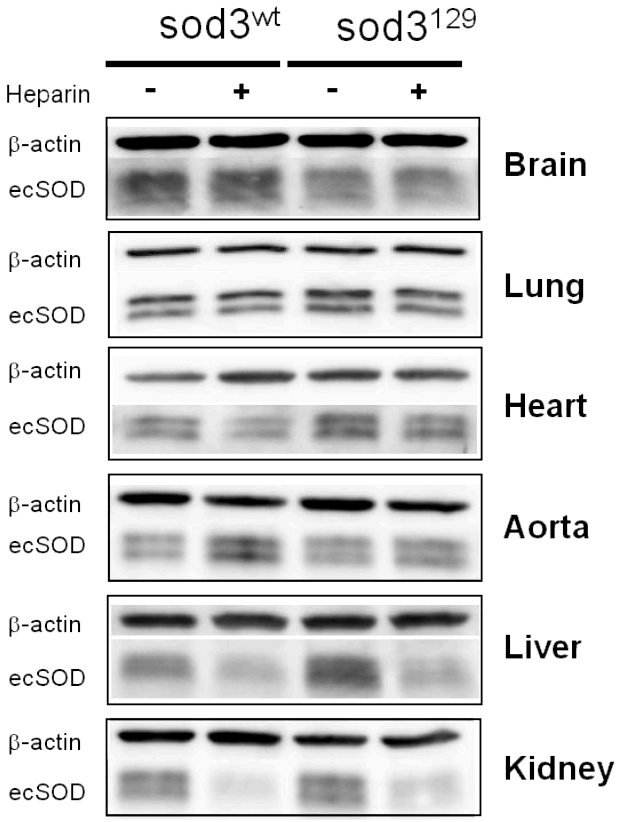
sod3wt
sod3129
Heparin
-
+
-
+
β-actin
ecSOD
Brain
Lung
Heart
Aorta
Liver
Kidney

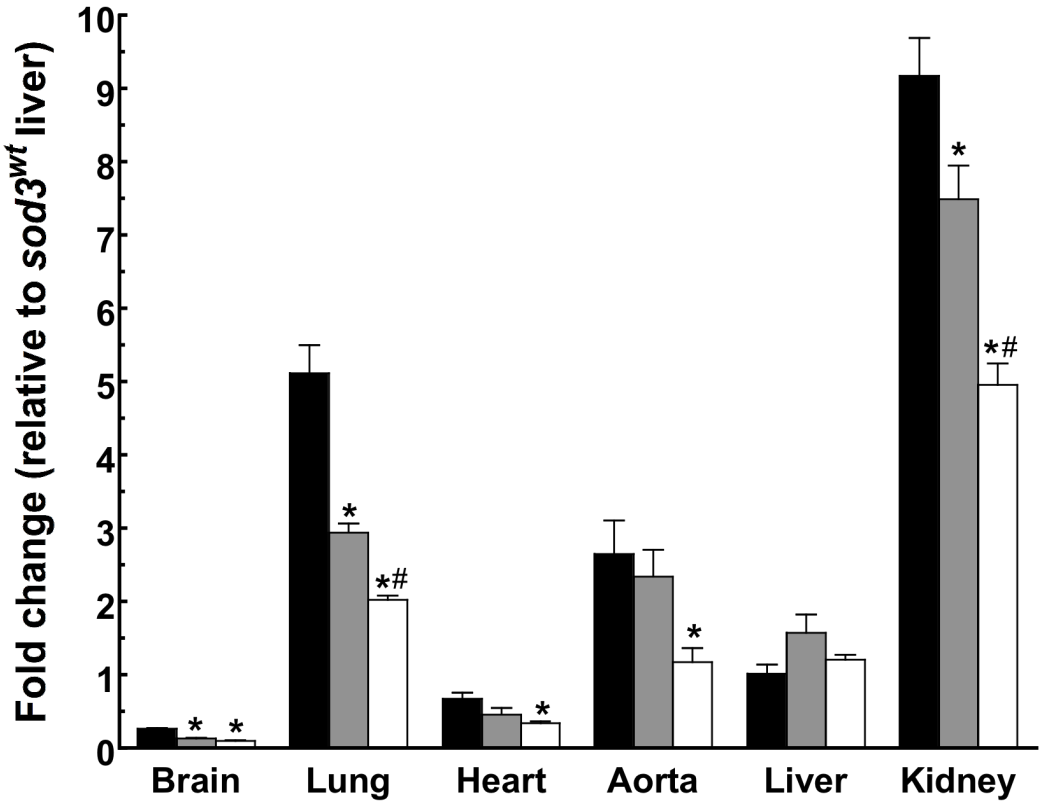

Figure 4. **Relative abundance of ecSOD mRNA in selected tissues of mice.**

mRNA levels were measured as described in the Materials and Methods from C57.129-*sod3*^{wt} (black bars), C57.129-*sod3*^{129} (grey bars) and the founder 129P3/J mice (clear bars). Ribosomal protein S15 was used as a control for each tissue. Bars represent means ± SEM of four to five animals in each group.

* indicates a significant difference (at $p<0.05$) from C57.129-*sod3*^{wt} mice (black bars)

# indicates a significant difference (at $p<0.05$) from C57.129-*sod3*^{129} mice (grey bars).

DISCUSSION

C57BL/6J and 129P3/J are some of the most commonly used mouse strains for disease studies and for generating genetically engineered mice. Interestingly, these strains differ significantly in their response to proliferative lung disease, brain ischemia and vascular remodeling and susceptibility to atherosclerosis [25-28]. Even though it is widely accepted that oxidative stress is an important component of the etiology of these conditions, studies have yet to identify the gene(s) responsible for these differences.

We recently reported that the 129P3/J strain expresses a novel ecSOD allele which differs in several aspects from the *wt* allele expressed by the C57BL/6J and C3H strains: it contains an N21D (or N-4D of the mature protein) substitution in the signal sequence of ecSOD, an A186S substitution in the catalytic domain and a 10bp deletion in the 3' untranslated region of the mRNA [1]. These mice have higher activity and amount of circulating and heparin-releasable ecSOD, when compared to C57BL/6J mice. Because of its function, ecSOD may be an important component of the anti-oxidant defense repertoire. To be able to compare the effect of two different ecSOD isoforms in an identical environment, we generated congenic mice that express either of the ecSOD alleles on a C57BL/6J genomic background. Based on the extent backcrossing (10 generations) and the additional use of 6 microsatellite polymorphism markers and an analysis by the Affimetrix Parallele Mouse 5K SNP panel, the congenic mice we generated are well over 99.8% identical to the C57BL/6J mice. The extensive backcrossing also eliminates any potential epigenetic factors that may have existed in the founder mice.

Our data show that the congenic mice recapitulate the ecSOD phenotype in an allele-specific manner, in terms of free and heparin-releasable plasma ecSOD levels and activities,

tissue enzyme distribution and relative tissue mRNA abundance. These results suggest that a substantial portion of the observed ecSOD phenotype is allele-dependent.

It should be noted that the analysis of total tissue enzyme activity and levels does not discriminate between enzymes localized extracellularly or still within the secretory pathway. Heparin administration, on the other hand, can only clear enzyme that is accessible: bound to the vascular cell surface or the endothelial lining of various organs [35]. Our data suggest that the *sod*^{129} mice have a larger pool size of the enzyme in most, but especially highly vascular tissues, including the liver and kidney and thus a higher heparin-accessible pool size. The physiological consequence of this is yet to be determined. The mature enzyme differs in a single amino acid substitution (A186S) which is unlikely to have an effect on its ability to form tetramers and thus influence the amounts of heparin-releasable enzyme. Both isoforms of the enzyme elute, upon FPLC chromatography at an identical point corresponding to ~130 kDa (data not shown). Heparin administration is not informative in tissues like lung or brain. The physiologically relevant location of ecSOD in the alveolae may make the enzyme inaccessible to heparin, while the extent of heparin penetration of the blood-brain barrier is uncertain. The apparent and consistent increase in aortic ecSOD content and activity after heparin administration may be due to a large influx of uncleaved ecSOD (released from peripheral tissues) that is able to re-bind to the endothelial lining of the vessel, while the concentration of heparin may be falling, due to "trapping" in the peripheral tissues.

The significant discrepancy in the relative enzyme content in the tissues of congenic mice vs. the amounts of corresponding mRNA is also of interest. At this point we can only speculate about potential differences in the mRNA translational efficiency and protein processing during the synthetic/secretory pathway. Our data using a stably transfected CHO cell line expressing

either of the ecSOD alleles are consistent with this observation. Given equal copy numbers of the ecSOD allele, CHO cells transfected with the *129* allele consistently secrete larger amounts of ecSOD [36].

We suggest that the N21D (N-4D in the mature protein) mutation may play an important role. The effect of this change may result in significant changes in the signal peptide processing. While the precise processing site of the *wt* signal peptide is not known, the well-accepted -3, -1 rule [34, 37] and computer analysis (SignalP 3.0 http://www.cbs.dtu.dk/services/SignalP/), points to the -4 aa (Asn in *wt*, Asp in *129* alleles). The relative cleavage site probability at this point rises from 0.611 in the *wt* product to 0.771 in the *129* isoform. The change at this position from a polar, uncharged Asn to a negatively charged Asp may thus lead to increased efficiency of processing and secretion. Different susceptibilities of the two transcripts to translational regulation or degradation may also play a role. Clearly more work is required in the future to elucidate this discrepancy.

A similar transcript (N21D and a 10 bp deletion) has been identified in apoE/LDLR KO mice and its appearance was erroneously reported to occur due post-transcriptional modification induced by atherosclerosis [38]. A more likely explanation is the significant extent of heterozygosity, with respect to ecSOD, in the apoE/LDLR KO mice as described previously [1]. A substantial portion of these mice carry over the 129 allele for ecSOD from the embryonic stem cells derived from the 129 strain and used in the generation of the knock-out mice.

Recently, Ganguly et al. [39] identified an ecSOD transcript variant in the JF1/Ms (JF1) mouse strain, which has several mutations, including two (A61G and G556T) point mutations that are shared with the 129 strain and associated with lower lung function [40]. The JF1 mouse strain has 2-3 fold lower mRNA as well as protein levels in the lung compared to C3H strain

which express *wt* ecSOD. It does not share the 10bp deletion in the 3' UTR of its transcript (L. Dory, unpublished observation). It should be emphasized however that the comparison of different variants of ecSOD transcripts and their products is not informative, when compared in a context of large differences in the rest of the genome. This is precisely the reason we generated the congenic mice.

The availability of congenic mice with different ecSOD phenotypes within an otherwise identical genome provides an important tool to investigate the role of this enzyme in various diseases and a tool to study the transcription and translational regulation of ecSOD expression.

REFERENCES

[1] Pierce, A.; Whitlark, J.; Dory, L. Extracellular superoxide dismutase polymorphism in mice. *Arterioscler. Thromb. Vasc. Biol.***23:**1820-1825; 2003.

[2] Beckman, J. S.; Beckman, T. W.; Chen, J.; Marshall, P. A.; Freeman, B. A. Apparent hydroxyl radical production by peroxynitrite: Implications for endothelial injury from nitric oxide and superoxide. *Proc. Natl. Acad. Sci. U. S. A.***87:**1620-1624; 1990.

[3] Oury, T. D.; Day, B. J.; Crapo, J. D. Extracellular superoxide dismutase: A regulator of nitric oxide bioavailability. *Lab. Invest.***75:**617-636; 1996.

[4] Brahmajothi, M. V.; Campbell, D. L. Heterogeneous basal expression of nitric oxide synthase and superoxide dismutase isoforms in mammalian heart : Implications for mechanisms governing indirect and direct nitric oxide-related effects. *Circ. Res.***85:**575-587; 1999.

[5] Ushio-Fukai, M. Redox signaling in angiogenesis: Role of NADPH oxidase. *Cardiovasc. Res.***71:**226-235; 2006.

[6] Capettini, L. S.; Cortes, S. F.; Gomes, M. A.; Silva, G. A.; Pesquero, J. L.; Lopes, M. J.; Teixeira, M. M.; Lemos, V. S. Neuronal nitric oxide synthase-derived hydrogen peroxide is a major endothelium-dependent relaxing factor. *Am. J. Physiol. Heart Circ.*

*Physiol.***295:**H2503-11; 2008.

[7] Faraci, F. M.; Didion, S. P. Vascular protection: Superoxide dismutase isoforms in the vessel wall. *Arterioscler. Thromb. Vasc. Biol.***24:**1367-1373; 2004.

[8] Fattman, C. L.; Tan, R. J.; Tobolewski, J. M.; Oury, T. D. Increased sensitivity to asbestos-induced lung injury in mice lacking extracellular superoxide dismutase. *Free Radic. Biol. Med.***40:**601-607; 2006.

[9] Jung, O.; Marklund, S. L.; Geiger, H.; Pedrazzini, T.; Busse, R.; Brandes, R. P. Extracellular superoxide dismutase is a major determinant of nitric oxide bioavailability: In vivo and ex vivo evidence from ecSOD-deficient mice. *Circ. Res.***93:**622-629; 2003.

[10] Kim, H. W.; Lin, A.; Guldberg, R. E.; Ushio-Fukai, M.; Fukai, T. Essential role of extracellular SOD in reparative neovascularization induced by hindlimb ischemia. *Circ. Res.***101:**409-419; 2007.

[11] Sheng, H.; Kudo, M.; Mackensen, G. B.; Pearlstein, R. D.; Crapo, J. D.; Warner, D. S. Mice overexpressing extracellular superoxide dismutase have increased resistance to global cerebral ischemia. *Exp. Neurol.***163:**392-398; 2000.

[12] Chen, E. P.; Bittner, H. B.; Davis, R. D.; Folz, R. J.; Van Trigt, P. Extracellular superoxide dismutase transgene overexpression preserves postischemic myocardial function in isolated

murine hearts. *Circulation***94:**II412-7; 1996.

[13] Ghio, A. J.; Suliman, H. B.; Carter, J. D.; Abushamaa, A. M.; Folz, R. J. Overexpression of extracellular superoxide dismutase decreases lung injury after exposure to oil fly ash. *Am. J. Physiol. Lung Cell. Mol. Physiol.***283:**L211-8; 2002.

[14] Levin, E. D. Extracellular superoxide dismutase (EC-SOD) quenches free radicals and attenuates age-related cognitive decline: Opportunities for novel drug development in aging. *Curr. Alzheimer Res.***2:**191-196; 2005.

[15] Gao, F.; Koenitzer, J. R.; Tobolewski, J. M.; Jiang, D.; Liang, J.; Noble, P. W.; Oury, T. D. Extracellular superoxide dismutase inhibits inflammation by preventing oxidative fragmentation of hyaluronan. *J. Biol. Chem.***283:**6058-6066; 2008.

[16] Kliment, C. R.; Tobolewski, J. M.; Manni, M. L.; Tan, R. J.; Enghild, J.; Oury, T. D. Extracellular superoxide dismutase protects against matrix degradation of heparan sulfate in the lung. *Antioxid. Redox Signal.***10:**261-268; 2008.

[17] Kliment, C. R.; Englert, J. M.; Gochuico, B. R.; Yu, G.; Kaminski, N.; Rosas, I.; Oury, T. D. Oxidative stress alters syndecan-1 distribution in lungs with pulmonary fibrosis. *J. Biol. Chem.***284:**3537-3545; 2009.

[18] Sandstrom, J.; Carlsson, L.; Marklund, S. L.; Edlund, T. The heparin-binding domain of extracellular superoxide dismutase C and formation of variants with reduced heparin affinity. *J. Biol. Chem.***267:**18205-18209; 1992.

[19] Karlsson, K.; Edlund, A.; Sandstrom, J.; Marklund, S. L. Proteolytic modification of the heparin-binding affinity of extracellular superoxide dismutase. *Biochem. J.***290 (Pt 2):**623-626; 1993.

[20] Petersen, S. V.; Oury, T. D.; Ostergaard, L.; Valnickova, Z.; Wegrzyn, J.; Thogersen, I. B.; Jacobsen, C.; Bowler, R. P.; Fattman, C. L.; Crapo, J. D.; Enghild, J. J. Extracellular superoxide dismutase (EC-SOD) binds to type i collagen and protects against oxidative fragmentation. *J. Biol. Chem.***279:**13705-13710; 2004.

[21] Sandstrom, J.; Karlsson, L.; Edlund, T. ; Marklund, S. L. Heparin-affinity patterns and composition of extracellular superoxide dismutase in human plasma and tissues. *Biochem J.* 294 (Pt 3):853-7; 1993.

[22] Stralin, P.; Karlsson, K.; Johansson, B. O.; Marklund, S. L. The interstitium of the human arterial wall contains very large amounts of extracellular superoxide dismutase. *Arterioscler. Thromb. Vasc. Biol.***15:**2032-2036; 1995.

[23] Karlsson, K.; Sandstrom, J.; Edlund, A.; Marklund, S. L. Turnover of extracellular-superoxide dismutase in tissues. *Lab. Invest.***70:**705-710; 1994.

[24] Oury, T. D.; Day, B. J.; Crapo, J. D. Extracellular superoxide dismutase in vessels and airways of humans and baboons. *Free Radic. Biol. Med.***20:**957-965; 1996.

[25] Warshamana, G. S.; Pociask, D. A.; Sime, P.; Schwartz, D. A.; Brody, A. R. Susceptibility to asbestos-induced and transforming growth factor-beta1-induced fibroproliferative lung disease in two strains of mice. *Am. J. Respir. Cell Mol. Biol.***27:**705-713; 2002.

[26] Fujii, M.; Hara, H.; Meng, W.; Vonsattel, J. P.; Huang, Z.; Moskowitz, M. A. Strain-related differences in susceptibility to transient forebrain ischemia in SV-129 and C57black/6 mice. *Stroke***28:**1805-10; discussion 1811; 1997.

[27] Ward, N. L.; Moore, E.; Noon, K.; Spassil, N.; Keenan, E.; Ivanco, T. L.; LaManna, J. C. Cerebral angiogenic factors, angiogenesis, and physiological response to chronic hypoxia differ among four commonly used mouse strains. *J. Appl. Physiol.***102:**1927-1935; 2007.

[28] Paigen, B.; Ishida, B. Y.; Verstuyft, J.; Winters, R. B.; Albee, D. Atherosclerosis susceptibility differences among progenitors of recombinant inbred strains of mice. *Arteriosclerosis***10:**316-323; 1990.

[29] Prass, K.; Wiegand, F.; Schumann, P.; Ahrens, M.; Kapinya, K.; Harms, C.; Liao, W.; Trendelenburg, G.; Gertz, K.; Moskowitz, M. A.; Knapp, F.; Victorov, I. V.; Megow, D.; Dirnagl, U. Hyperbaric oxygenation induced tolerance against focal cerebral ischemia in mice is strain dependent. *Brain Res.***871:**146-150; 2000.

[30] Lowry, O. H.; Rosebrough, N. J.; Farr, A. L.; Randall, R. J. Protein measurement with the folin phenol reagent. *J. Biol. Chem.***193:**265-275; 1951.

[31] Marklund, S. L. Analysis of extracellular superoxide dismutase in tissue homogenates and extracellular fluids. *Methods Enzymol.***186:**260-265; 1990.

[32] Paoletti, F.; Mocali, A. Determination of superoxide dismutase activity by purely chemical system based on NAD(P)H oxidation. *Methods Enzymol.***186:**209-220; 1990.

[33] Laemmli, U. K. Cleavage of structural proteins during the assembly of the head of bacteriophage T4. *Nature***227:**680-685; 1970.

[34] Folz, R. J.; Guan, J.; Seldin, M. F.; Oury, T. D.; Enghild, J. J.; Crapo, J. D. Mouse extracellular superoxide dismutase: Primary structure, tissue-specific gene expression, chromosomal localization, and lung in situ hybridization. *Am. J. Respir. Cell Mol. Biol.***17:**393-403; 1997.

[35] Karlsson, K.; Marklund, S. L. Heparin-induced release of extracellular superoxide dismutase to human blood plasma. *Biochem. J.***242:**55-59; 1987.

[36] Mirossay, A.; Jun, S.; Dory, L. Cloning and characterization of two alleles of the murine extracellular superoxide dismutase gene. *Biochem. Biophys. Res. Commun.***352:**739-743; 2007.

[37] Folz, R. J.; Gordon, J. I. Computer-assisted predictions of signal peptidase processing sites. *Biochem. Biophys. Res. Commun.***146:**870-877; 1987.

[38] Fukai, T.; Galis, Z. S.; Meng, X. P.; Parthasarathy, S.; Harrison, D. G. Vascular expression of extracellular superoxide dismutase in atherosclerosis. *J. Clin. Invest.***101:**2101-2111; 1998.

[39] Ganguly, K.; Stoeger, T.; Wesselkamper, S. C.; Reinhard, C.; Sartor, M. A.; Medvedovic, M.; Tomlinson, C. R.; Bolle, I.; Mason, J. M.; Leikauf, G. D.; Schulz, H. Candidate genes controlling pulmonary function in mice: Transcript profiling and predicted protein structure. *Physiol. Genomics***31:**410-421; 2007.

[40] Ganguly, K.; Schulz, H. Association studies of lung function in mice. *Dtsch. Tierarztl. Wochenschr.***115:**276-284; 2008.

CHAPTER III

ALLELE-SPECIFIC EFFECTS ON EXTRACELLULAR SUPEROXIDE DISMUTASE (ECSOD) SYNTHESIS AND SECRETION

ABSTRACT

We recently reported that the altered ecSOD allele in 129P3/J strain (129) is associated with increased level of the enzyme in several tissues but only a fraction of the corresponding mRNA levels when compared to the wild type (*wt*) allele. These results suggest potentially significant allele-specific differences in the regulation of the protein synthesis and/or intracellular rates of processing/secretion. The *129* allele is characterized by two point mutations leading to amino acid substitution one of which is in the signaling peptide (N21D) of the protein and a 10 bp deletion from the 3' UTR of mRNA. This study tested the potential mechanisms, increased synthesis and processing, for the increased levels of *129* ecSOD enzymes in *in vitro* systems. *In vitro* translation using rabbit reticulocyte lysate showed no differences in translational efficiency of transcripts and processing of the newly synthesized enzymes. However, when it was tested in stably transfected to CHO cells with either ecSOD alleles, both rates of synthesis and secretion of the *129* ecSOD were significantly higher than those of *wt* ecSOD. The processing of *129* ecSOD was faster than that of the *wt* enzyme. Pulse chase experiments revealed a potential intracellular degradation of ecSOD regardless of genotype. In conclusion, the altered ecSOD sequence in *129* allele resulted in increased rate of synthesis and secretion of *129* ecSOD. This is most likely the

result of an amino acid substitution in the signal peptide sequence of the *129* allele. This observation may responsible for the higher steady-state levels of plasma and tissue ecSOD in the congenic mice expressing this allele.

INTRODUCTION

Extracellular superoxide dismutase (ecSOD or SOD3) is the only enzyme that scavenges superoxide specifically in the extracellular compartment and protects tissues from oxidative damage. The understanding of the etiology of a number of oxidative stress- related diseases as well as potential therapeutic approaches for their treatment would be significantly enhanced by understanding factors that regulate the expression of this enzyme. While the involvement of several transcription factors or epigenetic regulation of ecSOD expression has been examined (1-6), there is essentially no information regarding potential regulatory mechanisms at the posttranscriptional level, including translational and processing efficiency (7).

We previously reported that the 129P3/J strain of mice expresses an ecSOD allele which differs in several aspects from the wild-type (*wt*) allele, expressed by the C57BL/6J and most other strains (8). It contains an N21D (or N-4D of the mature protein) substitution in the signal sequence of ecSOD, an A186S substitution in the catalytic domain and a 10bp deletion in the 3' untranslated region (UTR) of the mRNA (8). This genotype has a profound effect on the ecSOD phenotype in that plasma ecSOD level and activity in the 129P3/J mice are 2-3 fold higher than those in the C57BL/6 mice, showing no apparent change in specific activity. The phenotype associated with this allele ("*129*") is mostly allele-driven, as congenic mice (C57.129-*sod3*) expressing either ecSOD genotype on a C57BL/6 background fully recapitulate the allele-specific ecSOD phenotype (9).

We also recently reported that normal or elevated enzyme amounts in various tissues expressing the *129* allele are associated with mRNA levels that represent only a fraction of those associated with the expression of the *wt* allele (9). These observations suggest allele-specific

differences in the regulation of ecSOD synthesis and/or intracellular processing/secretion, independent of the genotype/strain context. The discrepancy in the enzyme content in the tissues of congenic mice vs. the amounts of corresponding mRNA is of interest and may provide an opportunity to examine potential mechanisms of posttranscriptional regulation, including rates of synthesis, secretion and intracellular processing.

First, in order to examine the relative translational efficiency of the transcripts of the two ecSOD alleles, and the nature of *in vitro* processing of the newly synthesized enzyme, we employed an *in vitro* translation system using rabbit reticulocyte lysate with or without microsomal membranes.

In order to test whether regulation by miRNAs may play a role in allele- specific expression of ecSOD, the 3'UTR of either *wt* or *129* ecSOD was cloned to the firefly luciferase (FL) gene. These clones were then used for *in vitro* transcription and translation, using a rabbit reticulocyte lysate system, to examine the potential effect of interaction of known miRNAs with the transcript sequence containing the 10bp deletion.

Lastly we examined the effect of the signal peptide mutation on rates of ecSOD synthesis and secretion in stably transfected to CHO (Chinese Hamster Ovarian) cells by long-term labeling and pulse chase experiments.

EXPERIMENTAL PROCEDURES

***In vitro* transcription and translation**:

pcDNA3.1D/V5-His-TOPO plasmid with either *wt* or *129* ecSOD (described previously by Mirossay et al. (10)) were linearized with *Not* I (New England Biolabs) at 37ºC for 2 hr. The linearized plasmids were extracted with phenol, precipitated with ethanol, and resuspended in nuclease-free water (Ambion). *In vitro* transcription was performed with 5 μg linearized plasmid using the RiboMax T7 Large-Scale RNA Production kit (Promega), according to the manufacturer's protocol, followed by purification by the phenol:chloroform method. The sequences of the template ecSOD for the *in vitro* transcription were confirmed in both directions. *In vitro* transcribed mRNAs were modified by 7-methyl G capping and polyadenylation. The capping reaction was carried out according to the manufacturer's protocol (EPICENTRE) using 20 pmoles of mRNA/ capping reaction. Capped mRNAs were polyadenylated for 30 min at 37ºC in 25 μl, containing 10 pmoles of capped mRNA and 600 U PAP, according to the manufacturer's protocol (Ambion). Polyadenylated transcripts were purified using oligo-dT beads (Ambion). The *in vitro* transcribed RNAs and polyadenyled transcripts were monitored on 1% agarose-formaldehyde gels and were tested for quantity and quality by the Nanodrop and Experion microcapillary electrophoresis (Bio-Rad), respectively.

In vitro translation assay reactions were performed in nuclease-treated rabbit reticulocyte lysate (RRL, Promega, cat. #L4960) at 30ºC. The translation system was charged with the same amount of mRNA obtained by *in vitro* transcription. The relative translational efficiency of the ecSOD transcripts was examined by Western blotting. Semi-purified mouse plasma ecSOD, incubated with or without peptide:N-glycosidase F (PNGase F, New England Labs), was used as a size

control. Post-heparin plasma ecSOD was semi-purified by ConA-sepharose column as previously described (9).

***In silico* study:** miRNA species targeting the 3'UTR of murine ecSOD were searched by three miRNA target prediction tools, including miRanda, TargetScan and miRtarget. We also aligned the 3' UTR of *wt* and *129* allele to be able to compare the sequence using the NCBI blast tool.

Cloning the 3'UTR with a reporter system: To be able to test the extent of miRNA(s) interaction with the 3'UTR of ecSOD and the potential effect on synthesis, a reporter assay (Luciferase) with either *wt* or *129* 3'-UTR was constructed. Mouse genomic DNA was extracted from ear tissues of C5BL/6J and 129P3/J. The ecSOD 3' UTR for both alleles were amplified by PCR using primers harboring restriction enzyme sites. The restriction enzyme digested amplicons were cloned into N*he*I/A*pa*I site of modified pGL3 control vector (11), which contains firefly luciferase ORF (FL), and is designated as pGL3 wtUTR or pGL3 129UTR. Both sequences of FL with either 3'UTR were subcloned into H*ind*III/A*pa*I site of pcDNA^{TM} 3.1 (Invitrogen, USA) and were designated as pcd wtUTR or pcd 129UTR. FL without 3'UTR was also subcloned into H*ind*III/X*ba*I site of the vector to be used as control and designated as pcd FL.

***In vitro* assay**: The mRNAs for FL either with or without UTR were obtained by *in vitro* transcription from the linearized pcd vectors (Promega,US). The mRNA for renilla luciferase (RL) was also obtained by *in vitro* transcription from the linearized pCMV-RL. The RNAs were further modified by 5' capping and poly(A) polymerase tailing kits (EPICENTRE) to mimic the structure of *in vivo* transcripts. The *in vitro* transcribed RNAs were purified and tested as described above. The rabbit reticulocyte lysate (Promega, US), was charged with the same amount of each FL mRNA, along with miR-744 or 663 (Ambion, US). RL mRNA was used in

all translation reactions as an internal control, except for negative control. The relative translational efficiency of the transcripts was obtained by measuring luciferase activities with a dual luciferase assay system (Promega, US).

Cell culture: CHO cells stably transfected with either *wt* or *129* allele of ecSOD, established as previously published (10), were incubated with DMEM/10% FBS with G-418 as a selection marker at 37˚C in a humidified atmosphere containing 5% CO_2. To purify mRNA and genomic DNA, cells were washed with ice-cold PBS and dissolved in 1mL of TRIreagent® (Molecular Research Center) and kept at -80˚C until used.

Real-time RT-PCR:

RNA and genomic DNA of CHO cells were purified according to the manufacturer's protocol (Molecular Research Center). We evaluated ecSOD mRNA levels in stably transfected CHO cells by real-time RT-PCR, as previously published (9).

Long-term labeling and pulse-chase study: CHO cells ($1.8x10^6$ cells/well) were seeded in 6-well plates in DMEM/10% FBS without G-418. For continuous labeling studies (up to 8hrs) cells were washed 2 times in methionine- and cysteine-free DMEM, followed by incubation in the labeling medium (Met- and Cys-free DMEM, containing 60 μCi/ml [^{35}S]-Met and Cys (Perkin Elmer, USA). Incubations were stopped at 30min to 1hour intervals, for up to 8 hours. Short-term, pulse-label studies were carried out in a similar manner; incubations were stopped at 30 min to 1hour intervals. In pulse-chase experiments, cells were chased in regular DMEM for up to 6 hours. At the end of the incubations the medium was collected and cells were washed twice with ice-cold PBS, and scraped off in a lysis buffer (final volume, 1ml).

TCA precipitation: Total radiolabeled secreted (medium) or cellular protein synthesis was determined by trichloroacetic (TCA) acid precipitation, as previously described (12) The results

were calculated in terms of corrected cpm/mg cell protein. Cellular protein content was determined by the Lowry assay (13).

Immunoprecipitation: Incorporation of [^{35}S] Met and Cys into cellular and medium ecSOD was determined by immunoprecipitation with a rabbit anti ecSOD serum. Total media ecSOD was immunoprecipitated in the presence of 0.05 % Triton X-100 and protease inhibitor (Sigma) at 4°C for 24h, as previously described (12). The immunoprecipitate was resolved by 12% SDS-PAGE. Slab gels processed for fluorography were soaked first in gel soaking solution (1% glycerol, 7% acetic acid and 7% methanol) and next in enhancer solution (1M Salicylic acid) and dried. X-ray films were exposed at -80˚C and developed. The X-ray film was scanned and densitometry of ecSOD was done using the supplied software AlphaEaseFC (Alpha Innotech). Intracellular ecSOD was immunoprecipitated in a similar fashion, except that 1 % Triton X-100 was used and the cell lysates were pre-cleared by addition of non-immune rabbit serum, followed by protein A-agarose, to minimize background.

Statistical Analysis: Results from experiments were reported as mean $\pm$ SEM. Statistical analysis was done using a *t*-test or linear regression comparison (GraphPad Prism). $P<0.05$ was considered statistically significant.

RESULTS

The *in vitro* translational efficiency and processing of the *wt* and *129* ecSOD transcript

We first examined the translational efficiency using *in vitro* transcribed *wt* or *129* ecSOD transcripts in the nuclease-treated rabbit reticulocyte lysate. The translated *wt* and *129* ecSOD proteins appear to be the same size as full-length, deglycosylated mouse plasma ecSOD. The translation efficiency of the two transcripts appears to be similar, regardless of the transcript concentration (**Figure 1A**). We next tested the processing efficiency, including the cleavage of the signal peptide and glycosylation. The presence of canine microsomal membranes results in a synthesis of glycosylated and full-length ecSOD for both transcripts. The processing efficiency for each transcript also appears to be similar (**Figure 1B**). Since the efficiency of translation as well as processing is likely dependent on the mRNA structure, 5' capped and poly (A) tailed transcripts were also tested, but were not different (**Figure 1B**).

The effect of candidate miRNAs on the translational efficiency of luciferase with ecSOD 3'UTRs in an *in vitro* system

A major difference between the two ecSOD transcripts is a 10bp deletion in the 3'UTR in the *129* allele. Since the 3'UTR sequence of many transcripts is subject to translational regulation by miRNA, we examined the effects of two selected miRNAs. Using three miRNA target prediction tools, including miRanda, TargetScan and miRtarget, miRNAs targeting ecSOD 3'UTR were searched. Five known miRNAs (miR-744, 764-5p, 339-3p, 490 and 33) are predicted by two search tools (miRanda and TargetScan) to bind to mouse ecSOD mRNA. Two miRNAs, miR-744 and miR-663 (predicted by miRanda only), are expected to bind to the

3'UTR of the mouse ecSOD in an area overlapping the 10bp deletion (10-19bp) region in the *129* ecSOD mRNA (**Figure 2A**). The 10 bp deletion in the *129* ecSOD mRNA results in 2 (miR-744) or 3 (miR-663) mismatches of miRNA binding sites, when compared to *wt* allele (**Figure 2B and C**). The effect of these two miRNAs on the translational efficiency was examined by using a firefly luciferase cloned to a 3'UTR of either the *wt* or *129* ecSOD. Neither miR-744 nor miR-663 significantly altered the rates of synthesis of the luciferase regardless of the source of 3'UTR. These results do not eliminate the possibility of other, yet to be defined miRNAs may modulate translational efficiency of the either transcript.

Rates of ecSOD synthesis and secretion in stably transfected CHO cells

To test the phenotype in mammalian cells, we established stably transfected CHO cells, as previously described (10). The genomic copy number and the mRNA level of ecSOD were checked by realtime qPCR. We selected CHO cell clones with similar mRNA copy numbers per total mRNA.

To compare the rates of synthesis and secretion, we employed a continuous labeling technique. Labeled cellular ecSOD levels increased with time and both products reached plateau at about 180 min of incubation, indicating that the intracellular ecSOD pool is fully labeled within 3 hours. As shown in **Figure 3A and B**, the synthetic rate of *129* ecSOD appears to be nearly 2-fold (1.79-fold) higher than that of *wt* ecSOD (3.05±0.18 vs. 5.47±0.35 IDV/ μg of protein/min), matching exactly the differences (1.84-fold) in the cellular pool size of ecSOD (439±17 vs. 807±74 IDV/μg of protein). As expected, rates of total protein synthesis or cellular pool size were identical in both CHO cell clones (Figure 3C).

To check if the increased synthetic rates of *129* ecSOD are coupled to higher rates of secretion, ecSOD was also immunoprecipitated from the medium and the fluorography is shown in **Figure 4A**. As expected, increased rates of *129* ecSOD synthesis (1.79-fold) in comparison of *wt* synthesis were matched with similar (1.60-fold) increase in rates of secretion (3.61±0.15 vs. 5.76 ± 0.19 IDV/ μg of protein/min; *wt* vs. *129*, respectively), as shown in **Figure 4B**. Furthermore, the time of appearance in the medium was almost 35 minutes earlier for *129* allele, when compared to *wt* (121.4 vs 87.5 min of labeling). The secretion of labeled total protein was indistinguishable between the two CHO clones **(Figure 4C).**

ecSOD half-life and internal degradation in stably transfected CHO cells

The observed rates of synthesis and secretion of the *129* ecSOD were significantly (nearly 2-fold) higher than those of *wt* ecSOD; the fold-difference in the rates of synthesis were somewhat lower than the fold difference in the observed rates of secretion. At steady-state, the rate of protein secretion must be balanced by the sum of the rate of synthesis and degradation; these results suggest that half-life or extent of internal degradation of ecSOD may be different between alleles. To measure the half-life and the extent of internal degradation of ecSOD, pulse chase experiments were carried out and shown in **Figure 5A**. As observed in continuous labeling experiments, cellular *129* ecSOD pool size at time 0 of chase (**Figure 5B**) is clearly higher (1.9-fold) than that of *wt* ecSOD. The secretion rate is also shown to be significantly higher in *129* ecSOD when compared to the *wt* in the media (1.5-fold) (**Figure 5C**). Albeit different in design, both labeling experiments (continuous and pulse-chase) provide qualitatively very similar data: both, rates of synthesis and secretion are significantly higher for the 129 allele product. As expected, a delay in ecSOD secretion is not observed in pulse-chase experiments. Moreover, the

small but consistent difference in the synthetic and secretory rates for both alleles suggest continuous enzyme degradation during this process.

The half-life of cellular *129* ecSOD is not different from that of *wt* ecSOD (86.2 vs. 86.7 min) (**Figure 5D**). The internal degradation turned out to be a similar proportion of intracellular level as well (~20%).

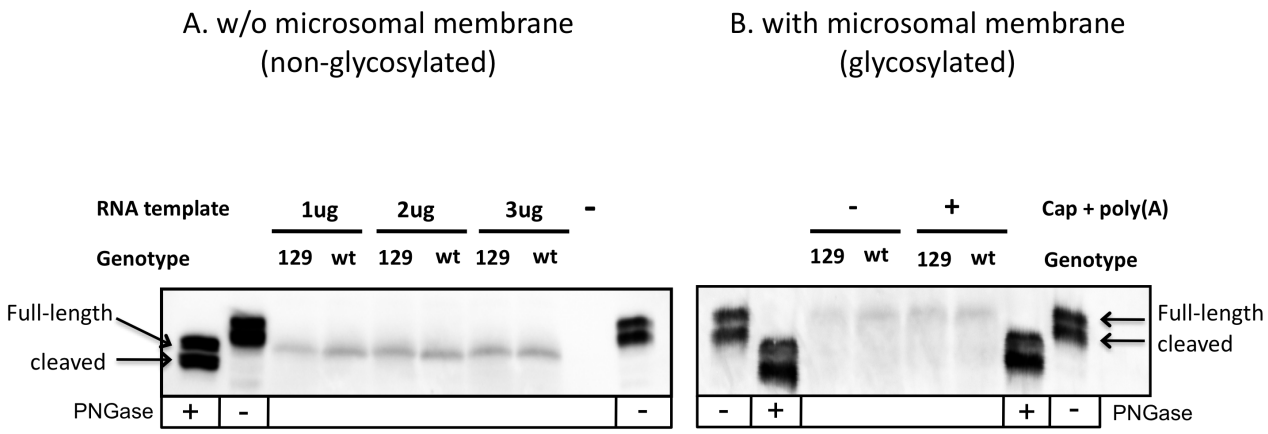

Figure 1. *In vitro* translation of *wt* and *129* ecSOD. (A) *In vitro* translated ecSODs using same amount (1-3 μg) of *in vitro* transcribed *wt* or *129* ecSOD mRNA was detected by western blot to compare translation efficiency. ConA purified mouse plasma ecSOD and deglycosylated ecSOD by PNGase F treatment was used as a control. The size of *wt* and *129* ecSOD are similar to deglycosylated full-length plasma ecSOD. (B) *In vitro* translation of 1μg of *wt* or *129* ecSOD mRNA with canine pancreatic microsomal membrane. The microsomal membrane is for post-translational processing including signal peptide cleavage and glycosylation. The incubation with microsomal membrane clearly attenuated mobility of both *wt* and *129* ecSOD and they are similar in size to the full-length plasma ecSOD (glycosylated). The processing efficiency was not different between *wt* and *129* transcripts regardless mRNA modifications, capping and polyadenylation.

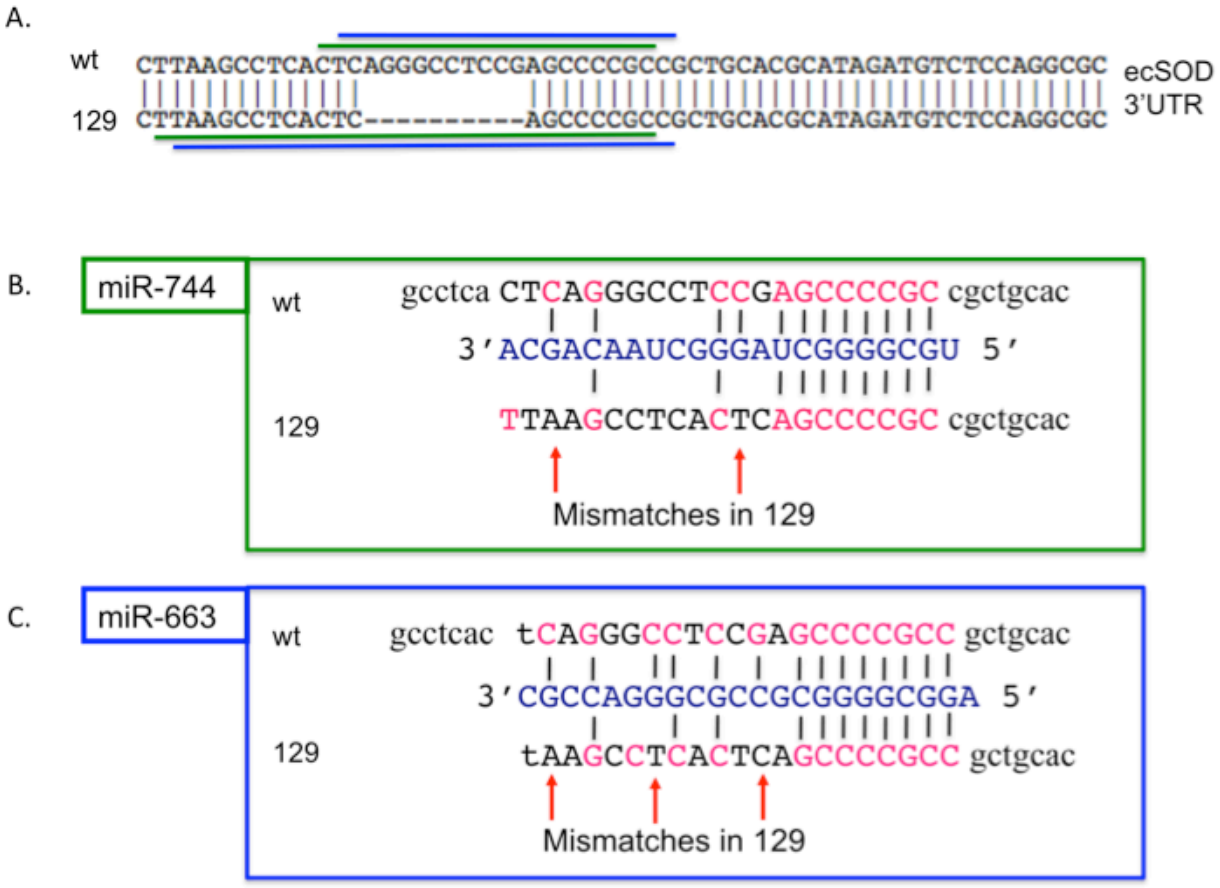

Figure 2. Alignment of miRNAs with *wt* and *129* ecSOD sequence. (A) Alignment of *wt* and *129* ecSOD 3' UTRs with miR-744 (green line) and miR-663 (blue line). (B) Green box shows alignment of miR-744 with ecSOD 3' UTRs. (C) Blue box shows alignment of miR-663 with ecSOD 3' UTRs. Sequences in blue is the miRNAs and pink is the sequences that is complementary to miRNAs. Arrows (↑) indicate additional mismatches of *129* sequences to miRNAs where *wt* is matched.

Figure 3. The rate of [^{35}S] ecSOD synthesis by stably transfected CHO cells. (A) Fluorograph (exposed for 15 days in -80 ºC) of cell immunoprecipitable *129* (top) and *wt* (bottom) ecSOD. A representative experiment (out of 3) is shown. (B) Densitometric analysis of labeled ecSOD. The slope of the linear portion of the curve (30-150 min) representing incorporation of [^{35}S]-met and cys into cellular ecSOD, which was normalized by total protein level, was used to calculate the rate of ecSOD synthesis (IDV/μg /minute). IDV stands for integrated density value. Steady state pool sizes were calculated by averaging intensity during 180-240 min when the labeled ecSOD reached plateau. (C) Total labeled protein level in cell lysate. TCA precipitated proteins were counted for 1 minute (cpm) for [^{35}S].

Figure 3.

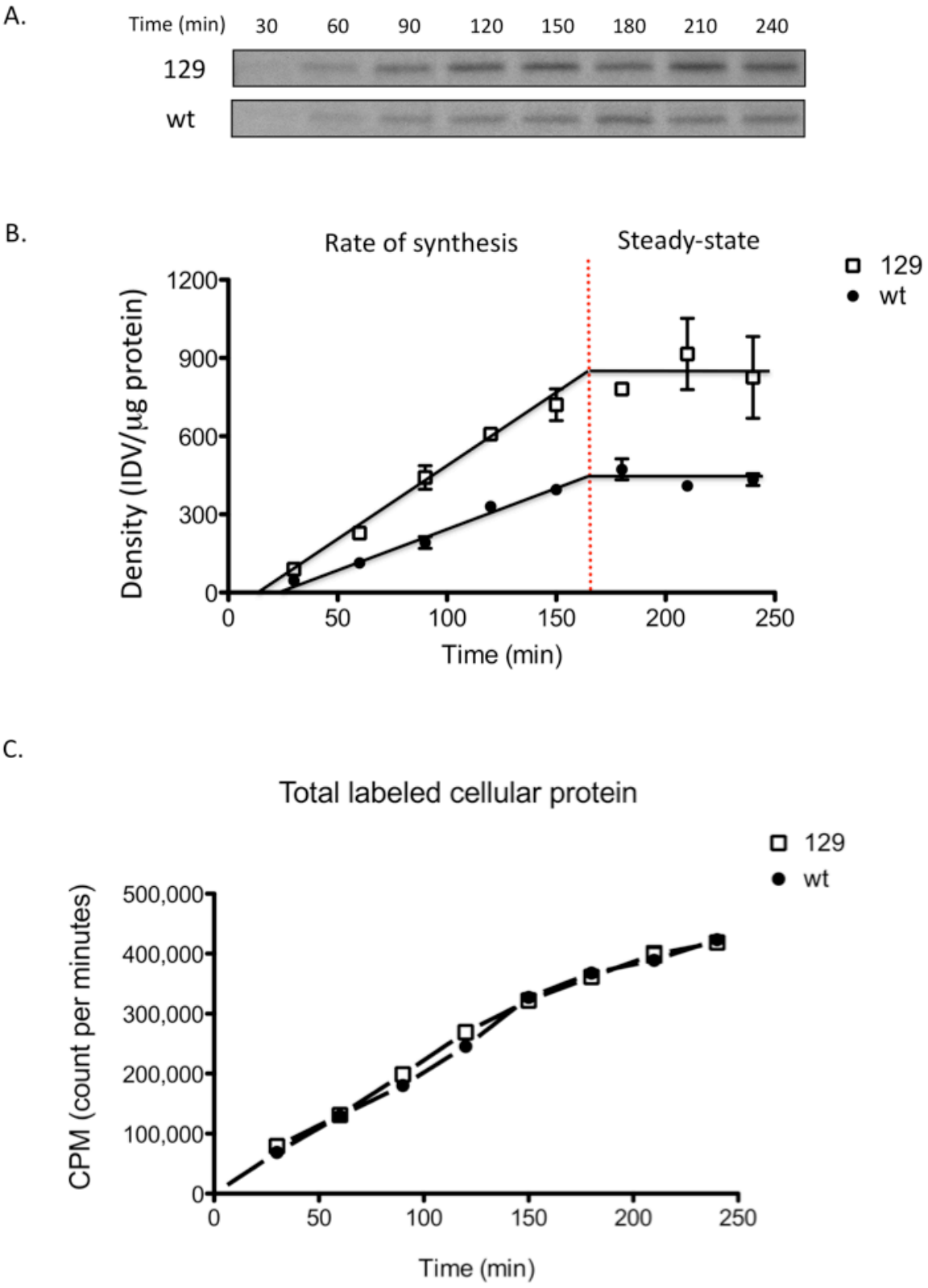
A.
Time (min) 30 60 90 120 150 180 210 240
129
wt
B.
Rate of synthesis
Steady-state
129
wt
Density (IDV/µg protein)
1200
900
600
300
0
0 50 100 150 200 250
Time (min)
C.
Total labeled cellular protein
129
wt
CPM (count per minutes)
500,000
400,000
300,000
200,000
100,000
0
0 50 100 150 200 250
Time (min)

Figure 4. The rate of [^{35}S]ecSOD secretion by stably transfected CHO cells. (A) A typical (out of 4 separate experiments) fluorograph of media immunoprecipitable *129* (top) and *wt* (bottom) ecSOD. (B) Densitometric analysis of labeled ecSOD. The slope of the linear portion of the curve (150-360 min) representing labeled medium ecSOD, which was normalized by total protein level, was used to calculate the rate of ecSOD secretion (IDV/μg /minute). (C) Total labeled protein level in media. TCA precipitated proteins were counted for 1 minute (cpm) for [^{35}S].

Figure 4.

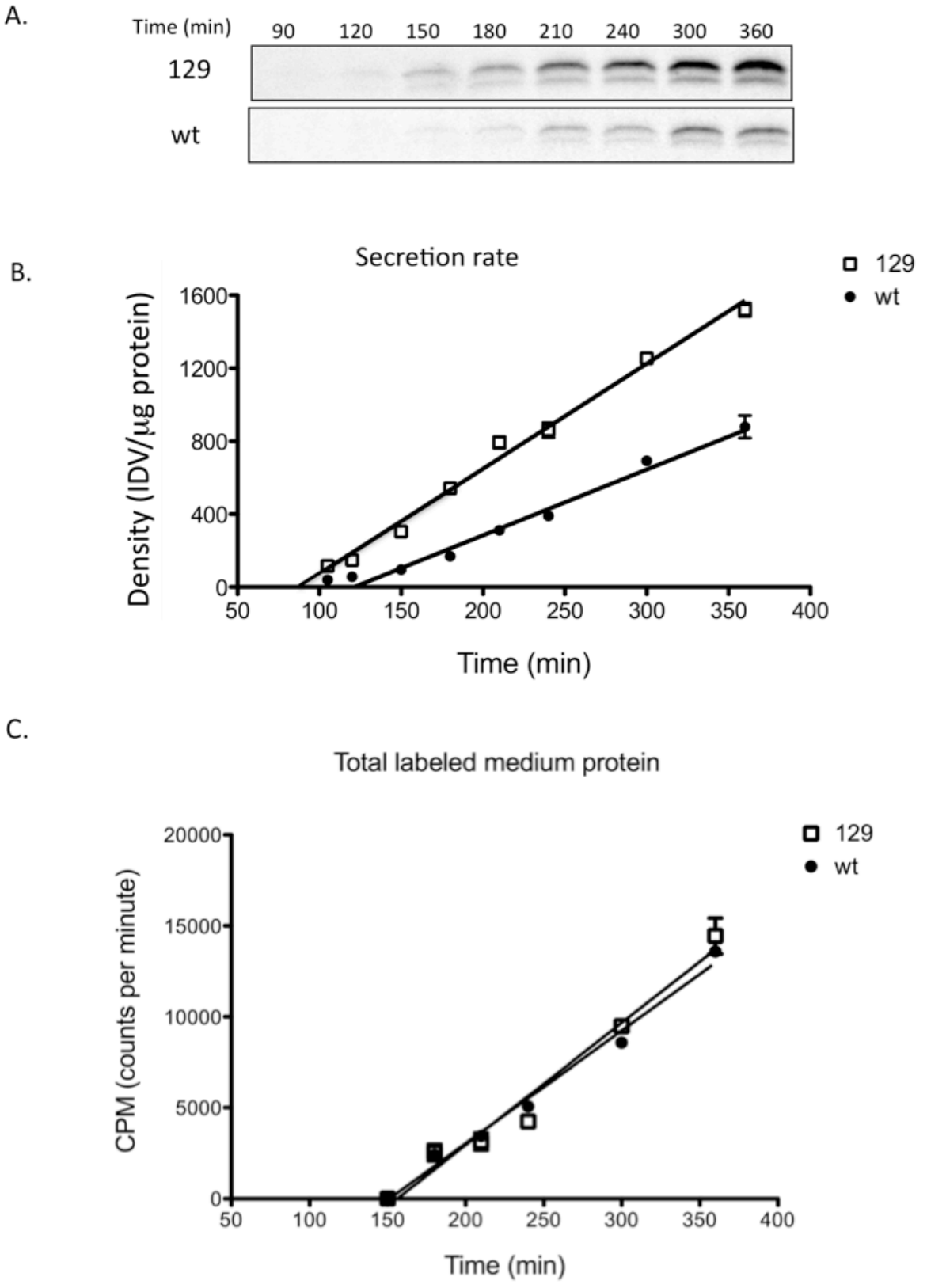
A.
Time (min)
90
120
150
180
210
240
300
360
129
wt
B.
Secretion rate
129
wt
Density (IDV/μg protein)
1600
1200
800
400
0
50
100
150
200
250
300
350
400
Time (min)
C.
Total labeled medium protein
129
wt
CPM (counts per minute)
20000
15000
10000
5000
0
50
100
150
200
250
300
350
400
Time (min)

Figure 5. [^{35}S]ecSOD half-life and internal degradation in stably transfected CHO cells. (A) A typical (out of 3 separate experiments) fluorograph of [^{35}S] labeled cellular and medium ecSOD at each time point of chase. Densitometric analysis of labeled cellular (B) and media (C) ecSOD. Each levels of intracellular ecSOD at 0 time chase were considered as 100 % and the relative [^{35}S]ecSOD levels in cell and media during chase are shown in (D). The half-life of *wt* and *129* ecSOD was calculated by the time when 50% of intracellular ecSOD is remaining. Intracellular degradation was calculated by subtracting the percentage of sum of cellular and media ecSOD from 100% at a time of half-life.

Figure 5.

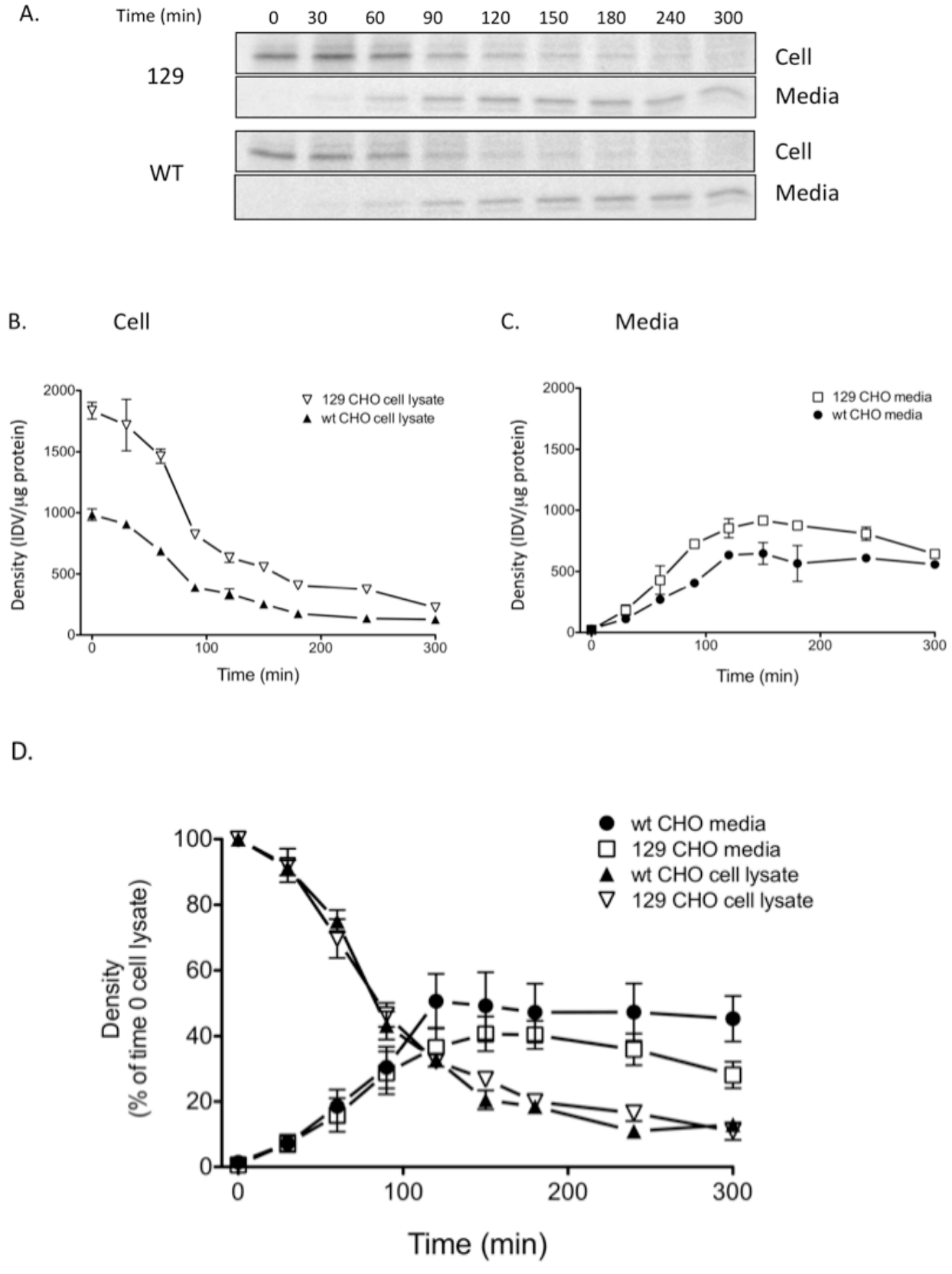
A.
Time (min)
0 30 60 90 120 150 180 240 300
129
Cell
Media
WT
Cell
Media
B.
Cell
Density (IDV/µg protein)
129 CHO cell lysate
wt CHO cell lysate
Time (min)
C.
Media
Density (IDV/µg protein)
129 CHO media
wt CHO media
Time (min)
D.
Density (% of time 0 cell lysate)
wt CHO media
129 CHO media
wt CHO cell lysate
129 CHO cell lysate
Time (min)

DISCUSSION

Our results clearly demonstrate that ecSOD polymorphism has a profound effect on several aspects of ecSOD phenotype, including rates of synthesis and secretion, independent of the genomic context. The synthetic rate and steady state levels of intracellular *129* ecSOD are nearly twice as high as those of *wt* ecSOD in stably transfected CHO cells, despite similar levels of mRNA. These observations are analogous to the *in vivo* situation we reported earlier (9). Similarly, rates of secretion and synthesis of the *129* allele product were nearly twice that of the *wt* allele product. These observations were made using two different experimental approaches: the continuous and the pulse-chase labeling design. These results strongly suggest that the allele-driven differences in synthetic and secretory rates may be responsible for the allelic differences observed *in vivo*, in tissue expression vs. mRNA levels (9).

Using the simplest expression system, the rabbit reticulocyte lysate in the presence or absence of microsomal membranes, the translational efficiency and processing rate were similar for both transcripts, regardless of capping or polyadenylation. These results suggest that the nuclease-treated rabbit reticulocyte lysate system may not contain the required components of the regulatory machinery responsible for the ecSOD phenotype *in vivo*.

miRNAs are evolutionarily conserved, single-stranded, non-coding RNA molecules that function as posttranscriptional gene regulators by pairing to the mRNA of protein-coding genes, which can result in the cleavage of mRNA (14) or the repression of productive translation (15). The 3'UTR of mRNA is known to be an important site for the miRNA-mediated events (16, 17). In addition, several studies showed that polymorphism in the 3'UTR of transcripts indeed has a significant effect on translational efficiency, by modifying the affinity of miRNA for the target

mRNA (18-20). A 10bp deletion in this region (such as observed in the *129* mRNA) may alter the translational efficiency in a fully reconstituted cell. In this study, we found two miRNAs (miR-744 and -663) that can potentially target the mouse ecSOD 3'UTR, the locus of the 10bp deletion in the *129* allele of ecSOD. The 10 bp deletion results in 2 (for miR-744) or 3 (for miR-663) mismatches in the miRNA binding region. However, we did not observe a translational repression effect by the two miRNA on either allele of ecSOD. These experiments do not exclude the possibility that other miRNAs may play a role in modulating translational efficiency of the ecSOD transcripts.

The continuous labeling studies show that the synthetic rate of *129* ecSOD is 1.8-fold greater than that of *wt* ecSOD, leading to 1.8-fold greater steady-state intracellular levels of the enzyme. At this point, it is not clear whether the increase of synthetic rate of *129* ecSOD is due to higher translation efficiency or the rate of processing of the co-translated protein (cleavage of signal peptide) or combination of both. The increased rate of processing of *129* ecSOD is supported by the earlier time of appearance in the medium (35min earlier than *wt* ecSOD). While the precise mechanism by which the *129* ecSOD is processed quicker remains to be determined, an analysis of signal peptide cleavage site suggests a possible mechanism. Even though the exact processing site of the *wt* signal peptide is not known, computer analysis (SignalP3.0 http://www.cbs.dtu.dk/ services/SignalP/) points to amino acid 21 in the prepropeptide, Asn (N) in *wt*, Asp (D) in *129* alleles, as signal peptide cleavage site of ecSOD. The relative cleavage site probability at this point rises from 0.611 in the *wt* product to 0.771 in the *129* isoform. Although it is not clear whether this increased probability can account for the nearly 2- fold increase in the apparent rate of synthesis, recent experiments have demonstrated that sequence variation among signal sequences can affect protein targeting and translocation, signal sequence cleavage and

even post-cleavage events (21). Importantly, the modulation of specific steps in the recognition and processing of signal sequences can have an essential role in protein biogenesis (21). Signal sequences regulate the timing and efficiency of cleavage which can control the exit of proteins from the ER; the exceptionally slow cleavage of the native HIV gp 120 signal sequence causes prolonged retention of the protein in the ER (21, 22). Furthermore, an amino acid substitution at the -1 position of signal peptide cleavage site of human preproapolipoprotein A-II was shown to lower the processing efficiency by signal peptidase activity (23). These studies suggest that the amino acid substitution in *129* ecSOD signal peptide (N21D) might modulated the cleavage efficiency and thus the *129* ecSOD appears faster in the media.

Several studies report that signal peptidase cleavage site mutations have significant clinical implications. A substitution at the -3 position with respect to the signal peptide-processing site in Factor $X_{\text{Santo Domingo}}$ prevents signal peptide cleavage and the mutant protein is not secreted, leading to a bleeding disorder (24). An Ala to Thr change at the -1 position in preprovasopressin, causing familial central diabetes insipidus, also leads to a failure of signal peptide processing and reduced secretion (25). Same change at -1 position (A25T) of ADAMTS10 signal peptide cleavage site affects the secretion of full-length protein, causing recessive Weill-Marchesani syndrome (WMS) (26). These studies show that 1 amino acid change in signal peptide can modulate the protein secretion and how important is the signal peptide in the protein biogenesis.

It is highly unlikely that the substitution in catalytic domain (A186S) play a role in the protein production. It also appeared to have no effect on the specific activity as shown previously (9).

It has been suggested that ecSOD can be stored in intracellular vesicles in tissues (27-29).

Previous study, which has shown localization of ecSOD in the endosomal fraction (30), suggests that there might be some degradation of intracellular ecSOD. In this study, we observed about 20% of degradation regardless of the genotype. Internal ecSOD T1/2 is also allele independent (~86min). These results suggest that the increased efficiency of *129* ecSOD processing is most likely responsible for the increased protein levels in the tissues of mice expressing the 129 allele.

129 ecSOD transcript levels in the lung tissue expressing the *129* allele are significantly lower relative to those tissues expressing the *wt* allele, yet consistently express higher levels of protein. Such differences in tissue-specific expression of the enzyme may lead to significant differences in disease susceptibility. Indeed our preliminary work supports this hypothesis. Given the potentially important role of ecSOD in defending against extracellular superoxide, additional studies of ecSOD post-transcriptional regulation and processing should be useful for understanding the processes of superoxide dismutase-dependent diseases. These unusual phenotypes of *129* ecSOD highlight the potential that the congenic mice expressing either *wt* or *129* allele will provide an important tool to investigate those unknown regulatory mechanisms.

REFERENCES

1. Zelko, I. N., and Folz, R. J. (2003) *Biochem. J.* **369**, 375-386

2. Zelko, I. N., and Folz, R. J. (2004) *Free Radic. Biol. Med.* **37**, 1256-1271

3. Zelko, I. N., Mueller, M. R., and Folz, R. J. (2008) *Am. J. Respir. Cell Mol. Biol.* **39**, 243-251

4. Itoh, S., Ozumi, K., Kim, H. W., Nakagawa, O., McKinney, R. D., Folz, R. J., Zelko, I. N., Ushio-Fukai, M., and Fukai, T. (2009) *Free Radic. Biol. Med.* **46**, 95-104

5. Zelko, I. N., Mueller, M. R., and Folz, R. J. (2010) *Free Radic. Biol. Med.* **48**, 895-904

6. Laukkanen, M. O., Mannermaa, S., Hiltunen, M. O., Aittomaki, S., Airenne, K., Janne, J., and Yla-Herttuala, S. (1999) *Arterioscler. Thromb. Vasc. Biol.* **19**, 2171-2178

7. Miao, L., and St Clair, D. K. (2009) *Free Radic. Biol. Med.* **47**, 344-356

8. Pierce, A., Whitlark, J., and Dory, L. (2003) *Arterioscler. Thromb. Vasc. Biol.* **23**, 1820-1825

9. Jun, S., Pierce, A., and Dory, L. (2010) *Free Radic. Biol. Med.* **48**, 590-596

10. Mirossay, A., Jun, S., and Dory, L. (2007) *Biochem. Biophys. Res. Commun.* **352**, 739-743

11. Doench, J. G., Petersen, C. P., and Sharp, P. A. (2003) *Genes Dev.* **17**, 438-442

12. Dory, L. (1989) *J. Lipid Res.* **30**, 809-816

13. Lowry, O. H., Rosebrough, N. J., Farr, A. L., and Randall, R. J. (1951) *J. Biol. Chem.* **193**, 265-275

14. Yekta, S., Shih, I. H., and Bartel, D. P. (2004) *Science* **304**, 594-596

15. Pillai, R. S., Bhattacharyya, S. N., Artus, C. G., Zoller, T., Cougot, N., Basyuk, E., Bertrand, E., and Filipowicz, W. (2005) *Science* **309**, 1573-1576

16. He, L., and Hannon, G. J. (2004) *Nat. Rev. Genet.* **5**, 522-531

17. Chen, K., Song, F., Calin, G. A., Wei, Q., Hao, X., and Zhang, W. (2008) *Carcinogenesis* **29**, 1306-1311

18. Mishra, P. J., Humeniuk, R., Mishra, P. J., Longo-Sorbello, G. S., Banerjee, D., and Bertino, J. R. (2007) *Proc. Natl. Acad. Sci. U. S. A.* **104**, 13513-13518

19. Martin, M. M., Buckenberger, J. A., Jiang, J., Malana, G. E., Nuovo, G. J., Chotani, M., Feldman, D. S., Schmittgen, T. D., and Elton, T. S. (2007) *J. Biol. Chem.* **282**, 24262-24269

20. He, H., Jazdzewski, K., Li, W. *et al.* (2005) *Proc. Natl. Acad. Sci. U. S. A.* **102**, 19075-19080

21. Hegde, R. S., and Bernstein, H. D. (2006) *Trends Biochem. Sci.* **31**, 563-571

22. Li, Y., Bergeron, J. J., Luo, L., Ou, W. J., Thomas, D. Y., and Kang, C. Y. (1996) *Proc. Natl. Acad. Sci. U. S. A.* **93**, 9606-9611

23. Folz, R. J., Nothwehr, S. F., and Gordon, J. I. (1988) *J. Biol. Chem.* **263**, 2070-2078

24. Racchi, M., Watzke, H. H., High, K. A., and Lively, M. O. (1993) *J. Biol. Chem.* **268**, 5735-5740

25. Ito, M., Oiso, Y., Murase, T., Kondo, K., Saito, H., Chinzei, T., Racchi, M., and Lively, M. O. (1993) *J. Clin. Invest.* **91**, 2565-2571

26. Kutz, W. E., Wang, L. W., Dagoneau, N., Odrcic, K. J., Cormier-Daire, V., Traboulsi, E. I., and Apte, S. S. (2008) *Hum. Mutat.* **29**, 1425-1434

27. Boggess, K. A., Kay, H. H., Crapo, J. D., Moore, W. F., Suliman, H. B., and Oury, T. D. (2000) *Am. J. Obstet. Gynecol.* **183**, 199-205

28. Nozik-Grayck, E., Dieterle, C. S., Piantadosi, C. A., Enghild, J. J., and Oury, T. D. (2000) *Am. J. Physiol. Lung Cell. Mol. Physiol.* **279**, L977-84

29. Oury, T. D., Card, J. P., and Klann, E. (1999) *Brain Res.* **850**, 96-103

30. Chu, Y., Piper, R., Richardson, S., Watanabe, Y., Patel, P., and Heistad, D. D. (2006) *Arterioscler. Thromb. Vasc. Biol.* **26**, 1985-1990

CHAPTER IV

ECSOD ALLELE-SPECIFIC EFFECTS ON ASBESTOS-INDUCED FIBROPROLIFERATIVE LUNG DISEASE IN MICE

ABSTRACT

Previous work by others suggests that there is a strain-dependent variation in the susceptibility to inflammatory lung injury in mice. Specifically, the 129J mice appear to be more resistant to asbestos-induced pulmonary fibrosis than the C57BL/6 strain. A separate line of evidence suggests that extracellular superoxide dismutase (ecSOD) may play an important role in protecting the lung from such injuries. We have recently reported that the 129J strain of mice has an ecSOD genotype and phenotype distinctly different from those of the C57BL/6 mice. In order to identify ecSOD as a potential "asbestos-injury resistance" gene, we bred congenic mice, on the C57BL/6 background, carrying the wild type ($sod3^{wt}$) or the 129J ($sod3^{129}$) allele for ecSOD. This allowed us to examine the role of ecSOD polymorphisms in susceptibility to lung injury in an otherwise identical genetic background. As previously reported, asbestos administration resulted in a loss of ecSOD activity and protein from lung tissue of both congenic strains, but the lung ecSOD activity remained significantly higher in $sod3^{129}$ mice. As expected, asbestos treatment resulted in a significant recovery of ecSOD protein in bronchoalveolar lavage fluid (BALF). The BALF of $sod3^{129}$ mice also had significantly lower levels of proteins and inflammatory cells, especially neutrophils, accompanied by a significantly lower extent of lung injury, as measured by a pathology index score or hydroxyproline content. Our studies thus identify ecSOD as an important anti-inflammatory gene, responsible for most if not all of the resistance to asbestos-induced lung injury reported for the 129 strain of mice. The congenic mice

therefore represent a very useful model to study the role of this enzyme in other inflammatory diseases. Polymorphisms in human ecSOD have also been reported and it appears logical to assume that such variations may have a profound effect on disease susceptibility.

INTRODUCTION

Inhalation of asbestos fibers has long been known to cause asbestosis, pleural diseases, lung cancer, malignant mesothelioma and other cancers [1-3]. Asbestosis, a form of interstitial lung disease and one of the most frequent diseases caused by asbestos exposure, is characterized by inflammation and tissue fibrosis. It is a chronic, debilitating disease that leads to significant morbidity and mortality [2]. Although occupational exposures to asbestos fibers has decreased in recent years, the 20 to 40 year delay from exposure to manifestation of disease has resulted in increased incidence of asbestosis in exposed populations [1, 4, 5]. Thus, this disease currently is and will remain a significant health problem.

In the last 20 years, much work has been done to investigate both the pathogenesis and treatment of asbestos-related diseases. Nevertheless, many aspects remain poorly understood. A number of studies suggest that reactive oxygen species (ROS)-mediated inflammation and tissue damage contribute to the development and progression of interstitial pulmonary fibrosis (reviewed in [6, 7]). Previous studies have demonstrated that asbestos fibers, particularly of the amphibole class, can cause oxidative damage to the lung, primarily through the infiltration of the activated macrophages and neutrophils [8-10], although asbestos fibers can also directly generate ROS via reactive surface iron [11, 12]. In addition, over-expression of a number of antioxidant enzymes, including manganese superoxide dismutase and catalase [13, 14], as well as the addition of iron chelators [15] have been shown to be protective in a number of models of asbestos-induced lung disease.

The antioxidant enzyme extracellular superoxide dismutase (ecSOD) is the most abundant extracellular antioxidant in the lung [16-18]. This enzyme exists as a 135 kDa

homotetramer composed of four 28 kDa subunits. EcSOD in the lung is bound to extracellular matrix (ECM) components through interaction with a positively charged heparin- binding domain located at the C-terminus of the enzyme (reviewed in [19]).

Exposure of mice to a variety of injurious agents, including asbestos fibers, leads to the development of pulmonary fibrosis [7, 20, 21]. This is accompanied by loss of ecSOD from the alveolar septa and accumulation of the enzyme in the BALF [22, 23]. Evidence suggests that release of the enzyme may be mediated by proteolytic cleavage of the heparin-binding domain by proteases of neutrophil and macrophage origin [24, 25].

While it is not clear whether loss of ecSOD contributes to and/or is a result of the ongoing pathology, the former seems to be the case, as lung pathology is significantly exaggerated in ecSOD knockout mice [26, 27]. Recent studies indicate that inhibition of oxidative fragmentation of ECM probably represents one mechanism by which ecSOD inhibits inflammation in response to lung injury [28].

It should be noted that the 129P3/J (or 129J) mice are significantly more resistant to asbestos-induced pulmonary fibrosis than the C57BL/6 mice [29-31]. This phenotype is also associated with reduced expression of pro-fibrotic cytokines at sites of fiber deposition. Since the 129 strain of mice differs from the C57BL/6 strain in a number of other genes, finding the "susceptibility" gene(s) by a direct comparison of the two strains would be a difficult if not impossible task.

We [32] previously reported the existence of an allelic variant of ecSOD found only in the 129P3/J strain of mice (*129*). Relative to the wild-type allele (*wt*), found in the C57BL/6 and other strains, this variant yields mRNA with a 10 bp deletion in the 3' untranslated region (UTR) and several point mutations in the coding sequence. Two of the point mutations result in amino

acid substitutions: one within the signal peptide (N21D) and one within the catalytic region (A186S). This genotype has a profound effect on the ecSOD phenotype: both, plasma ecSOD levels and activities in the 129P3/J mice are 2- 3 fold higher than those in the C57BL/6 mice suggesting no apparent change in specific activity. In order to investigate further the role of ecSOD as a "susceptibility" gene in asbestos- induced injury, we generated congenic mice expressing either the *129* or *wt* allele on the C57BL6 background (C57.129-*sod3*) [33]. The congenic mice that express the 129 allele ($sod3^{129}$) recapitulate the phenotypic differences in an allelespecific manner, in terms of free and heparin-releasable plasma ecSOD levels, activities, tissue enzyme distribution and relative tissue mRNA abundance [33]. These results suggest that most if not all of the observed ecSOD phenotype is allele-driven. This animal model enabled us to investigate specifically the role of ecSOD in an otherwise essentially identical (>99.9%) genetic environment.

We now present evidence that substituting the ecSOD allele from 129P3/J on the genetic background of a C57BL/6 mouse significantly changes the response of the animal to a fibrotic stimulus; specifically, the congenic $sod3^{129}$ mice are significantly protected against asbestos-induced inflammation and fibrotic lung disease relative to $sod3^{wt}$ mice. Our findings demonstrate that a single gene polymorphism can modulate disease susceptibility and highlight the significance of active ecSOD in the amelioration of asbestos-induced lung disease.

METHODS

Animals & asbestos exposure: 8-10 weeks old female congenic *sod3*^{wt} and *sod3*^{129} mice, derived as previously described [33], were treated with 0.1 mg NIEHS crocidolite asbestos (> 10 μm in length) or 0.9% saline by intratracheal instillation, as previously described [23, 25]. Mice were euthanized at 14 days post-treatment. BALF was obtained by intratracheal instillation and recovery of 1 ml of 0.9% saline. Lungs were perfused with ice-cold PBS via cardiac puncture to remove residual blood. Lungs were removed and either flash-frozen in liquid nitrogen and stored at -80 ºC until used for biochemical analysis or inflation-fixed with 10% formalin for histological analysis. All animals were treated by experimental protocols approved by the UNT HSC Institutional Animal Care and Use Committee.

Lung ecSOD activity: Frozen lungs were ground to a fine powder in liquid nitrogen, and homogenized with 50 mM potassium phosphate buffer containing 0.3 M KBr and 3 mM EDTA, pH 7.4 containing a 1:1000 dilution of a protease inhibitor cocktail (100 μM 4-(2- aminoethyl) benzensulfonyl fluoride, 10 μM leupeptin, 10 μM E-64, 1 μM bestatin, 15 nM aprotinin, 1.0 μM pepstatin-A). The protein concentration of tissue homogenates was determined by Lowry assay [34]. ecSOD was partially purified using ConA Sepharose (Sigma) as described [35], using 2mg of lung homogenate protein. The activity of ecSOD (released from ConA) was determined using an assay based on the oxidation of NAD(P)H [36]. Dismutase activity was estimated from a standard curve constructed by measuring the activity of increasing and known amounts of Cu/Zn SOD (Sigma, cat. #S2515). Activities are therefore expressed as ng of Cu/Zn SOD equivalents.

Western blots: Rabbit anti-mouse ecSOD antiserum was produced against a synthetic mouse-specific 21-amino acid peptide corresponding to the N-terminus of the mature protein, as

previously described [32]. 20μL aliquots of BALF or 10μg of lung homogenate protein were dissolved and boiled in Laemmli buffer containing 5% β- mercaptoethanol [37] for 5 min, separated by 12% SDS-PAGE at 100 V for 3.5 hours and transferred to polyvinylidine fluoride membranes (Bio-Rad) for 2 hours. After blocking in 5% milk TBST for 1 hour, the membranes were incubated with the primary antibody against ecSOD (1:20,000) and/or β-actin (1:5,000) rabbit anti-mouse antiserum (Sigma) overnight at 4 ˚C. Secondary antibodies (goat anti-rabbit IgG), conjugated to horseradish peroxidase (Jackson Immunoresearch) were added for 2 hours at RT (1:5,000 dilution). ecSOD and ß-actin bands were visualized by the ECL system (Amersham) using FluorChem® FC2 Imaging System (Alpha Innotech) and densitometric analysis was done using the software supplied (AlphaEaseFC) for the instrument. Transfer efficiency between runs was checked and corrected for by using aliquots of pooled mouse lung homogenates in each of the outside lanes. Moreover, scans were also corrected for loading by detecting ß-actin in lung samples.

Analysis of BALF: Total protein in BALF was determined by Lowry assay [34]. Total cell counts in BALF were obtained using a Beckman Coulter Z1 particle counter (Beckman Coulter, Fullerton, CA). To obtain differential cell counts, total BALF cells were collected by spinning 1000xg at 4 ºC for 10 min and sorted for cell type by flow cytometry.

Flow cytometry: Collected BALF cells were incubated with anti-CD16/CD32 FcRII/III blocker at 4 ºC for 10 min. Multi-color immunofluorescence staining was performed using PE-labeled anti-mouse Ly6G (1A8), PE labeled anti-mouse SiglecF, PEcy7-labeled anti-mouse CD11b, alexafluo 488 (AF488)-labeled anti-mouse F4/80, APC-labeled antimouse CD19 and FITC-labeled anti-mouse B220 (CD45R) at 4 ºC for 30 min. After washing twice, positive cells for immunostaining were identified using the Cytomic FC500 flow cytometry analyzer (Beckman–

Coulter). Further analysis to determine proper cell population was performed using CXCP software (Beckman-Coulter). Anti-mouse antibodies for Ly6G, SiglecF, CD11b and B220 and Fc blocker were purchased from BD Biosciences (San Jose, CA). Anti-mouse antibodies for F4/80 and CD19 were purchased from Caltag® (InVitrogen Co. Carlsbad, CA).

Histological analysis: Five-micron thick lung sections from three levels (anterior, medial and posterior) were subjected to hematoxylin and eosin staining (Derm-Prep, FL, USA) and scored by Dr. Suarez (pathologist, Derm-Prep), blinded to sample groups. Individual fields were examined with a light microscope. Scoring in each level was based on the severity of bronchioles/alveolar tissue with interstitial fibrosis as well as inflammation according to the following scale: 0 = negative, 1 = minimal, 2 = moderate, 3 = moderate/severe, 4 = severe. Scores were calculated for each animal, and the group scores were averaged together for statistical comparisons.

Hydroxyproline assay: Whole lungs were dried and acid hydrolyzed in sealed oxygen purged glass ampoules containing 2 ml of 6 N HCl for 24 h at 110 ºC. Samples were centrifuged at 14,000 rpm and supernatant was taken for hydroxyproline analysis using chloramine-T, as previously described [38].

Statistical Analyses: Results from experiments are reported as means ± SEM. All quantitative data are assessed for significance using either a Student's t-test or a one-way ANOVA with Tukey's post-hoc test (GraphPad Prism). A p value < 0.05 is used to establish significance.

RESULTS

ecSOD protein levels, C-terminal processing and activity levels.

To examine the effect of the 129 allele on distribution of ecSOD protein in the lung parenchyma and airspaces after 14 days post asbestos-treatment, Western blots were performed on lung homogenates and BALF. As we previously reported [33], saline treated congenic *sod3*^{129} mice expressed higher level of ecSOD in the lung compared to *sod3*^{wt} mice (Figure 1A and 1B). Asbestos treatment resulted in decreased ecSOD protein abundance in both groups of mice after 14 days, but the decrease in the *sod3*^{129} lung was significant, while the changes were smaller in *sod3*^{wt} lungs (Figure 1B).

Following asbestos treatment both groups of mice had similar amount of ecSOD protein remaining in their lung tissues. As previously reported [23, 25, 27], there was a marked release of ecSOD into the BALF regardless of ecSOD genotype (Figure 1C); the extent of asbestos-induced ecSOD protein release was not significantly different in the two treatment groups.

As expected, the enzyme recovered from the BALF from both treatment groups was predominantly in the cleaved form, which lacks the heparin-binding domain (Figure 1A and 1D). In addition, the ratio of cleaved to uncleaved (full length) subunits of ecSOD increased in the lungs as well as BALF after asbestos-treatment, regardless of the ecSOD genotype (Figure 1D).

Asbestos-elicited changes in lung ecSOD enzyme level were accompanied by similar changes in ecSOD activities, as shown in Figure 2. Lung ecSOD activities in saline treated mice were higher in *sod3*^{129} mice than in *sod3*^{wt} mice and asbestos treatment significantly reduced this activity in both groups; significant differences in ecSOD activities however remain. It should be noted that the decrease in lung ecSOD activity of the *sod3*^{wt} mice was significant, while the

decrease in enzyme level was not, suggesting a decrease in lung ecSOD specific activity. These observations suggest that asbestos treatment resulted in ecSOD of a higher relative "specific activity" in *sod3*^{129} mice.

Sod3*^{129} *mice exhibit reduced levels of acute lung injury markers.

To evaluate the effect of the 129 allele on asbestos-induced lung injury, BALF from saline- or asbestos- treated *sod3*^{129} or *sod3*^{wt} mice was analyzed for markers of acute lung injury. The two groups of saline-treated mice did not differ in BALF protein or cell content (Figure 3 A and B). As expected, asbestos treatment resulted in a significant increase in both markers in BALF isolated from asbestos- treated *sod3*^{129} or *sod3*^{wt} mice. However, both the amount of protein and the total number of inflammatory cells in BALF isolated from asbestos-treated *sod3*^{129} mice were significantly lower (~30% decrease) than those in BALF from *sod3*^{wt} mice (304.0±30.16 μg vs. 444.0±45.93 μg and 2.16±0.24 x 106 vs. 3.27±0.37 x 106 cells, respectively).

Flow cytometry further revealed the presence of macrophages, B cells, neutrophils and eosinophils in the BALF of both groups of mice (Figure 4). There were no significant differences in the numbers of each cell type found in BALF of saline-treated mice of either ecSOD genotype. Macrophages were the dominant cell type in both groups of mice. Asbestos treatment induced a profound increase in eosinophils and neutrophils, and a marked reduction in macrophages. The relative increase in neutrophils and, to lesser extent eosinophils was markedly reduced in *sod3*^{129} mice. These results suggest a reduced inflammatory response to asbestos in the *sod3*^{129} lungs. In agreement with previous study [27], asbestos instillation reduced the macrophage content in BALF of both congenic mice (Figure 4A).

Asbestos-induced lung fibrosis is reduced in sod3^{129} mice

To evaluate the effect of the129 allele on asbestos-induced lung fibrosis, lungs from saline- or asbestos- treated mice were assessed for fibrosis. Analysis of lung tissue pathology from asbestos-treated *sod3^{129}* and *sod3^{wt}* mice indicated that both strains respond to the presence of asbestos fibers by mounting an inflammatory response that progress into patchy, heterogeneous fibrotic lesions by 14 days post-treatment (Figure 5A). A semi-quantitative assessment of lung tissue pathology, shown in Figure 5B, indicated a significantly reduced (~20%) fibrosis in the *sod3^{129}* lungs (2.64 ± 0.21) relative to the *sod3^{wt}* mice (3.20 ± 0.18). Saline treatment did not lead to significant fibrosis in either group of mice.

The extent of fibrosis in the lungs of asbestos-treated animals was also evaluated by hydroxyproline level- an index of collagen deposition. In agreement with the pathology index data, hydroxyproline levels were also significantly elevated in asbestos- treated animals relative to saline treated controls (Figure 5C). Moreover, the hydroxyproline level in asbestos- treated *sod3^{129}* mice (109.21 ± 4.46 μg / lung) was significantly lower when compared to that of the lungs of *sod3^{wt}* mice (124.0 ± 4.82 μg / lung).

Figure 1. The effect of asbestos treatment on ecSOD protein in lung tissue and BALF.

Lung and BALF ecSOD isolated from saline and asbestos-exposed *sod3*^{129} (grey bars) and *sod3*^{wt} (solid bars) mice 14 days after treatment (5-7 mice per group). Western blot (A) was performed using 10 μg of total lung protein or 20 μl of BALF and densitometric analyses of lung and BALF ecSOD are shown in B and C, respectively. Lung ecSOD densitometry was normalized to β-actin as an internal loading control. (D) The ratio of cleaved to full-length forms of ecSOD in lung and BALF. Error bars represent +SEM.

* $p < 0.05$ versus *sod3*^{wt} mice;

# $p < 0.05$ versus saline control;

+ $p < 0.05$ versus lung.

Figure 1.

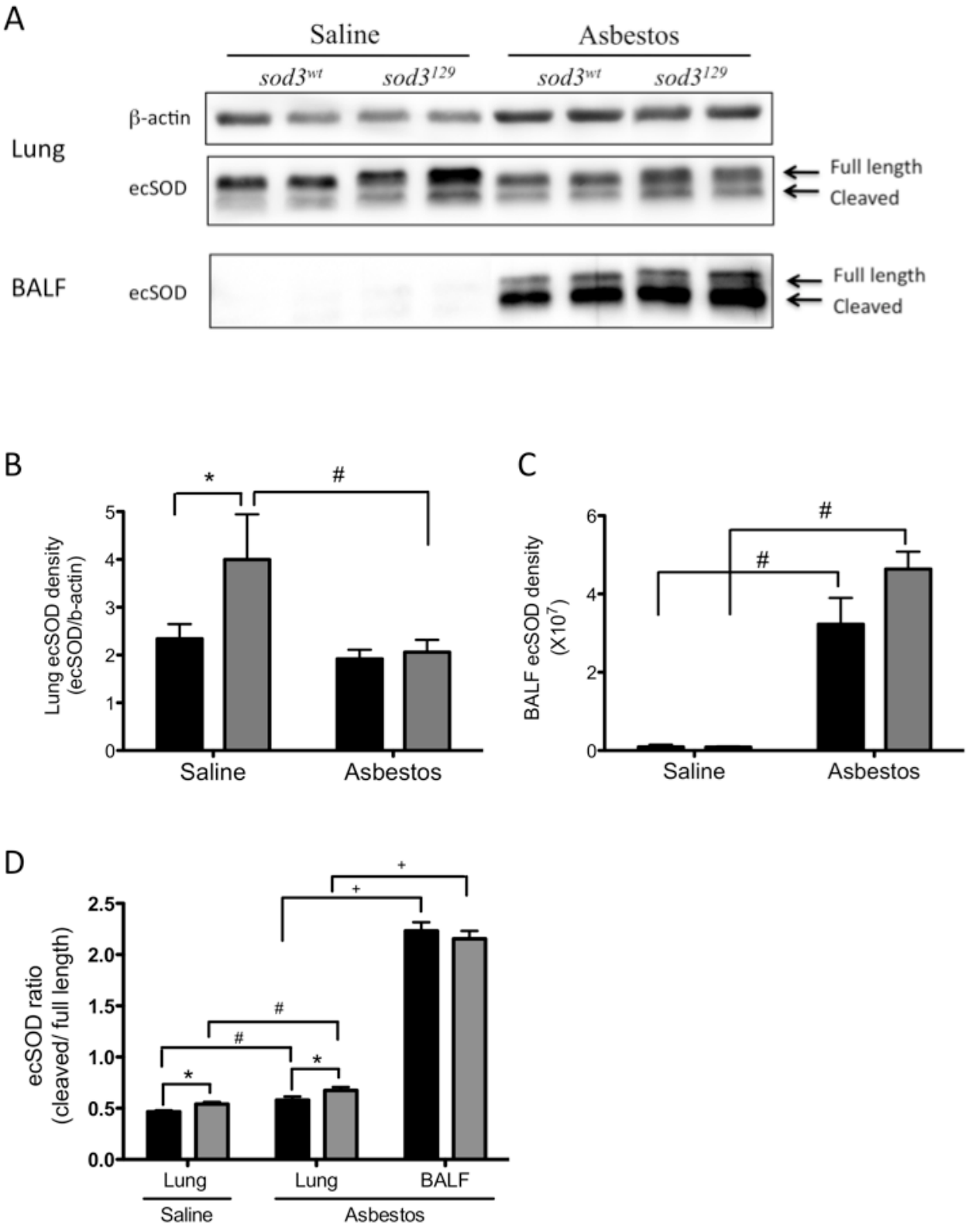
A
Saline
Asbestos
sod3wt
sod3129
sod3wt
sod3129
β-actin
Lung
ecSOD
Full length
Cleaved
BALF
ecSOD
Full length
Cleaved
B
Lung ecSOD density (ecSOD/b-actin)
Saline
Asbestos
C
BALF ecSOD density (X10^7)
Saline
Asbestos
D
ecSOD ratio (cleaved/ full length)
Lung
Lung
BALF
Saline
Asbestos

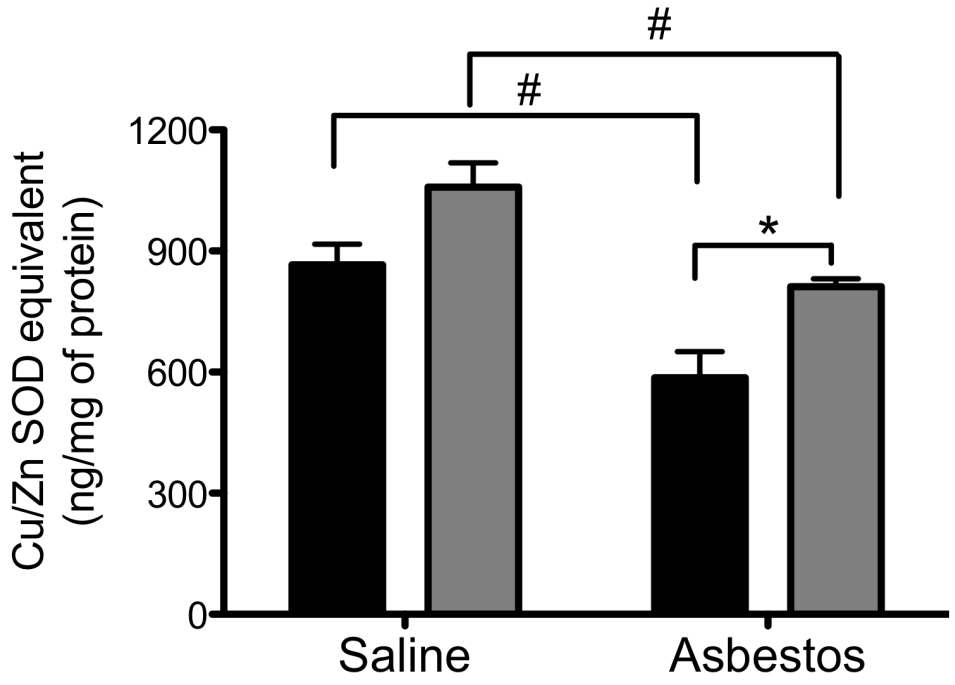

Figure 2. Lung ecSOD activity in saline- and asbestos- treated mice.

Activities of ecSOD, isolated from lung homogenates by ConA-affinity chromatography from control and asbestos- treated *sod3*^{129} (grey bars) and *sod3*^{wt} (solid bars) mice (5-7 mice per group). Error bars represent +SEM.

* $p < 0.05$ versus *sod3*^{wt} mice;

# $p < 0.05$ versus saline control.

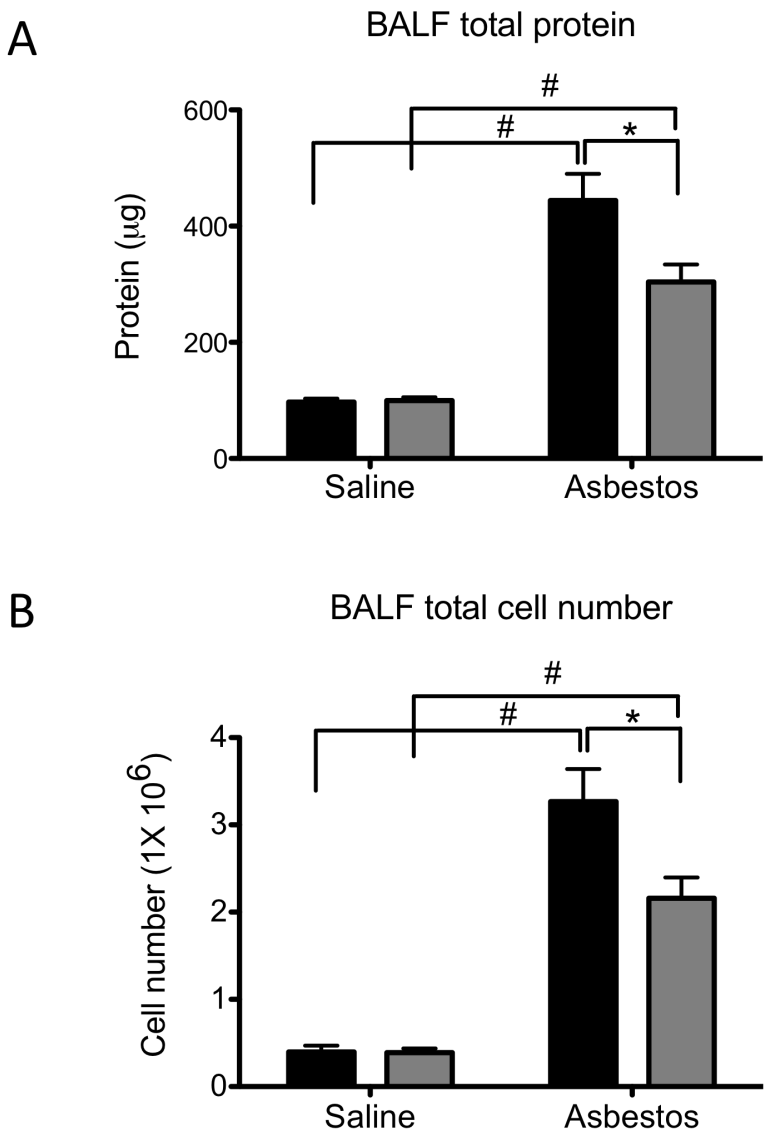

Figure 3. Total protein (A) and cell content (B) of BALF isolated from saline and asbestos-treated mice.

Total protein content (A) and cell content (B) in BALF isolated from saline- and asbestos-treated *sod3*^{129} (grey bars) and *sod3*^{wt} (solid bars) mice (5-7 mice per group).

Error bars represent +SEM.

* $p < 0.05$ versus *sod3*^{wt} mice;

# $p < 0.05$ versus saline control.

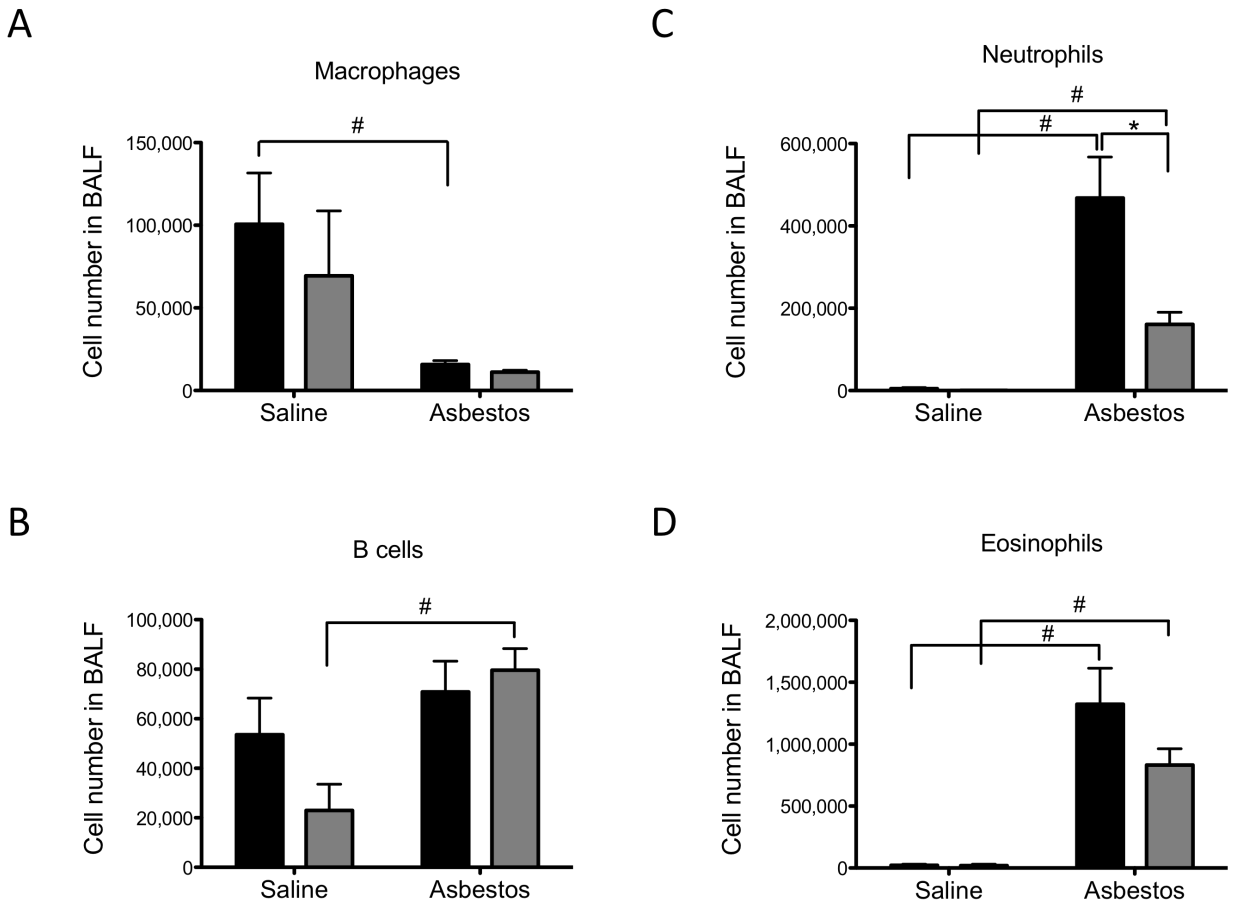

Figure 4. Analysis of BALF cell content by flow cytometry.

Macrophages (A), B cells (B), neutrophils (C) and eosinophils (D) in BALF isolated from saline- and asbestos- treated *sod3*^{129} (grey bars) and *sod3*^{wt} (solid bars) mice (5-7 mice per group). Error bars represent +SEM.

* $p < 0.05$ versus *sod3*^{wt} mice;

# $p < 0.05$ versus saline control.

Figure 5. H & E staining and typical micrographs (A), pathology indices (B) and hydroxyproline content of lung tissues isolated from saline- or asbestostreated mice.

Hematoxylin and eosin (H & E) staining was performed on 5 μ thick sections of lung tissue, obtained from saline- and asbestos- treated mice, as described in Methods. Typical micrographs (40X magnification) are shown in (A). Mean pathology index scores (B) of lung tissue sections were determined, as described in Methods. The extent of collagen deposition, as measured by hydroxyproline content of lung tissue is shown in (C). Lung tissue from saline- and asbestos-treated *sod3*^{129} (grey bars) *and sod3*^{wt} (solid bars) was used (5-7 mice per group). Error bars represent +SEM.

* $p < 0.05$ versus *sod3*^{wt} mice;

# $p < 0.05$ versus saline control.

Figure 5.

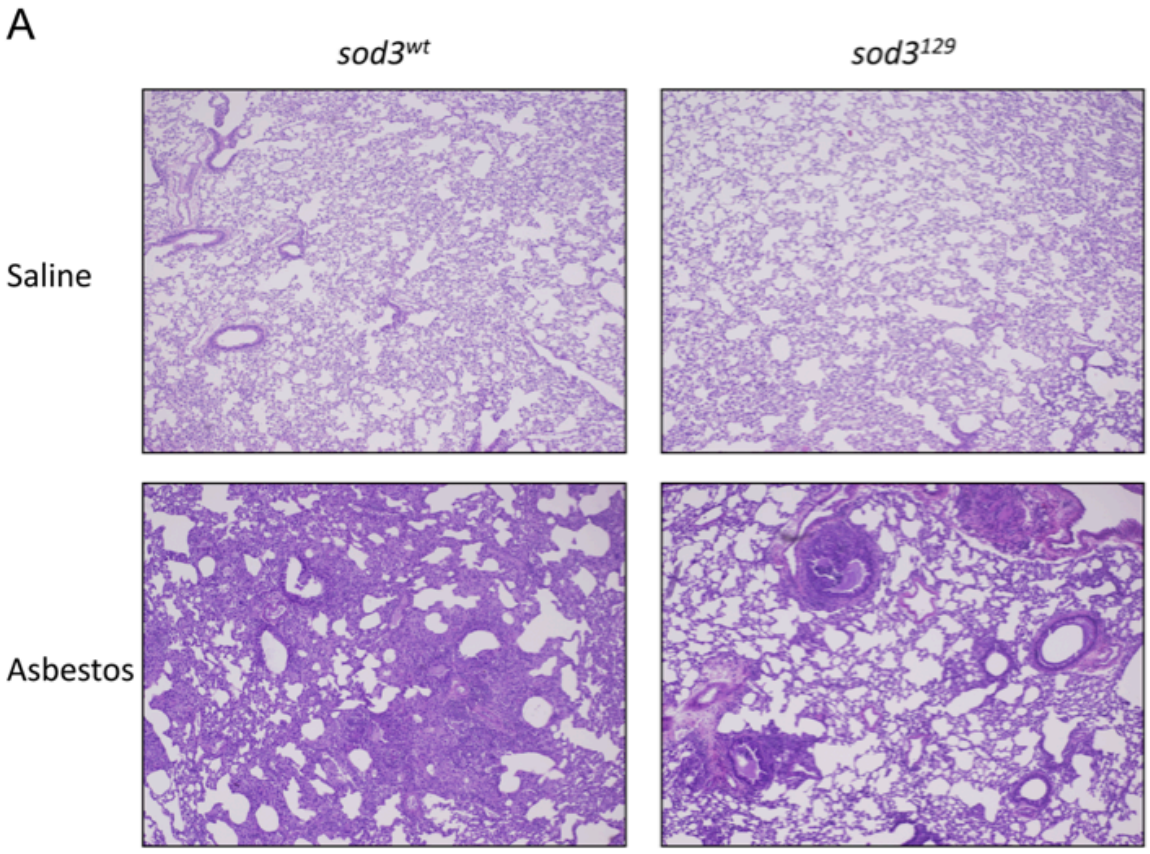

Figure 5. continued

B

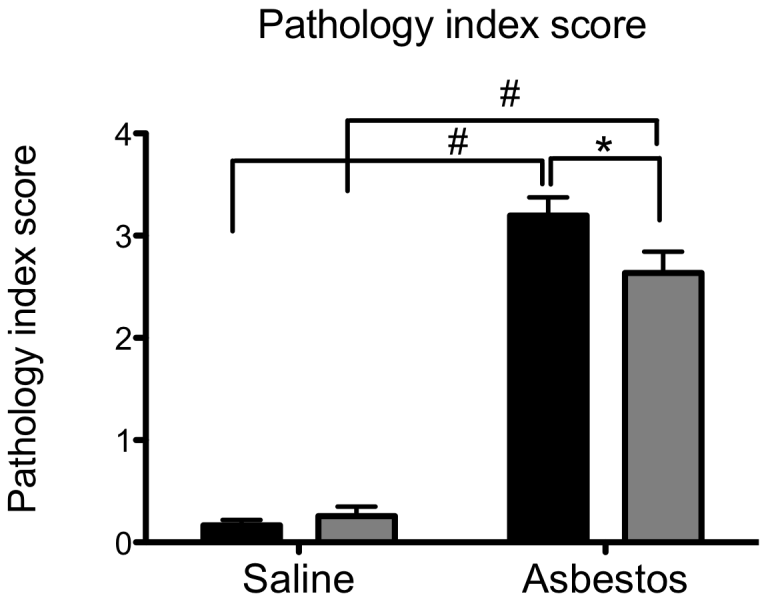

C

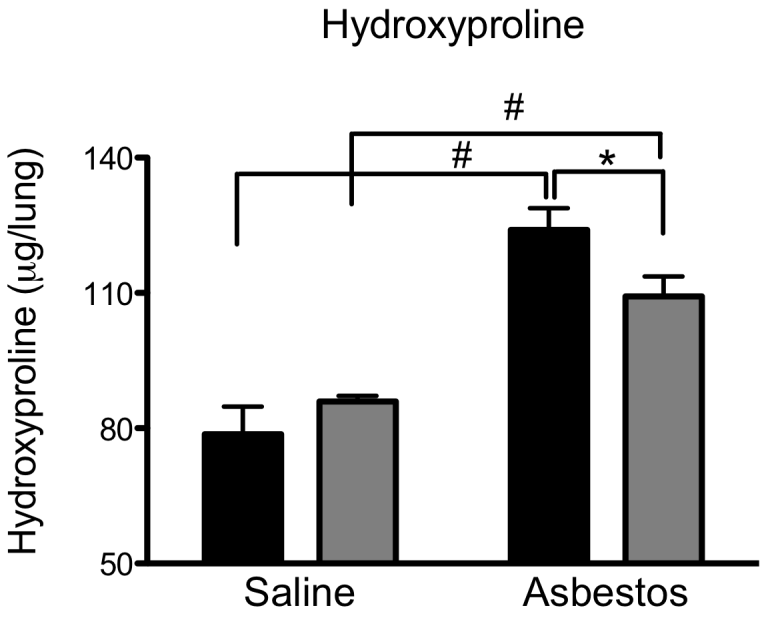

DISCUSSION

Strain-specific differences in susceptibility to asbestos- induced injury have been previously reported. Brass et al. have previously shown that 129P3/J (or 129J) mice develop a reduced fibro-proliferative response to inhaled asbestos, relative to 'fibrosis sensitive' C57BL/6 mice [29]. They also showed that primary lung fibroblasts from the 129J mice proliferate more slowly, make less collagen, and have a reduced response to pro-fibrotic growth factors [30]. In addition, even with direct application of pro-fibrotic TGF-β to the lung parenchyma, the 129 mice have a reduced degree of disease and a delay in the development of fibrogenesis [31]. To-date there is little or no information regarding the genetic loci responsible for the observed differences between the strains.

In an independent line of research, studies have described a protective role for ecSOD in acute and fibrotic lung injuries [26]. An acute loss of this enzyme by a conditional knockout model using Cre-Lox technology leads to severe lung damage in the presence of ambient air [39]. A protective role for ecSOD is further supported by the fact that ecSOD KO mice are significantly more susceptible to injuries that cause pulmonary fibrosis, including asbestos exposure [26, 27, 40].

Given the strain-specific response to asbestos, the potential importance of ecSOD and our recent report that the 129 strain of mice express an allelic variant of ecSOD of a profoundly different phenotype, we decided to breed congenic mice, on the C57 background, which express either allele of ecSOD [33]. This experimental model enables us to examine the role of ecSOD specifically, independent of the genomic environment, in a number of inflammatory diseases.

Our results support the previous observations that increased levels of ecSOD in the lung

of mice attenuate inflammation [41-43]. The *sod3*^{129} mice have significantly higher lung ecSOD activity even after asbestos treatment. Although asbestos treatment reduced the ecSOD enzyme protein and activities in both congenic strains, the reduction in protein in the *sod3*^{wt} lungs is less extensive than that of *sod3*^{129} lungs and, more importantly, less than the observed loss of activity. Analysis of the BALF as well as histological analysis of the tissue suggests that the lack of significant change in ecSOD protein level of the *sod3*^{wt} lungs is likely due to the compensatory acquisition of "exogenous" ecSOD from the large number of infiltrating inflammatory cells. The inflammatory cell- derived enzyme appears to be rapidly degraded/inactivated in the *sod3*^{wt} strain, possibly by an oxidative stress-mediated mechanism. Indeed, previous work by Tan et al clearly demonstrates that the influx of inflammatory/immune cells into lungs [25] can be a source of substantial ecSOD activity and amount after asbestos-treatment. We suggest that the increased initial ecSOD activity in the *sod3*^{129} mice reduces the asbestos-induced oxidative stress and the resulting magnitude of inflammation.

Our data are also in accord with previous observations that ecSOD specifically inhibits neutrophil influx in response to asbestos [27]. Several studies have shown that ecSOD may inhibit pulmonary inflammation, specifically neutrophil chemotaxis, in part by preventing superoxide- mediated fragmentation of ECM components such as hyaluronan and syndecan-1 [28, 44, 45]. A similar mechanism is likely operating in our experiments: the increased initial activity of ecSOD in *sod3*^{129} lungs quenches the ROS induced by asbestos which, in turn, leads to a reduction in the oxidative fragmentations of ECM, decreased recruitment of neutrophils and decreased fibrosis.

Our results demonstrate that ecSOD is a prominent "fibrosis-resistance/anti-inflammatory" gene, responsible for the increased resistance of the 129 strain of mice to lung

injury and fibrosis. Indeed, expanding our observations to those of Fattman et al. [27], these studies cover a range of mice with high (*sod3*^{129}), intermediate (*sod3*^{wt}) and no (ecSOD KO) enzyme activity on an identical (C57BL/6) genetic background. It is clear that the extent of lung injury in response to asbestos is inversely proportional to lung ecSOD activity. Our recent studies demonstrate that the increased expression of the *129* form of ecSOD is allele-driven: the *129* ecSOD phenotype is observed even when immersed in the C57 genome [33].

Human ecSOD polymorphism is associated with a number of diseases, including chronic obstructive pulmonary disease (COPD), ischemic heart disease, atherosclerosis and diabetes [46-49]. While protective against COPD, the R213G substitution, associated with elevated ecSOD levels in plasma, is associated with increased risk of ischemic heart disease in heterozygotes [48, 50, 51]. The A40T polymorphism appears to be associated with susceptibility to Type 2 diabetes, and insulin resistance and hypertension [49]. Clearly, variations in ecSOD expression due to polymorphism may play a major role in disease susceptibility in humans.

In conclusion, ecSOD gene polymorphism clearly modulates susceptibility to asbestos-induced lung injury in mice. The congenic mice used in this study may provide an excellent model to examine the role of ecSOD in other diseases involving oxidative stress and an inflammatory response.

REFERENCE

[1] Kamp, D. W.; Weitzman, S. A. Asbestosis: Clinical spectrum and pathogenic mechanisms. *Proc. Soc. Exp. Biol. Med.***214:**12-26; 1997.

[2] Manning, C. B.; Vallyathan, V.; Mossman, B. T. Diseases caused by asbestos: Mechanisms of injury and disease development. *Int. Immunopharmacol.***2:**191-200; 2002.

[3] Kamp, D. W. Asbestos-induced lung diseases: An update. *Transl. Res.***153:**143-152; 2009.

[4] Murphy, R. L.,Jr. The diagnosis of nonmalignant diseases related to asbestos. *Am. Rev. Respir. Dis.***136:**1516-1517; 1987.

[5] Selikoff, I. J.; Hammond, E. C.; Seidman, H. Latency of asbestos disease among insulation workers in the united states and canada. *Cancer***46:**2736-2740; 1980.

[6] Fattman, C. L.; Chu, C. T.; Oury, T. D. Experimental models of asbestos-related diseases. *In* Roggli, V. L., Sporn, T., and Oury, T. D., editors. Pathology of Asbestos-Associated Diseases, 2nd ed. Little, Brown and Company, Boston ; 2002.

[7] Kinnula, V. L.; Fattman, C. L.; Tan, R. J.; Oury, T. D. Oxidative stress in pulmonary fibrosis: A possible role for redox modulatory therapy. *Am. J. Respir. Crit. Care Med.***172:**417-422; 2005.

[8] Dorger, M.; Allmeling, A. M.; Kiefmann, R.; Munzing, S.; Messmer, K.; Krombach, F. Early inflammatory response to asbestos exposure in rat and hamster lungs: Role of inducible nitric oxide synthase. *Toxicol. Appl. Pharmacol.***181:**93-105; 2002.

[9] Hansen, K.; Mossman, B. T. Generation of superoxide ($O2^{-\cdot}$) from alveolar macrophages exposed to asbestiform and nonfibrous particles. *Cancer Res.***47:**1681-1686; 1987.

[10] Rola-Pleszczynski, M.; Rivest, D.; Berardi, M. Asbestos-induced chemiluminescence response of human polymorphonuclear leukocytes. *Environ. Res.***33:**1-6; 1984.

[11] Hardy, J. A.; Aust, A. E. The effect of iron binding on the ability of crocidolite asbestos to catalyze DNA single-strand breaks. *Carcinogenesis***16:**319-325; 1995.

[12] Schapira, R. M.; Ghio, A. J.; Effros, R. M.; Morrisey, J.; Dawson, C. A.; Hacker, A. D. Hydroxyl radicals are formed in the rat lung after asbestos instillation in vivo. *Am. J. Respir. Cell Mol. Biol.***10:**573-579; 1994.

[13] Mossman, B. T.; Marsh, J. P.; Sesko, A.; Hill, S.; Shatos, M. A.; Doherty, J.; Petruska, J.; Adler, K. B.; Hemenway, D.; Mickey, R. Inhibition of lung injury, inflammation, and interstitial pulmonary fibrosis by polyethylene glycol-conjugated catalase in a rapid inhalation model of asbestosis. *Am. Rev. Respir. Dis.***141:**1266-1271; 1990.

[14] Mossman, B. T.; Surinrut, P.; Brinton, B. T.; Marsh, J. P.; Heintz, N. H.; Lindau-Shepard, B.; Shaffer, J. B. Transfection of a manganese-containing superoxide dismutase gene into hamster tracheal epithelial cells ameliorates asbestos-mediated cytotoxicity. *Free Radic. Biol. Med.***21:**125-131; 1996.

[15] Panduri, V.; Weitzman, S. A.; Chandel, N.; Kamp, D. W. The mitochondria-regulated death pathway mediates asbestos-induced alveolar epithelial cell apoptosis. *Am. J. Respir. Cell Mol. Biol.***28:**241-248; 2003.

[16] Marklund, S. L. Extracellular superoxide dismutase and other superoxide dismutase isoenzymes in tissues from nine mammalian species. *Biochem. J.***222:**649-655; 1984.

[17] Marklund, S. L. Extracellular superoxide dismutase in human tissues and human cell lines. *J. Clin. Invest.***74:**1398-1403; 1984.

[18] Marklund, S. L. Human copper-containing superoxide dismutase of high molecular weight. *Proc. Natl. Acad. Sci. U. S. A.***79:**7634-7638; 1982.

[19] Fattman, C. L.; Schaefer, L. M.; Oury, T. D. Extracellular superoxide dismutase in biology and medicine. *Free Radic. Biol. Med.***35:**236-256; 2003.

[20] Cantin, A. M.; North, S. L.; Fells, G. A.; Hubbard, R. C.; Crystal, R. G. Oxidant-mediated epithelial cell injury in idiopathic pulmonary fibrosis. *J. Clin. Invest.***79:**1665-1673; 1987.

[21] Thannickal, V. J.; Toews, G. B.; White, E. S.; Lynch, J. P.,3rd; Martinez, F. J. Mechanisms of pulmonary fibrosis. *Annu. Rev. Med.***55:**395-417; 2004.

[22] Fattman, C. L.; Chu, C. T.; Kulich, S. M.; Enghild, J. J.; Oury, T. D. Altered expression of extracellular superoxide dismutase in mouse lung after bleomycin treatment. *Free Radic. Biol. Med.***31:**1198-1207; 2001.

[23] Tan, R. J.; Fattman, C. L.; Watkins, S. C.; Oury, T. D. Redistribution of pulmonary EC-SOD after exposure to asbestos. *J. Appl. Physiol.***97:**2006-2013; 2004.

[24] Tan, R. J.; Fattman, C. L.; Niehouse, L. M.; Tobolewski, J. M.; Hanford, L. E.; Li, Q.; Monzon, F. A.; Parks, W. C.; Oury, T. D. Matrix metalloproteinases promote inflammation and fibrosis in asbestos-induced lung injury in mice. *Am. J. Respir. Cell Mol. Biol.***35:**289-297; 2006.

[25] Tan, R. J.; Lee, J. S.; Manni, M. L.; Fattman, C. L.; Tobolewski, J. M.; Zheng, M.; Kolls, J. K.; Martin, T. R.; Oury, T. D. Inflammatory cells as a source of airspace extracellular superoxide dismutase after pulmonary injury. *Am. J. Respir. Cell Mol. Biol.***34:**226-232; 2006.

[26] Fattman, C. L.; Chang, L. Y.; Termin, T. A.; Petersen, L.; Enghild, J. J.; Oury, T. D. Enhanced bleomycin-induced pulmonary damage in mice lacking extracellular superoxide dismutase. *Free Radic. Biol. Med.***35:**763-771; 2003.

[27] Fattman, C. L.; Tan, R. J.; Tobolewski, J. M.; Oury, T. D. Increased sensitivity to asbestos-induced lung injury in mice lacking extracellular superoxide dismutase. *Free Radic. Biol. Med.***40:**601-607; 2006.

[28] Gao, F.; Koenitzer, J. R.; Tobolewski, J. M.; Jiang, D.; Liang, J.; Noble, P. W.; Oury, T. D. Extracellular superoxide dismutase inhibits inflammation by preventing oxidative fragmentation of hyaluronan. *J. Biol. Chem.***283:**6058-6066; 2008.

[29] Brass, D. M.; Hoyle, G. W.; Poovey, H. G.; Liu, J. Y.; Brody, A. R. Reduced tumor necrosis factor-alpha and transforming growth factor-beta1 expression in the lungs of inbred mice that fail to develop fibroproliferative lesions consequent to asbestos exposure. *Am. J. Pathol.***154:**853-862; 1999.

[30] Brass, D. M.; Tsai, S. Y.; Brody, A. R. Primary lung fibroblasts from the 129 mouse strain exhibit reduced growth factor responsiveness in vitro. *Exp. Lung Res.***27:**639-653; 2001.

[31] Warshamana, G. S.; Pociask, D. A.; Sime, P.; Schwartz, D. A.; Brody, A. R. Susceptibility to asbestos-induced and transforming growth factor-beta1-induced fibroproliferative lung

disease in two strains of mice. *Am. J. Respir. Cell Mol. Biol.***27:**705-713; 2002.

[32] Pierce, A.; Whitlark, J.; Dory, L. Extracellular superoxide dismutase polymorphism in mice. *Arterioscler. Thromb. Vasc. Biol.***23:**1820-1825; 2003.

[33] Jun, S.; Pierce, A.; Dory, L. Extracellular superoxide dismutase polymorphism in mice: Allele-specific effects on phenotype. *Free Radic. Biol. Med.***48:**590-596; 2010.

[34] Lowry, O. H.; Rosebrough, N. J.; Farr, A. L.; Randall, R. J. Protein measurement with the folin phenol reagent. *J. Biol. Chem.***193:**265-275; 1951.

[35] Marklund, S. L. Analysis of extracellular superoxide dismutase in tissue homogenates and extracellular fluids. *Methods Enzymol.***186:**260-265; 1990.

[36] Paoletti, F.; Mocali, A. Determination of superoxide dismutase activity by purely chemical system based on NAD(P)H oxidation. *Methods Enzymol.***186:**209-220; 1990.

[37] Laemmli, U. K. Cleavage of structural proteins during the assembly of the head of bacteriophage T4. *Nature***227:**680-685; 1970.

[38] Woessner, J. F.,Jr. The determination of hydroxyproline in tissue and protein samples containing small proportions of this imino acid. *Arch. Biochem. Biophys.***93:**440-447; 1961.

[39] Gongora, M. C.; Lob, H. E.; Landmesser, U.; Guzik, T. J.; Martin, W. D.; Ozumi, K.; Wall, S. M.; Wilson, D. S.; Murthy, N.; Gravanis, M.; Fukai, T.; Harrison, D. G. Loss of extracellular superoxide dismutase leads to acute lung damage in the presence of ambient air: A potential mechanism underlying adult respiratory distress syndrome. *Am. J. Pathol.***173:**915-926; 2008.

[40] Carlsson, L. M.; Jonsson, J.; Edlund, T.; Marklund, S. L. Mice lacking extracellular superoxide dismutase are more sensitive to hyperoxia. *Proc. Natl. Acad. Sci. U. S. A.***92:**6264-6268; 1995.

[41] Bowler, R. P.; Nicks, M.; Tran, K.; Tanner, G.; Chang, L. Y.; Young, S. K.; Worthen, G. S. Extracellular superoxide dismutase attenuates lipopolysaccharide-induced neutrophilic inflammation. *Am. J. Respir. Cell Mol. Biol.***31:**432-439; 2004.

[42] Folz, R. J.; Abushamaa, A. M.; Suliman, H. B. Extracellular superoxide dismutase in the airways of transgenic mice reduces inflammation and attenuates lung toxicity following hyperoxia. *J. Clin. Invest.***103:**1055-1066; 1999.

[43] Bowler, R. P.; Nicks, M.; Warnick, K.; Crapo, J. D. Role of extracellular superoxide dismutase in bleomycin-induced pulmonary fibrosis. *Am. J. Physiol. Lung Cell. Mol. Physiol.***282:**L719-26; 2002.

[44] Kliment, C. R.; Englert, J. M.; Gochuico, B. R.; Yu, G.; Kaminski, N.; Rosas, I.; Oury, T. D. Oxidative stress alters syndecan-1 distribution in lungs with pulmonary fibrosis. *J. Biol. Chem.***284:**3537-3545; 2009.

[45] Kliment, C. R.; Tobolewski, J. M.; Manni, M. L.; Tan, R. J.; Enghild, J.; Oury, T. D. Extracellular superoxide dismutase protects against matrix degradation of heparan sulfate in the lung. *Antioxid. Redox Signal.***10:**261-268; 2008.

[46] Siedlinski, M.; van Diemen, C. C.; Postma, D. S.; Vonk, J. M.; Boezen, H. M. Superoxide dismutases, lung function and bronchial responsiveness in a general population. *Eur. Respir. J.***33:**986-992; 2009.

[47] Yamada, H.; Yamada, Y.; Adachi, T.; Fukatsu, A.; Sakuma, M.; Futenma, A.; Kakumu, S. Protective role of extracellular superoxide dismutase in hemodialysis patients. *Nephron.* **84:**218-223; 2000.

[48] Juul, K.; Tybjaerg-Hansen, A.; Marklund, S.; Heegaard, N. H.; Steffensen, R.; Sillesen, H.; Jensen, G.; Nordestgaard, B. G. Genetically reduced antioxidative protection and increased ischemic heart disease risk: The copenhagen city heart study. *Circulation.***109:**59-65; 2004.

[49] Tamai, M.; Furuta, H.; Kawashima, H.; Doi, A.; Hamanishi, T.; Shimomura, H.; Sakagashira, S.; Nishi, M.; Sasaki, H.; Sanke, T.; Nanjo, K. Extracellular superoxide dismutase gene polymorphism is associated with insulin resistance and the susceptibility to

type 2 diabetes. *Diabetes Res. Clin. Pract.***71:**140-145; 2006.

[50] Young, R. P.; Hopkins, R.; Black, P. N.; Eddy, C.; Wu, L.; Gamble, G. D.; Mills, G. D.; Garrett, J. E.; Eaton, T. E.; Rees, M. I. Functional variants of antioxidant genes in smokers with COPD and in those with normal lung function. *Thorax.* **61:**394-399; 2006.

[51] Juul, K.; Tybjaerg-Hansen, A.; Marklund, S.; Lange, P.; Nordestgaard, B. G. Genetically increased antioxidative protection and decreased chronic obstructive pulmonary disease. *Am. J. Respir. Crit. Care Med.***173:**858-864; 2006.

CHAPTER V

ALLELE-SPECIFIC EFFECTS OF ECSOD IN BACTERIAL INFECTION

ABSTRACT

Extracellular superoxide dismutase (ecSOD) is the only enzyme that scavenges superoxide specifically in the extracellular compartment and provides protection to tissues from oxidative damage. Many studies using lipopolysaccharide (LPS) indicate that ecSOD is important for protecting tissues from oxidative damage by dampening immune responses. These studies imply that ecSOD may impair the ability to mount a proper innate immune response, against invading microorganisms**.** Although many studies have revealed the importance of the reactive oxygen species (ROS) in bacterial killing, the role of ecSOD during bacterial infection has not been studied yet. In this study, *Listeria monogytogene* and *Streptococcus pneumoniae* were used to infect mice expressing various level of ecSOD: congenic mice $sod3^{129}$ (relatively high), $sod3^{wt}$ and *sod3 KO* mice (none). ecSOD expression is inversely related to bacterial clearance, suggesting that ecSOD expression can negatively impact the innate immune response. On the other hand, bacterial infection significantly decreases ecSOD activity in infected tissues, while the protein levels are not affected. The induction of iNOS expression is significantly lower in the liver and spleen of *sod3 KO* mice when compared to those of congenic $sod3^{129}$ and $sod3^{wt}$ mice. The NO levels in liver and spleen were independent on the level of iNOS induction. However, the NO levels in plasma were significantly induced regardless of the genotype. The oxidative stress levels measured by nitrotyrosine immunoblotting in plasma and liver were significantly higher in *sod3 KO* mice compared to the congenic $sod3^{129}$ and $sod3^{wt}$ mice.

In conclusion, high ecSOD expression impairs the bacterial clearance and the infection diminishes the ecSOD activity. Congenic mice expressing various levels of ecSOD represent an important tool to investigate the role of ecSOD in bacterial infection.

INTRODUCTION

Inflammation is a response of the organism to injury related to physical or chemical noxious stimuli or microbiological toxins. The inflammatory response is intended to inactivate or destroy invading organisms, remove irritants, and set the stage for tissue repair (1). Conventionally, ROS have been considered to function primarily in host-defense as antimicrobial factors (2). Phagocytic cells, including neutrophils and macrophages, are among the most important components of the innate immune response. It is the first line of host-defense and the phagocyte-derived ROS are of crucial importance for host resistance to microbial pathogens (3). Two of the most important antimicrobial systems of phagocytic cells are the NADPH oxidase and inducible nitric oxide synthase (iNOS) pathways, which are responsible for the generation of superoxide ($O_2^{\bullet -}$) and nitric oxide radicals ($NO^{\bullet}$) respectively, during the oxidative burst triggered during infection (3). Nitric oxide may play regulatory roles at virtually every stage of the development of inflammation: in the regulation of pro-inflammatory properties of endothelium and in the early stages of inflammatory cell transmigration into the sites of inflammation (1). Superoxide anions activate endothelial cells and increase neutrophil infiltration (4, 5), by generating chemotactic mediators, such as leukotriene B4 (6), or by up-regulating adhesion molecules, such as intracellular adhesion molecule (ICAM)-1 (7, 8). Under the inflammatory conditions, nitric oxide and the superoxide anion react together to produce significant amounts of highly toxic, peroxynitrite anion ($ONOO^-$), which is a potent oxidizing agent that can cause DNA fragmentation and lipid oxidation (9).

Superoxide dismutase (SOD) is an endogenous cellular defense system that catalyzes the dismutation of two superoxide radicals into oxygen and hydrogen peroxide. Extracellular superoxide dismutase (ecSOD or SOD3) is the only enzyme that scavenges superoxide

specifically in the extracellular compartment and provides protection to tissues from oxidative damage. Furthermore, by limiting the availability of superoxide, the level of peroxynitrite can be controlled by these enzymes. Although many studies have revealed the importance of the ROS in bacterial killing (3) and surprisingly the role of ecSOD during bacterial infection has not been studied yet.

The expression of ecSOD has been implicated in protection against inflammation due to its ability to reduce oxidative stress and tissue damage. Importantly, mice overexpressing human ecSOD have increased survival rates and decreased neutrophil recruitment in response to LPS stimulation, when compared to wild-type mice (10). On the other hand mice lacking ecSOD show increased lung neutrophil recruitment and injury in response to LPS (11). The overexpression of human ecSOD also protects mice from lung injury due to influenza virus infection (12). These studies indicate that ecSOD is important for protecting tissues from oxidative damage by dampening immune responses but imply that the immunosuppressive effect may be counterproductive during acute infections.

A limited number of studies have shown that exogenous SOD can inhibit killing of *Listeria* (13, 14); macrophages from mice that overexpress human SOD1 are also impared in their ability to kill *E. coli* (15). These studies imply that ecSOD may impair the ability to mount a proper innate immune response, against invading microorganisms. Thus, understanding the role of ecSOD during bacterial infection is important.

We previously reported that the 129P3/J strain expresses a novel ecSOD allele which differs in several aspects from the wild-type (*wt*) allele expressed by the C57BL/6J strains: it contains an N21D substitution in the signal sequence of ecSOD, an A186S substitution in the catalytic domain and a 10bp deletion in the 3' untranslated region (UTR) of the mRNA (16). Our

recent study showed that the altered ecSOD allele in 129P3/J strain (129) is associated with increased level of the enzyme in several tissues (17). This is an allele-driven phenomenon, as similar observations were made in congenic mice (C57.129-*sod3*) expressing either ecSOD alleles on a same genetic background, C57BL/6 strain of mouse (17).

Listeria monocytogenes (*Listeria*) is a gram-positive bacterium that can induce septicemia, meningitis, or spontaneous abortion in infected individuals (18). *Streptococcus pneumoniae* (*Streptococcus*) is a gram-positive bacterium and the most frequent cause of acute lower respiratory infection and death due to sepsis (19). *Listeria* and *Streptococcus* infected mice are a well-characterized infection model, and we used them for the studies described below. In this study, we examined the effect of various ecSOD expression on 1) bacterial clearance 2) changes of ecSOD distribution in tissues/organs 3) changes in nitric oxide level and iNOS expression and 4) oxidative stress levels after infection in the congenic mice $sod3^{129}$ (high), $sod3^{wt}$ (normal) along with ecSOD KO mice (none).

METHODS

Animal procedures: 10-12 weeks old congenic mice *sod3*^{129} (high), *sod3*^{wt} (normal) along with ecSOD KO mice (none) were infected intravenously with *Listeria* or instilled *Streptococcus* via intranasal passages as previously described (20, 21). Mice were euthanized at 3 days (*Listeria*) or 18hrs (*Streptococcus*) post-infection. Since the main target organ for *Listeria* is the liver and spleen, and for *Streptococcus* infection is lung, spleen and blood, these tissues/organs were collected. Blood was collected via retro-orbital plexus after anesthesia. The removed tissues were homogenized in sterile water (*Listeria*) or PBS (*Streptococcus*) for bacterial colony-forming unit (CFU) analysis as previously described (20, 21) or flash-frozen in liquid nitrogen for biochemical analyses.

Sample preparation: Frozen tissues (Liver, spleen and lung) was ground to a fine powder in liquid nitrogen, and homogenized with 50 mM potassium phosphate buffer containing 0.3 M KBr and 3 mM EDTA, pH 7.4 containing a 1:1000 dilution of a protease inhibitor cocktail (sigma; cat# P8340). Homogenate was centrifuged 10,000 xg for 10min at 4˚C. The protein concentration of tissue homogenate was determined by Lowry assay (22). Homogenates (liver spleen and lung) or 1:1 diluted plasma were applied to Microcon (Millipore; cat# 42407) and centrifuged 10,000 X g for 30-60min. Filtrates were kept -20˚C until assayed.

Plasma and tissue ecSOD activities: ecSOD was partially purified using ConA Sepharose (Sigma) as described (23), using 100 μl of plasma or 2-6 mg of tissue homogenate protein. The columns (0.5x10 mm) were washed with 50mM Na-HEPES (pH 7.0) and 0.25 M NaCl, and ecSOD was eluted with a washing buffer containing 0.5 M α-methyl mannoside (Sigma), pH

6.0. ConA-Sepaharose efficiency and binding capacity were monitored by Western blotting of the wash.

The activity of ecSOD (released from ConA) was determined using a system based on the oxidation of NAD(P)H (24). Briefly, 23.5µl of sample was combined with 187µl of 100 mM triethanolamine/diethanolamine-HCl buffer pH 7.4, 6µl of 100mM EDTA/50mM $MnCl_2$ solution, and 10µl 7.5 mM NAD(P)H. The reaction was started with the addition of 23.5µl of 10 mM ß-mercaptoethanol. Samples were tested for NAD(P)H oxidase activity before the addition of ß-mercaptoethanol. Dismutase activity was estimated from a standard curve constructed by measuring the activity of increasing and known amounts of Cu/Zn SOD (Sigma, cat. #S2515). Activities are therefore expressed as ng of Cu/Zn SOD equivalents.

Western blot: Aliquots of whole mouse plasma (0.25ul) or 100ug of tissue protein was dissolved and boiled in Laemmli buffer (25)(5 min), separated by SDS-12% PAGE and transferred to PVDF membranes (Bio-Rad, Inc.). ecSOD was detected as described before using rabbit anti-ecSOD serum. Peroxynitrite formation was evaluated by detection of nitrotyrosine residues by performing Western immunoblotting with a monoclonal anti-nitrotyrosine antibody of high specificity (clone 1A6; Upstate Biotechnology, Lake Placid, NY). Membranes were processed as manufacture's protocol using 1:2000 dilutions of anti-Nitrotyrosine (Upstate Biotechnology; cat# 05-233) and a goat anti-mouse HRP IgG, (Upstate Biotechnology; cat# 12-349) in 3% milk-PBS. Detection was done using FC camera system (Alpha Innotech). Notrotyrosine blots were stripped and reblotted with anti- b-actin (sigma; cat# A2066) and goat anti-rabbit HRP IgG (Jackson immunoresearch, cat# 111-035-144). To test the effect of ecSOD on the iNOS induction after bacterial infection, tissue iNOS level was detected using anti-iNOS

(BD bioscience, 1:2000 dilution) after separation of protein by 8% SDS-PAGE. Protein levels in tissues were adjusted with β-actin as a loading control. In case of plasma, the loaded protein level was checked with ponceau S training.

Nitric oxide quantitation: Total nitrate levels were measured using a Nitric Oxide Quantitation Kit (Active Motif Inc.; cat# 40020) as the manufacturer's protocol. 50ul (plasma) or 70ul (homogenates) of filtrates/well was used for the assay. Nitrate values in tissue samples were normalized to protein content.

Statistical Analysis: Results from experiments are reported as mean±SEM. All quantitative data were assessed for significance using either Student's t-test or one-way ANOVA with Tukey's post-hoc test. A p value < 0.05 was used to establish significance.

RESULTS

Effect of ecSOD level in bacterial clearance and susceptibility

To determine if the ecSOD expression levels have an effect on bacterial clearance and susceptibility, mice that expressing various levels of ecSOD were infected with *Listeria* or with *Streptococcus*, the colony-forming units (CFU) in major target organs were measured. Significant differences in *Listeria* CFU's were seen in the different groups of mice, as shown in Figure 1A (Courtesy of Timothy Break and Rance Berg in Department of Molecular Biology and Immunology, UNTHSC). In both the liver and spleen, the ecSOD KO mice had decreased CFU in comparison to the other groups of mice. Importantly, the congenic $sod3^{129}$ mice showed increased *Listeria* CFU's in the liver and spleen when compared to the other mice. The decreased bacterial clearance in the congenic $sod3^{129}$ mice is correlated with the decreased survival (data not shown). Similar results were shown in *Streptococcus* CFU's in lungs that congenic $sod3^{129}$ mice showed increased bacterial load (Figure 1B), even though the CFUs from other organs, spleen and blood were not significant (Courtesy of Byung-Jin Kim and Harlan Jones in Department of Molecular Biology and Immunology, UNTHSC). These results show that level of ecSOD is inversely related to bacterial clearance during infection, suggesting that ecSOD expression can negatively impact the innate immune response.

ecSOD level after bacterial infection

To-date the effect of bacterial infection on the expression of ecSOD is not studied in detail. Several studies have shown that ecSOD levels in the lungs were decreased after LPS treatment and most likely it is associated with a loss in proteolytically processed ecSOD (10, 11). Since the mechanism of inflammation induced by LPS might be different from that induced by

bacterial infection, we tested the effect of *Listeria* or *Streptococcus* infection on tissue ecSOD level and activity. As previously shown, the congenic $sod3^{129}$ female mice express significantly increased level of ecSOD in plasma and liver when compared to the $sod3^{wt}$ mice (Figure 2A). In addition, ecSOD in spleen was detected this study and the level in $sod3^{129}$ mice was marginally higher ($p<0.058$) than that of $sod3^{wt}$ mice. Similar to the females, the congenic $sod3^{129}$ male mice express significantly increased level of ecSOD in plasma and marginally increased in lungs relative to the $sod3^{wt}$ mice (Figure 3A).

Bacterial infection did not affect to the level of ecSOD in tissues (Figure 2A and 3A). The plasma ecSOD level of congenic $sod3^{wt}$ mice was increased in 1day post infection of *Listeria* compared to non-infected group and decreased back to normal level in 3day post infection (data not shown). Spleen ecSOD level increase by day 3 after *Listeria* infection from both congenic $sod3^{wt}$ and $sod3^{129}$ mice, however, the change did not reach the significance ($p = 0.1$ and 0.2, respectively) (figure 2A). The levels of ecSOD in plasma and lung were not changed 18 hrs post-infection with *Streptococcus* (Figure 3A). ecSOD amount and activity in tissues of KO mice was not detectable, as previously published (26).

We next examined ecSOD activity in tissues after bacterial infections. The enzyme activities in tissues without infection were very similar to the trend of the enzyme amount (Figure 2C and 2D). However, ecSOD activities were significantly decreased after *Listeria* infection from all tissues including plasma, liver and spleen. On the other hand, ecSOD activity was not significantly changed in tissues 18hrs post-infection with *Streptococcus*. It is interesting that all tissue ecSOD levels were not changed or increased after *Listeria* infection but the activities rapidly diminished.

Effect of ecSOD on iNOS induction and nitric oxide (NO) level after infection

It is well known that inducible nitric oxide synthase (iNOS) expression is upregulated by bacterial infection to increase NO, an important antimicrobial system (3). However, whether or not the iNOS induction after infection is associated with ecSOD level is not studied. Thus, in this study, the level of iNOS was determined in tissues after *Listeria* infection. iNOS expressions are significantly increased in spleens by 3 day post-infection regardless ecSOD genotype, as shown in Figure 4. The induction in spleen was significantly higher in congenic $sod3^{129}$ and $sod3^{wt}$ mice when compared to the KO mice. On the other hand, the induction of iNOS was not significant in livers regardless genotype, although the iNOS levels after infection were significantly higher in $sod3^{129}$ relative to the KO mice. These results clearly show that the level of ecSOD affect the iNOS induction in spleen post *Listeria* infection.

Since the NO is known as a bactericidal agent, we checked the NO level in tissues. It has been suggested that ecSOD is the major determinant of NO bioavailability in blood vessels and thus, the levels of NO in non-infected mice tissues were expected to be higher in the $sod3^{wt}$ than *sod3 KO* and lower than $sod3^{129}$. Indeed, the level of NO in blood was highest in 129 and lowest in KO as expected, as shown in Figure 5, however, the difference was not significant. After infection, the NO level in blood was significantly increased by 3 days post infection from all genotypes but they were not significantly different, even though $sod3^{wt}$ tend to have higher level then *KO* and lower then $sod3^{129}$. In fact, we could detect substantial amount of NO only from blood in all genotypes but very limited amount in other tissues (liver and spleen). None of them reached statistical significance between genotypes and between groups of infection. These results suggest that the expression of *129* ecSOD allele increased the protective effect of NO in the

vessels at least. It is interesting that the level of iNOS induction was very significant by day 3 in both liver and spleen yet the changes of NO in those tissues were not significant.

Effect of ecSOD on oxidative stress after infection

Since ecSOD is an antioxidant enzyme, we next tested level of oxidative stress after infection. Nitrotyrosine residues of protein modified by peroxinitrite are a well-known marker for the oxidative stress. We thus examined the level of nitrotyrosine in tissue proteins during *Listeria* infection. Levels of nitrotyrosine in plasma and liver were significantly lower in congenic $sod3^{129}$ and $sod3^{wt}$ mice than those in *sod3 KO* mice (Figure 6). The nitrotyrosine levels in the tissues were inversely correlated with ecSOD levels. However, the level of nitrotyrosine was not increased by the LM infection but rather decreased, significant in KO plasma, 3 days post-infection.

Figure 1. Bacterial burden in tissues post LM or SP infection.

Congenic *sod3*^{129} (grey bars), *sod3*^{wt} (solid bars) and *sod3* KO (white bars) mice were infected intravenously with *Listeria* or instilled *Streptococcus via* intranasal passages. By day 3 (*Listeria*) or 18 hrs (*Streptococcus*) post-infection, the colony-forming units (CFU) in major target organs were measured. (A) LM CFU in liver and spleen (5-7 mice per group) (Courtesy of Timothy Break and Rance Berg in the Department of Molecular Biology and Immunology, UNTHSC). (B) SP CFU in lung, spleen and blood (7 mice per group) (Courtesy of Byung-Jin Kim and Harlan Jones in the Department of Molecular Biology and Immunology, UNTHSC). The CFUs are presented in Log_{10} scale. Error bars represent ±SEM.

* $p < 0.05$ versus *sod3 KO* mice;

# $p < 0.05$ versus *sod3*^{wt}.

Figure 1.

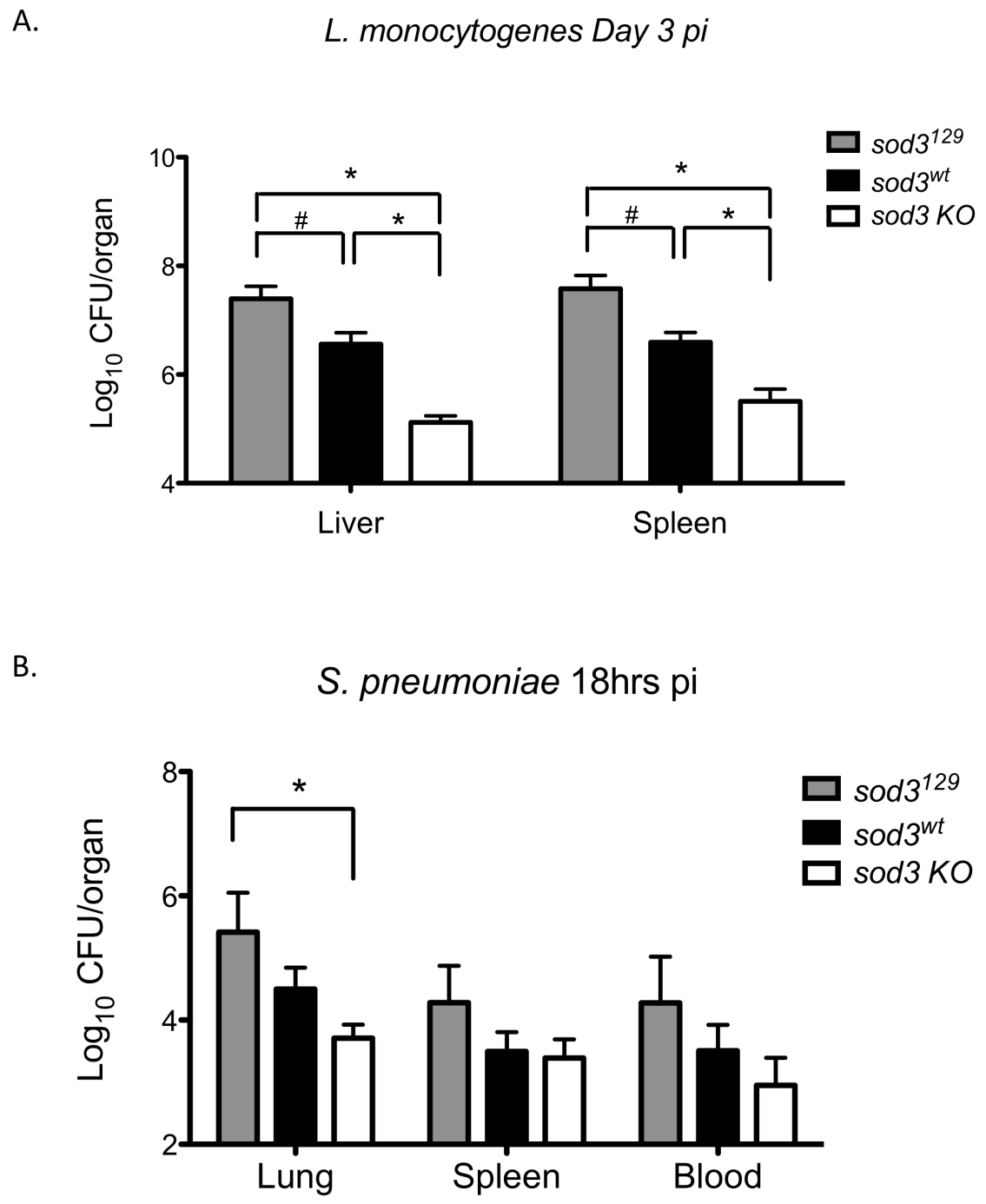

Courtesy of Timothy Break and Rance Berg (A), and Byung-Jin Kim and Harlan Jones (B) in the Department of Molecular Biology and Immunology, UNTHSC.

Figure 2. The effect of *Listeria* infection on ecSOD protein amount and activity in plasma, liver and spleen.

Plasma, liver and spleen were isolated from non-infected control and *Listeria*-infected congenic $sod3^{129}$ (grey bars) and $sod3^{wt}$ (solid bars) mice 3 days after infection (5-7 mice per group). Western blot was performed using 100 μg of total tissue protein or 20 μl of plasma and densitometric analyses of are shown in A. Tissue ecSOD densitometry was normalized to β-actin as an internal loading control. (B) Activities of ecSOD, isolated from tissue homogenates by ConA-affinity chromatography (5-7 mice per group). Error bars represent ±SEM.

* $p < 0.05$ versus *sod3 KO* mice;

# $p < 0.05$ versus $sod3^{wt}$.

+ $p < 0.05$ versus control (no infection).

Figure 2.

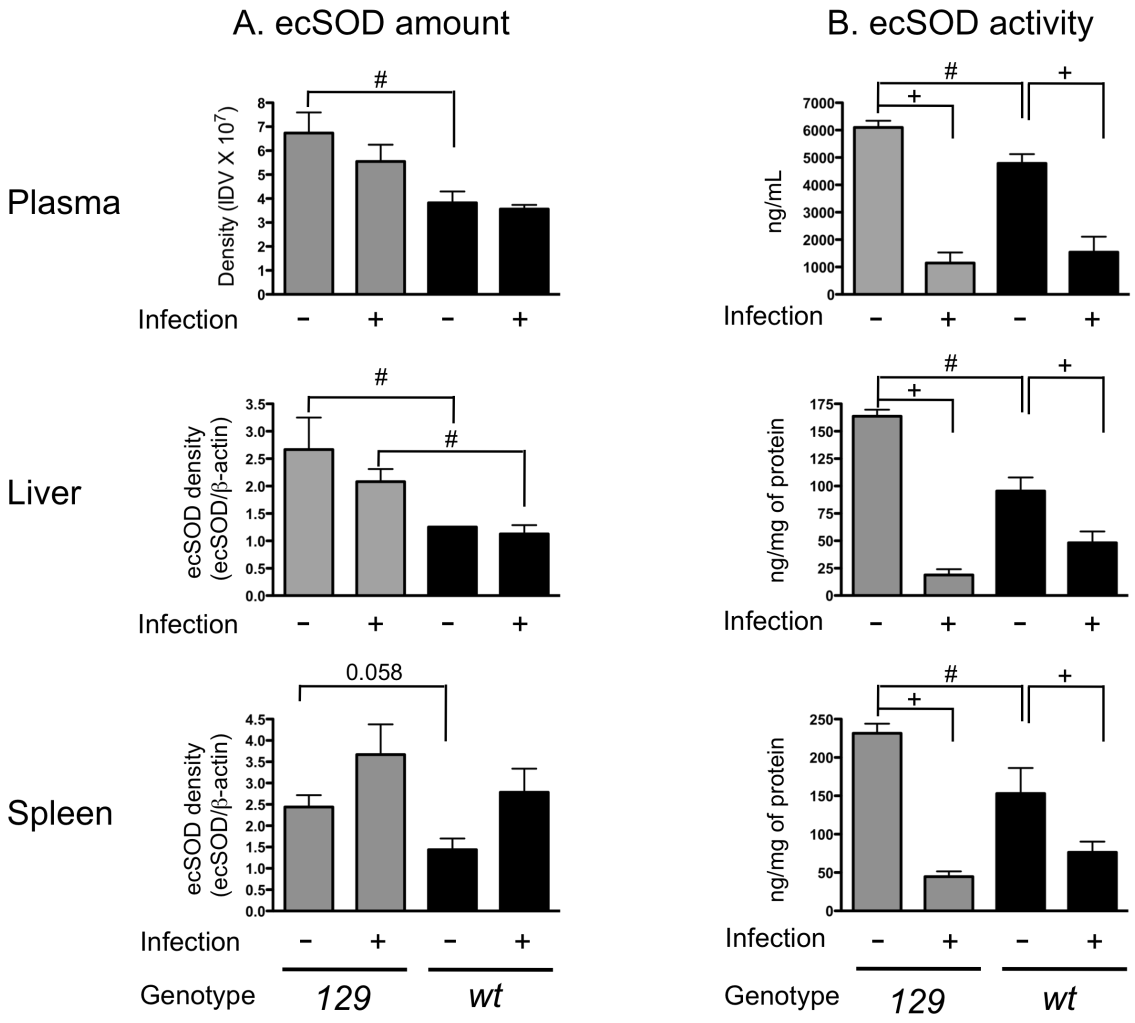
A. ecSOD amount
B. ecSOD activity
Plasma
Liver
Spleen
Density (IDV X 10^7)
ecSOD density (ecSOD/β-actin)
ng/mL
ng/mg of protein
#
+
0.058
Infection
Genotype
129
wt

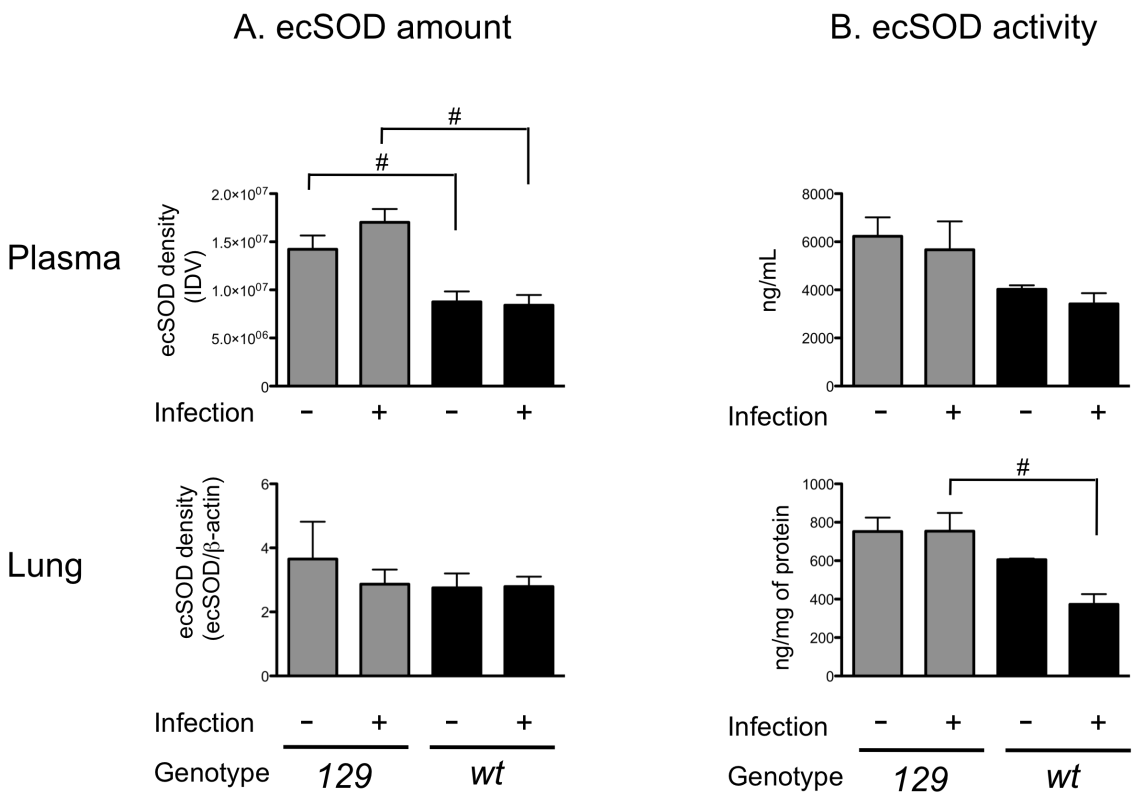

Figure 3. The effect of *Streptococcus* infection on ecSOD protein amount and activity in plasma and lung.

Plasma and lung were isolated from non-infected control and LM-infected congenic *sod3*^{129} (grey bars) and *sod3*^{wt} (solid bars) mice 3 days after infection (5-7 mice per group). Western blot was performed using 10 μg of total lung protein or 20 μl of plasma and densitometric analyses of are shown in (A). Tissue ecSOD densitometry was normalized to β-actin as an internal loading control. (B) Activities of ecSOD, isolated from lung homogenates or plasma by ConA-affinity chromatography (5-7 mice per group). Error bars represent ±SEM.

# $p < 0.05$ versus *sod3*^{wt}.

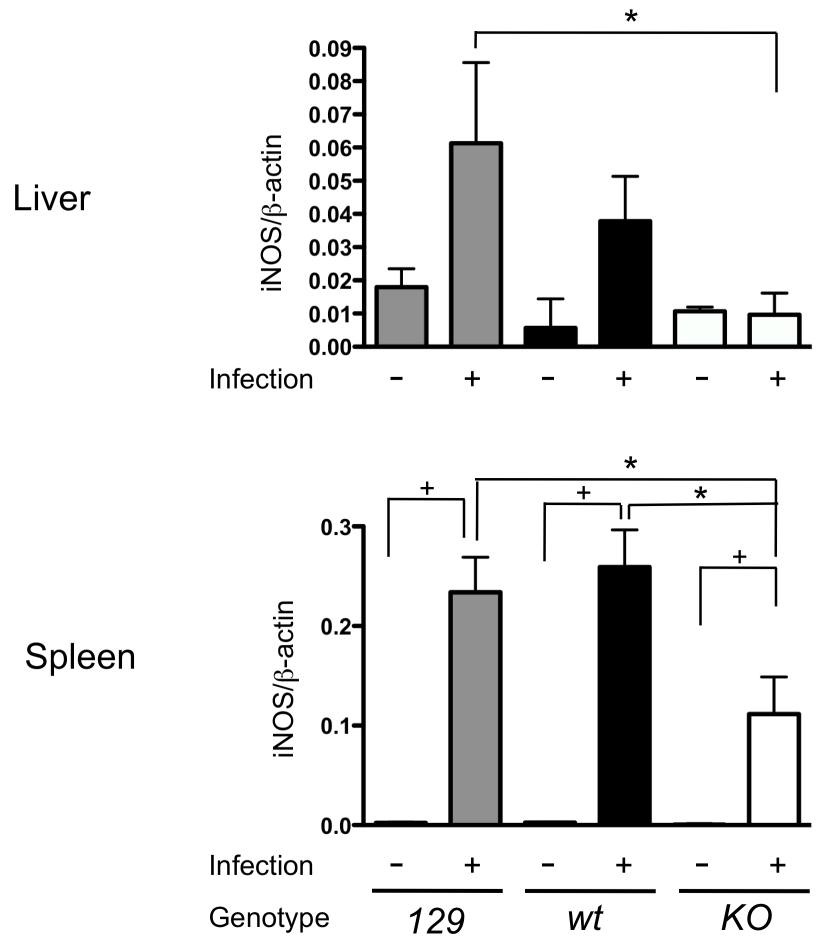

Figure 4. The effect of ecSOD on iNOS induction in liver and spleen after *Listeria* infection. Liver and spleen were isolated from non-infected control and *Listeria*-infected congenic $sod3^{129}$ (grey bars) and $sod3^{wt}$ (solid bars) mice 3 days after infection (5-7 mice per group). Western blot for iNOS was performed using 100 μg of total tissue protein and densitometric analyses of are shown. Tissue iNOS densitometry was normalized to β-actin as an internal loading control. Error bars represent ±SEM.

* $p < 0.05$ versus *sod3 KO* mice;

+ $p < 0.05$ versus control (no infection).

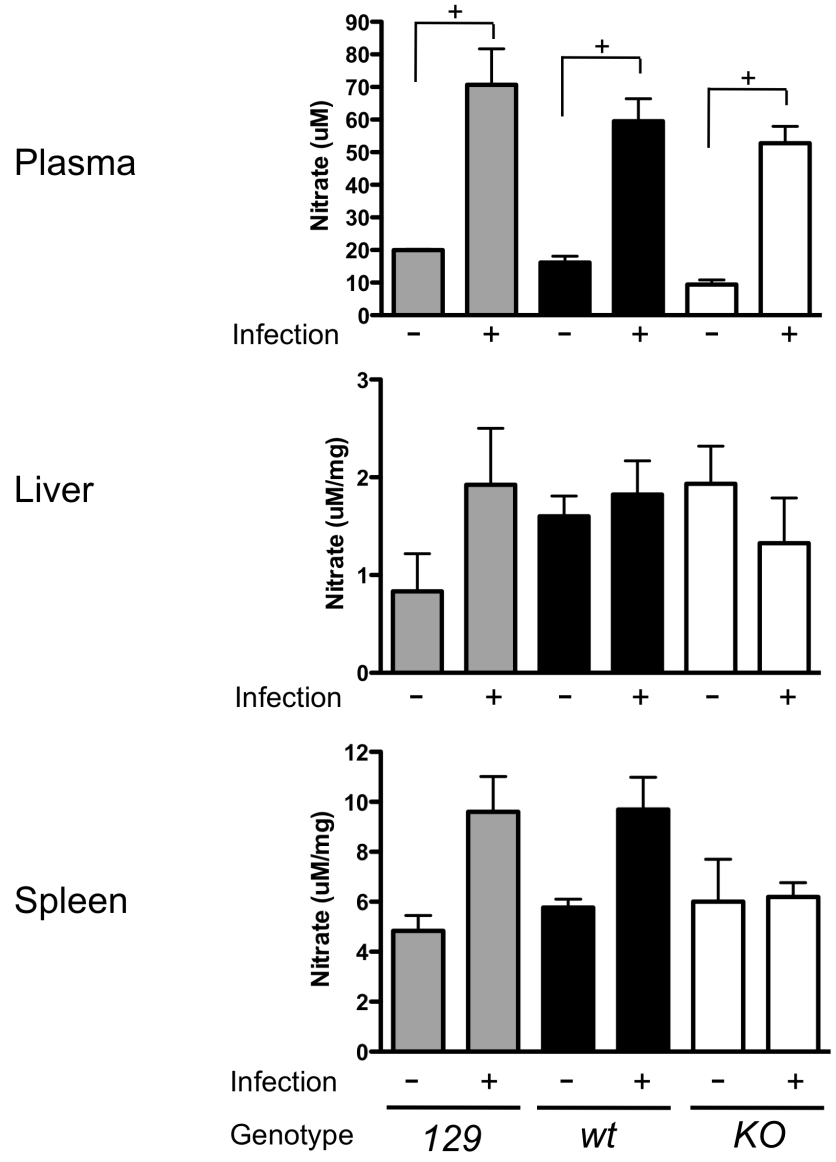

Figure 5. NO levels in plasma, liver and spleen after *Listeria* infection.

Plasma, liver and spleen were isolated from non-infected control and *Listeria*-infected congenic *sod3*^{129} (grey bars) and *sod3*^{wt} (solid bars) mice 3 days after infection (5-7 mice per group). Homogenates (liver and spleen) or 1:1 diluted plasma were filtered and applied to NO assay. Tissue NO levels were normalized by total protein levels. Error bars represent ±SEM. + $p < 0.05$ versus control (no infection).

Figure 6. The effect of ecSOD on oxidative stress in plasma, liver and spleen after *Listeria* infection.

Plasma, liver and spleen were isolated from non-infected control and *Listeria*-infected congenic $sod3^{129}$ (grey bars) and $sod3^{wt}$ (solid bars) mice 3 days after infection (5-7 mice per group). Western blot for nitrotyrosine was performed using 100 μg of total tissue protein or 20 μl of plasma and densitometric analyses of are shown. Tissue nitrotyrosine densitometry was normalized to β-actin as an internal loading control. Error bars represent ±SEM.

* $p < 0.05$ versus *sod3 KO* mice;

+ $p < 0.05$ versus control (no infection).

Figure 6.

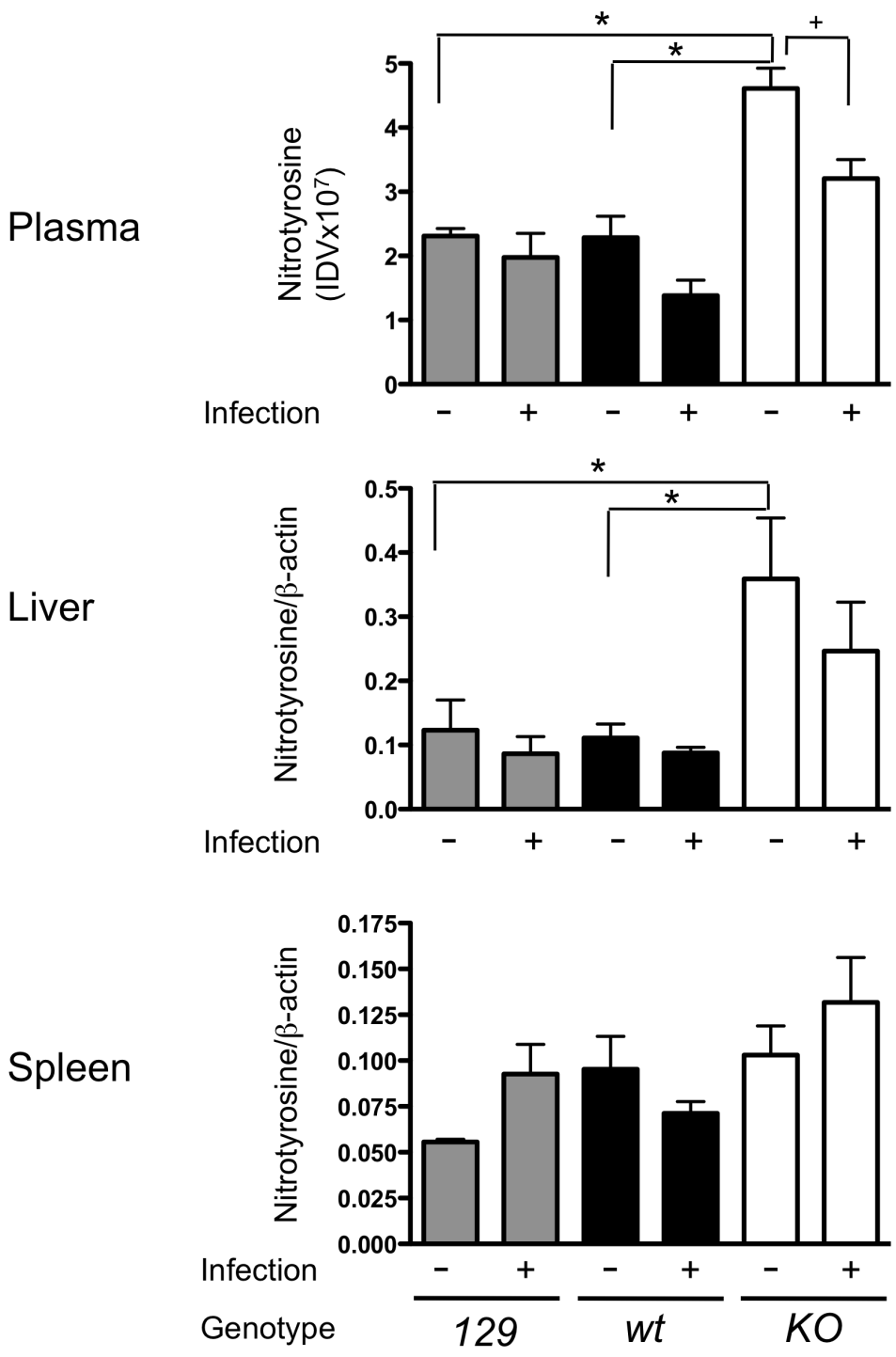
Plasma
Nitrotyrosine (IDVx10^7)
Infection
Liver
Nitrotyrosine/β-actin
Infection
Spleen
Nitrotyrosine/β-actin
Infection
Genotype
129
wt
KO

DISCUSSION

No work has been done concerning the effects of host ecSOD on the bacterial infection susceptibility. Most of the research in this area has been performed on the effect of ecSOD on LPS-induced injury (10, 27, 28). These studies demonstrate a protective effect of ecSOD on LPS induced inflammation and septic shock, by scavenging excessive ROS and thus attenuating neutrophil recruitment to the site of injury (10, 27, 28). We show that increased ecSOD levels can be harmful during acute infection; specifically, the ecSOD level is inversely correlated with the bacterial clearance. The detailed mechanism by which the ecSOD levels affect bacterial clearance needs to be studied further. However, it is likely that increased ecSOD actually reduces ROS production and thus dampens the acute inflammatory response. A recent study showed that the extracellular $O_2^{\bullet -}$ produced by phagocytic cells, including macrophages are targeting the periplasmic site of pathogens instead of cytoplasmic molecules or DNA (29). Many studies showed that bacteria also express SODs including Cu/Zn SOD, into the periplasmic space, where they are likely to play a defensive role against extracellular oxidative stress (30). Indeed, several types of SOD including Cu/Zn SOD and MnSOD are linked with a virulence of bacterial pathogens including *Listeria* and *Streptococcus* (31, 32). The mutation of bacterial SOD was associated with reduced virulence as well as tolerance against host immune system (31-34). These results suggest that the increased level of ecSOD in the host not only dampens the inflammatory response but may also help bacteria to survive from oxidative burst by host immune system.

Interestingly, we also found for the first time that bacterial infection, especially *Listeria*, triggers an extensive inactivation of ecSOD. The mechanism of inactivation is unknown; the most likely explanation is a consequence of increased oxidative stress and several studies

suggests that is a mechanism. Inactivation of SODs during aging is well known and the subtle denaturation by reactive oxygen species and glycation was implicated in the inactivation of SODs (35, 36). In addition, Hink et al have reported that ecSOD has peroxidase activity in which H_2O_2, the dismutation product of $O_2^{\bullet-}$, can inactivate ecSOD by reacting with the copper center of ecSOD, thereby forming the Cu–OH radical and leading to enzyme inactivation with hypertension model (37). Since ecSOD has many cysteine and methionine residues, it is also possible those amino acids may be oxidized and loose their activity. Indeed, recent study indicates that ecSOD inactivation in pulmonary hypertension models is associated with increased protein thiol oxidation (38). It is also interesting that the activity decreased rapidly in the liver and blood from day 1 (data not shown) but spleen lost its ecSOD activity at day 3, indicating that each organ has a different timing of ecSOD inactivation.

In accordance with previous studies, iNOS induction in liver and spleen was shown after infection (**Figure 4**). However, the levels of iNOS in the KO mice were significantly lower relative to *sod3*^{129} mice. These results clearly show that the level of ecSOD affect the iNOS induction in spleen post *Listeria*-infection. It is interesting that the level of iNOS induction was significant by day 3 in spleen yet the changes of NO in this tissue was not significant. This result suggests that NO produced by iNOS react with $O_2^{\bullet-}$, which is simultaneously generated by activated immune cells, leading to the formation of $ONOO^-$. With the inactivation of ecSOD at 3 days post-infection, less $O_2^{\bullet-}$ may be scavenged and thus more formation of $ONOO^-$ is expected. Surprisingly, the nitration of tyrosine residues (nitrotyrosine) in protein was not increased post infection. These results suggest that $ONOO^-$ may react with targets other than tyrosine residue during *Listeria* infection. The fastest known reaction for $ONOO^-$ is the direct reaction with transition metal centers (39) and thus modifies proteins containing a heme prosthetic group, such

as hemoglobin (40). It is also known that the most prevalent reaction of $ONOO^-$ is with cysteine (41, 42). Importantly, the nitrotyrosine levels in plasma and liver of KO mice were significantly increased when compared to the *sod3*^{wt} and *sod3*^{129} mice, suggesting that the KO mice are under oxidative stress and it may affect the bacterial survival during the acute infection.

Previous work by others suggests that there is a strain-dependent variation in the susceptibility to bacterial infection; specifically, the 129J mice appear to be more susceptible to *Listeria* infection than the C57BL/6 strain (43). The present study provides evidence that the different susceptibilities to the *Listeria* infection are ecSOD allele-driven.

In conclusion, ecSOD expression is a major determinant of susceptibility to the bacterial infection and the congenic mice expressing different level of tissue ecSOD will be an important tool to investigate the mechanism by which the ecSOD regulates the bacterial clearance and immunologic responses.

REFERENCES

1. Guzik, T. J., Korbut, R., and Adamek-Guzik, T. (2003) *J. Physiol. Pharmacol.* **54**, 469-487

2. Fialkow, L., Wang, Y., and Downey, G. P. (2007) *Free Radic. Biol. Med.* **42**, 153-164

3. Fang, F. C. (2004) *Nat. Rev. Microbiol.* **2**, 820-832

4. Salvemini, D., Wang, Z. Q., Zweier, J. L., Samouilov, A., Macarthur, H., Misko, T. P., Currie, M. G., Cuzzocrea, S., Sikorski, J. A., and Riley, D. P. (1999) *Science* **286**, 304-306

5. Masini, E., Cuzzocrea, S., Mazzon, E., Marzocca, C., Mannaioni, P. F., and Salvemini, D. (2002) *Br. J. Pharmacol.* **136**, 905-917

6. Bjork, J., and Arfors, K. E. (1982) *Agents Actions Suppl.* **11**, 63-72

7. Cuzzocrea, S., Mazzon, E., Dugo, L., Caputi, A. P., Aston, K., Riley, D. P., and Salvemini, D. (2001) *Br. J. Pharmacol.* **132**, 19-29

8. Yasui, K., and Baba, A. (2006) *Inflamm. Res.* **55**, 359-363

9. Carr, A. C., McCall, M. R., and Frei, B. (2000) *Arterioscler. Thromb. Vasc. Biol.* **20**, 1716-1723

10. Bowler, R. P., Nicks, M., Tran, K., Tanner, G., Chang, L. Y., Young, S. K., and Worthen, G. S. (2004) *Am. J. Respir. Cell Mol. Biol.* **31**, 432-439

11. Ueda, J., Starr, M. E., Takahashi, H., Du, J., Chang, L. Y., Crapo, J. D., Evers, B. M., and Saito, H. (2008) *Free Radic. Biol. Med.* **45**, 897-904

12. Suliman, H. B., Ryan, L. K., Bishop, L., and Folz, R. J. (2001) *Am. J. Physiol. Lung Cell. Mol. Physiol.* **280**, L69-78

13. Bortolussi, R., Vandenbroucke-Grauls, C. M., van Asbeck, B. S., and Verhoef, J. (1987) *Infect. Immun.* **55**, 3197-3203

14. Peck, R. (1989) *J. Leukoc. Biol.* **46**, 434-440

15. Mirochnitchenko, O., and Inouye, M. (1996) *J. Immunol.* **156**, 1578-1586

16. Pierce, A., Whitlark, J., and Dory, L. (2003) *Arterioscler. Thromb. Vasc. Biol.* **23**, 1820-1825

17. Jun, S., Pierce, A., and Dory, L. (2010) *Free Radic. Biol. Med.* **48**, 590-596

18. Pamer, E. G. (2004) *Nat. Rev. Immunol.* **4**, 812-823

19. Andonegui, G., Goring, K., Liu, D., McCafferty, D. M., and Winston, B. W. (2009) *Shock* **31**, 423-428

20. Meeks, K. D., Sieve, A. N., Kolls, J. K., Ghilardi, N., and Berg, R. E. (2009) *J. Immunol.* **183**, 8026-8034

21. Gonzales, X. F., Deshmukh, A., Pulse, M., Johnson, K., and Jones, H. P. (2008) *Brain Behav. Immun.* **22**, 552-564

22. LOWRY, O. H., ROSEBROUGH, N. J., FARR, A. L., and RANDALL, R. J. (1951) *J. Biol. Chem.* **193**, 265-275

23. Marklund, S. L. (1990) *Methods Enzymol.* **186**, 260-265

24. Paoletti, F., and Mocali, A. (1990) *Methods Enzymol.* **186**, 209-220

25. Laemmli, U. K. (1970) *Nature* **227**, 680-685

26. Carlsson, L. M., Jonsson, J., Edlund, T., and Marklund, S. L. (1995) *Proc. Natl. Acad. Sci. U. S. A.* **92**, 6264-6268

27. Lund, D. D., Gunnett, C. A., Chu, Y., Brooks, R. M., Faraci, F. M., and Heistad, D. D. (2004) *Am. J. Physiol. Heart Circ. Physiol.* **287**, H805-11

28. Lund, D. D., Chu, Y., Brooks, R. M., Faraci, F. M., and Heistad, D. D. (2007) *J. Physiol.* **584**, 583-590

29. Craig, M., and Slauch, J. M. (2009) *PLoS One* **4**, e4975

30. Desideri, A., and Falconi, M. (2003) *Biochem. Soc. Trans.* **31**, 1322-1325

31. Dallmier, A. W., and Martin, S. E. (1990) *Appl. Environ. Microbiol.* **56**, 2807-2810

32. Yesilkaya, H., Kadioglu, A., Gingles, N., Alexander, J. E., Mitchell, T. J., and Andrew, P. W. (2000) *Infect. Immun.* **68**, 2819-2826

33. Edwards, K. M., Cynamon, M. H., Voladri, R. K., Hager, C. C., DeStefano, M. S., Tham, K. T., Lakey, D. L., Bochan, M. R., and Kernodle, D. S. (2001) *Am. J. Respir. Crit. Care Med.* **164**, 2213-2219

34. Sansone, A., Watson, P. R., Wallis, T. S., Langford, P. R., and Kroll, J. S. (2002) *Microbiology* **148**, 719-726

35. Maria, C. S., Revilla, E., Ayala, A., de la Cruz, C. P., and Machado, A. (1995) *FEBS Lett.* **374**, 85-88

36. Bartosz, G., Soszynski, M., and Retelewska, W. (1981) *Mech. Ageing Dev.* **17**, 237-251

37. Hink, H. U., Santanam, N., Dikalov, S., McCann, L., Nguyen, A. D., Parthasarathy, S., Harrison, D. G., and Fukai, T. (2002) *Arterioscler. Thromb. Vasc. Biol.* **22**, 1402-1408

38. Wedgwood, S., Lakshminrusimha, S., Fukai, T., Russell, J. A., Schumacker, P. T., and Steinhorn, R. H. (2010) *Antioxid. Redox Signal.*

39. Alvarez, B., and Radi, R. (2003) *Amino Acids* **25**, 295-311

40. Boccini, F., and Herold, S. (2004) *Biochemistry* **43**, 16393-16404

41. Radi, R., Beckman, J. S., Bush, K. M., and Freeman, B. A. (1991) *J. Biol. Chem.* **266**, 4244-4250

42. Pacher, P., Beckman, J. S., and Liaudet, L. (2007) *Physiol. Rev.* **87**, 315-424

43. Cheers, C., and McKenzie, I. F. (1978) *Infect. Immun.* **19**, 755-762

CHAPTER VI

CONCLUSIONS AND FUTURE DIRECTIONS

The data presented in this dissertation clearly demonstrate that murine ecSOD polymorphism has a significant effect on the ecSOD expression, tissue distribution and the animal's disease susceptibility. Congenic mice (**C57.129-*sod3***) that carry either the *wt* or *129* ecSOD alleles in an otherwise identical C57BL/6J background, recapitulate the differences observed in the founder mice: $sod3^{129}$ mice have significantly higher activity and amount of circulating and heparin-releasable ecSOD, when compared to $sod3^{wt}$ mice. The $sod3^{129}$ mice have a larger pool size of the enzyme in most, but especially highly vascular tissues, including the liver and kidney and thus a higher heparin-accessible pool size. These results clearly demonstrate that the ecSOD phenotype is largely allele-driven, independent of other strain-specific factors.

In addition, tissues of the $sod3^{129}$ mice have consistently lower levels of ecSOD mRNA, even though enzyme expression levels are similar or higher. The discrepancy in the relative enzyme content vs. the amounts of corresponding mRNA suggests significant allele-specific differences in the regulation of ecSOD synthesis and intracellular processing/secretion. Indeed, the data from *in vitro* system is consistent with the observation *in vivo*. The synthetic rate and steady state levels of intracellular *129* ecSOD in CHO cells are nearly twice as high as those of *wt* ecSOD, despite similar levels of mRNA. Similarly, rate of secretion of the *129* allele product was nearly twice that of the *wt* allele product. These results strongly suggest that the allele-driven differences in synthetic and secretory rates are responsible for the allelic differences observed *in vivo*, in tissue expression vs. mRNA levels.

It is not clear by which mechanism the synthesis and secretion of *129* ecSOD is increased. However, it is most likely that the N21D change within the signal peptide in *129* ecSOD results in significant increase in the efficiency of the cleavage and thus increase rates of processing, synthesis and secretion as shown in **Figure 1**. Translation of the secretory protein stops during translocation of the complex of signal-recognition particle (SRP), nascent polypeptide, and ribosome to the ER membrane. The nascent peptides including signal sequence are inserted to the membrane bound translocon. The translation resumes only after the signal peptide is cleaved by a signal peptidase in the ER lumen. The signal cleavage of *129* ecSOD likely occurs with a higher efficiency, according to computer analysis (SignalP3.0) pointing the relative cleavage probability rises from 61% in the *wt* product to 77% in the *129* isoform, and thus the translation efficiency increase and is extruded into the ER lumen faster through the translocon. With the increased processing efficiency by the amino acid substitution in signal peptide, the *129* ecSOD is translated more efficiently into ER and secreted through the Golgi and secretory vesicle rapidly to the extracellular space. Since the same proportion of newly synthesized ecSOD is secreted and degrade, increased synthesis results in increased steady state level.

The increased synthetic and secretion rates of *129* ecSOD are consistent with the observed plasma phenotype of congenic mice before and after heparin administration. With relatively higher tissue ecSOD levels in $sod3^{129}$, more tissue ecSOD is accessible to heparin resulting increased pool size of heparin-released plasma ecSOD as shown in **Figure 2**. Given the potentially important role of ecSOD in defending against extracellular superoxide, additional studies of ecSOD post-transcriptional regulation and processing should be useful for understanding the processes of superoxide dismutase-dependent diseases.

Studies indicate that ecSOD is important for protecting tissues from oxidative damage by dampening immune responses. The immunosuppressive effect may, however, be counterproductive during acute infections. Indeed, the increased ecSOD levels in tissues have a profound effect on disease susceptibility. First, this dissertation presents evidence that substituting the ecSOD allele from 129P3/J on the genetic background of a C57BL/6 mouse significantly changes the response of the animal to a fibrotic stimulus; specifically, the congenic *sod3*^{129} mice are significantly protected against asbestos- induced inflammation and fibrotic lung disease relative to *sod3*^{wt} mice. The increased initial activity of ecSOD in *sod3*^{129} lungs quenches the ROS induced by asbestos, which, in turn, leads to a reduction in the oxidative fragmentations of ECM, decreased recruitment of neutrophils and decreased fibrosis (**Figure 3**). On the other hand, the higher ecSOD expression results in increased bacterial burden after LM and SP infection. The increased ecSOD may attenuate ROS production and thus impair the proper inflammatory cell activation resulting in decreased bactericidal function. The detailed effects of ecSOD on the immunologic response are under investigation by Drs. Berg's and Jones' group. We also observed that bacterial infection, especially LM, triggers an extensive inactivation of ecSOD. Even though it is unknown whether the inactivation is a consequence of increased oxidative stress after infection, several studies implicated that denaturation by ROS, specifically H_2O_2, is responsible to inactivation of SODs during aging and hypertension (1-3). The mechanism of infection-induced loss of enzyme activity needs to be investigated further.

Previous work by others suggests that there is a strain-dependent variation in the susceptibility to several diseases. Specifically, the 129J mice appear to be more resistant to asbestos-induced pulmonary fibrosis, stroke and atherosclerosis than the C57BL/6 strain while they are more susceptible to *Listeria* infection (4-8). None of these studies identified specific

gene(s) that may account for the observed differences in the response of these strains. This dissertation demonstrates that variations in ecSOD expression due to the polymorphism in 129J mice are responsible for the different susceptibilities to asbestos-induced lung fibrosis and *Listeria* infection. These results suggest that the different susceptibility of 129 and C57 strain of mice to other diseases may also due to the ecSOD polymorphism.

In conclusion, the availability of congenic mice with different ecSOD phenotypes within an otherwise identical genome provides an important tool to investigate the role of this enzyme in various diseases and a tool to study the post-transcriptional regulation of ecSOD expression.

Figure 1. **Potential mechanism of increased synthesis and secretion of *129* ecSOD.** ecSOD synthesis begins on an unattached ribosome in the cytosol. When signal sequence is exposed, a signal-recognition particle (SRP) binds to the signal sequence (red color) of a nascent protein chain and the translation stops. The complex of SRP, nascent polypeptide, and ribosome translocates to the rough ER membrane and the signal sequence and adjacent polypeptide (green color) is inserted to the translocon. Once signal peptidase cleaves the signal sequence, the peptide chain continues to elongate until translation is completed and is extruded into the ER lumen through the translocon. The change within the signal peptide (N21D) in *129* ecSOD results in significant increase of the cleavage efficiency. The signal cleavage in *129* ecSOD occurs in a higher rate and thus increases rates of synthesis and secretion compared to *wt* ecSOD. With the increased processing efficiency, the *129* ecSOD secreted faster to the extracellular space. Similar proportion of ecSOD can be internally degraded in endosome.

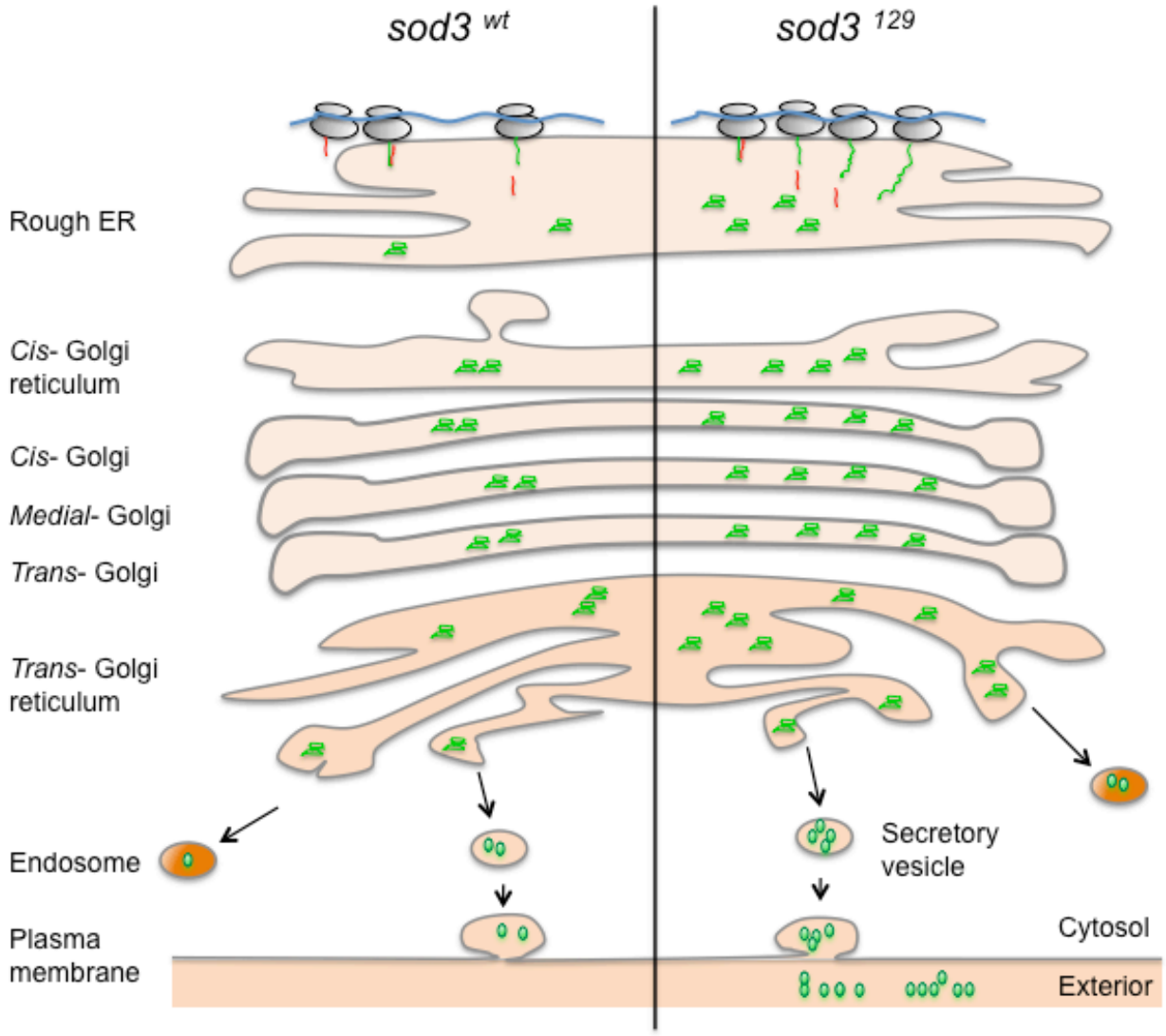
sod3 wt
sod3 129
Rough ER
Cis- Golgi reticulum
Cis- Golgi
Medial- Golgi
Trans- Golgi
Trans- Golgi reticulum
Endosome
Plasma membrane
Secretory vesicle
Cytosol
Exterior

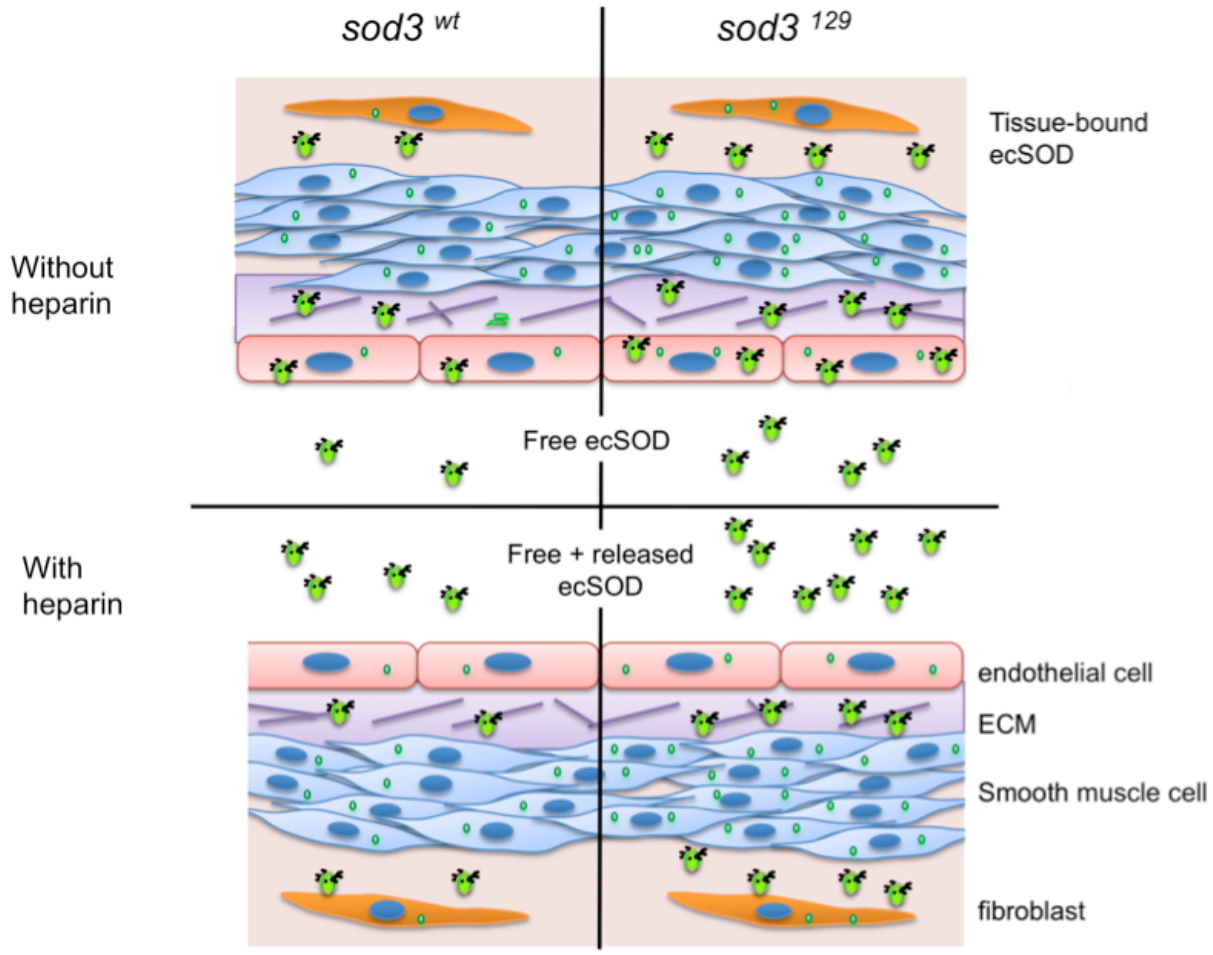

Figure 2. Potential effect of 129 allele on tissue ecSOD distribution. Cross-section of an artery from mice expressing the *wt* allele (left quadrants) or *129* allele (right quadrants) ecSOD. Before heparin administration, (upper quadrants) 129 mice have higher intracellular and tissue-bound ecSOD (shown in green). With the cleavage of heparin-binding domain, ecSOD circulate in the plasma. Due to greater level of tissue-bound ecSOD in mice expressing the *129* allele, more ecSOD is circulating in the plasma and more ecSOD is released after heparin administration (lower quadrants).

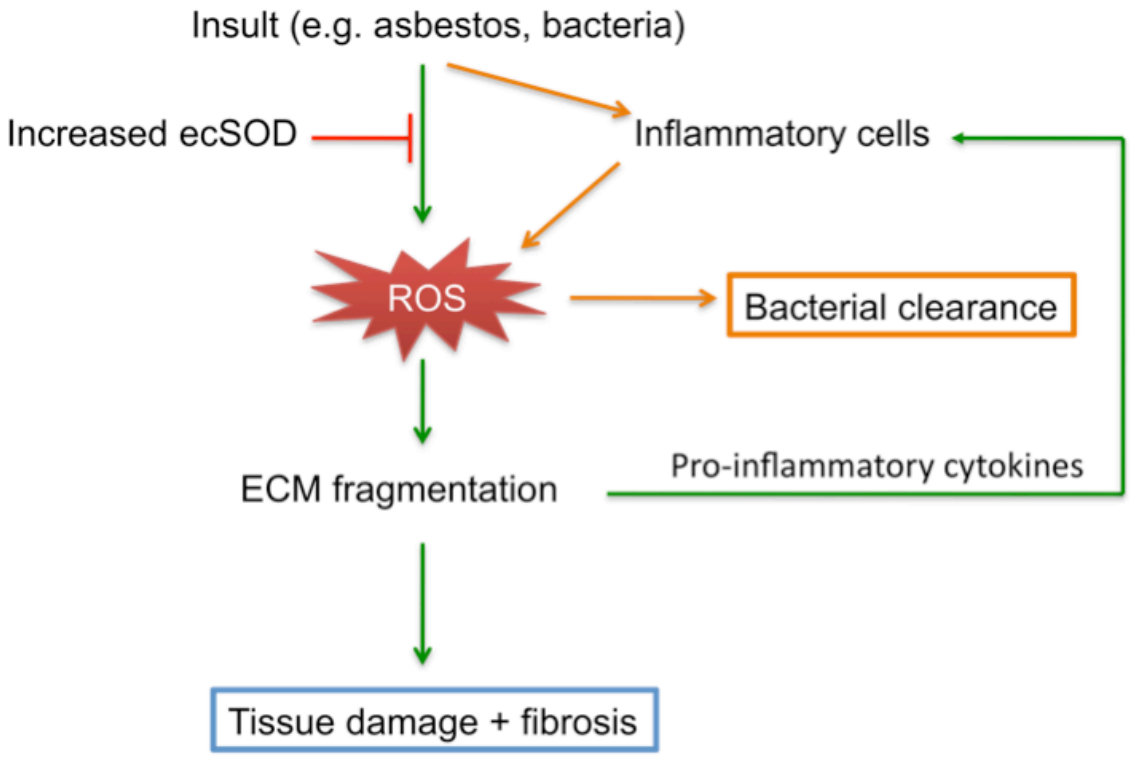

Figure 3. Effects of increased ecSOD level in the pathogenesis by asbestos and bacterial infection. Multiple factors create a redox imbalance by an initial injury, resulting in the production of ROS. The ROS can degrade several components of the extracellular matrix (ECM), causing ECM remodeling. The ECM fragments produced can lead to inflammatory cell recruitment to the site and further increases productions of ROS and pro-inflammatory cytokines. The persistent inflammation can clear bacteria in the site of infection but also can damage tissue and trigger the fibrogenic process. The increased level of *129* ecSOD can significantly reduce the initial ROS imbalance dampening immune responses. The immunosuppressive effect can be protective for tissue damage from non-infectious insults such as asbestos, however, it may be counterproductive during acute infections.

REFERENCES

1. Hink, H. U., Santanam, N., Dikalov, S., McCann, L., Nguyen, A. D., Parthasarathy, S., Harrison, D. G., and Fukai, T. (2002) *Arterioscler. Thromb. Vasc. Biol.* **22**, 1402-1408

2. Wedgwood, S., Lakshminrusimha, S., Fukai, T., Russell, J. A., Schumacker, P. T., and Steinhorn, R. H. (2010) *Antioxid. Redox Signal.*

3. Goldstone, A. B., Liochev, S. I., and Fridovich, I. (2006) *Free Radic. Biol. Med.* **41**, 1860-1863

4. Warshamana, G. S., Pociask, D. A., Sime, P., Schwartz, D. A., and Brody, A. R. (2002) *Am. J. Respir. Cell Mol. Biol.* **27**, 705-713

5. Fujii, M., Hara, H., Meng, W., Vonsattel, J. P., Huang, Z., and Moskowitz, M. A. (1997) *Stroke* **28**, 1805-10; discussion 1811

6. Paigen, B., Ishida, B. Y., Verstuyft, J., Winters, R. B., and Albee, D. (1990) *Arteriosclerosis* **10**, 316-323

7. Ward, N. L., Moore, E., Noon, K., Spassil, N., Keenan, E., Ivanco, T. L., and LaManna, J. C. (2007) *J. Appl. Physiol.* **102**, 1927-1935

8. Cheers, C., and McKenzie, I. F. (1978) *Infect. Immun.* **19**, 755-762